# Thermomechanical simulation in novel vanadium alloyed high strength interstitial free steels.

**Beh, Kok Yong**

# Thermomechanical Simulation in Novel Vanadium Alloyed High Strength Interstitial Free Steels

Kọk Yong Beh

Master of Philosophy (MPhil) Thesis

Academic Supervisor: Dr. George Fourlaris

Materials Research Centre,
School of Engineering,
Swansea University,
Swansea, SA2 8PP

# Declaration

This work has not previously been accepted in substance for any degree and is not being concurrently submitted in candidature for any degree.

Signed _____ (Candidate)
Date 08/07/08

## Statement 1

This thesis is the result of my own investigations, except where otherwise stated.

Other sources are acknowledged by footnotes giving explicit references. A bibliography is appended.

Signed _____ (Candidate)
Date 08/07/08

## Statement 2

I hereby give consent for my thesis, if accepted, to be available for photocopying and for inter-library loans after expiry of a bar on access approved by the University of Wales on the special recommendation of the Constituent Institution / University College concerned.

Signed _____ (Candidate)
Date 08/07/08

# Contents

# Acknowledgements

I wish to express my grateful to all who have given me the opportunity to complete my thesis. I would like to express my sincere gratitude to my academic supervisor Dr George Fourlaris for his valuable advice and help through my study.

Many thanks to my colleagues of Physical Metallurgy Group, Ooi, Khoo, Wong, Owen, Joel, Han, Ian and Carr for the good times and support during my study.

I would like to express my gratitude to Peter Davies for his help in SEM microscopy.

Finally, I would like to express my deep gratitude to my family and girl friend for their encouragement and support during my study.

# List of Tables

# List of Figures

# Abstract

The steel industry has been encouraged to develop high strength and good formability strip steels in order to address the needs of the automotive sector and address the competition from lightweight materials such as aluminium alloys. In order to meet these stringent requirements, high strength interstitial free steels have been developed. High strength interstitial free steels are characterised by high elongation values, high r-value, low yield strength and tensile strength higher than the conventional interstitial free steel. This study has focussed on two different grades of experimental high strength interstitial free steels.

The literature review provides the details of the processing route applied to obtain appropriate mechanical properties on high strength IF strip steels and the investigation of these properties for each microalloying element and also the various types of precipitates forming, including carbides, nitrides, carbonitrides and sulphides, which could be present in High Strength IF steels relevant to the present study.

In recent years, thermomechanical processing of strip steels has become the preferred processing route to produce high quality strip steel products and satisfy the requirements of the automotive industry. Experimental simulation is one way of obtaining an optimum processing route for subsequent application during thermomechanical heat treatment. In this part of the study, two experimental grades of high strength IF steels were studied a titanium stabilised and a titanium-vanadium stabilised grade, which were subjected to thermomechanical simulation via the Gleeble 3500 machine. Following Gleeble testing, a microstructure examination has been performed, coupled with hardness testing, grain size evolution, as well as with MT-Data thermodynamic calculations of precipitate formation.

This study identified the critical parameters for processing titanium and titanium-vanadium alloyed experimental HS-IF steels grades. These included, the identification of the effect the reheating, roughing, coiling and finishing temperatures. The recommendation of the optimised processing route is offered as part of this thesis.

# Chapter 1

## Introduction

Steel is one of the material which has been known from antiquity [1]. In China, steel was reported during the Han dynasty (202BC-220AD), produced by melting wrought iron together with cast iron and gaining an ultimate product with an intermediate carbon content, which was identified as "steel". Chinese had also developed methods for the production of creating wootz steel along with their original methods of forging steel, an idea imported from India to China during the $5^{th}$ century AD [2]. In the $11^{th}$ century, the production of steel using two techniques has taken place with evidence during the Song dynasty in China, and these two techniques reported to be the a precursors to the modern Bessemer process. The first techinique is reported to use partial decarburisation by repeated forging under a cold mount and the second technique is similar to the "berganesque" method that produces inferior, inhomogeneous steel [3].

In order to make steel, first we must make iron. Unlike other noble metals such as silver and gold, iron is never found as a pure element in the earth's crust but exists normally as an oxide. Originally, iron is extracted from iron ores and following the removal of oxygen, it is then combined with a preferred chemical partner such as carbon. This process is acknowledged as "smelting", this process was the first theoretical method applied to metals with lower melting points [4]. Different metals have a variety of melting points. For example; copper melts at $1082^0$C. However, these temperatures can be reached with established methods that have been used for more than 6000 years from the Bronze Age [4]. Compared to copper, the melting point of iron is quite high, therefore smelting results in a ferrous alloy that contains mainly iron and called steel [3]. Although,

the composition of steel varies significantly, the combination of iron and carbon is responsible for the existence of a number of different crystal structures with very different properties. This allotropic transformation of steel is the reason that steel still has a large potential for research and development nowadays. Steel is widely used in many different fields, such as construction, aerospace, automotive or even used to produce some small products like spoons and forks. Many different grades of steel have been researched and produced to fulfill the requirements of different engineering fields.

Since thin sheet steel was first developed by the American Rolling Company at Ohio (ARMCO) in 1923, it was soon adopted by the automotive industry to replace the wooden frames as a material of building self-support car bodies [5]. There are many reasons that caused the replacement of wooden frames. First, is the safety, the ability of energy absorption of the car body made by steel is much higher. Thus, the safety of car body made by steel is much higher. Furthermore, steel is also easier to form into complex shapes. Due to the need of reducing harmful emissions coupled with the need of reducing consumption energy, the design of lightweight autobody vehicle has become necessary. To achieve this requirement, thinner sheet and highly formable steel grades have been developed. Today, Al alloys are the main competitor of steels in the automotive market, due to their lightweight character that contributes in fuel saving, but for safety reasons and lower production costs steel is still the preferred material for the automotives market. Furthermore, it has been reported that [6], steel has better formability and elongation compared to Al alloys as shown in Figure 1.1

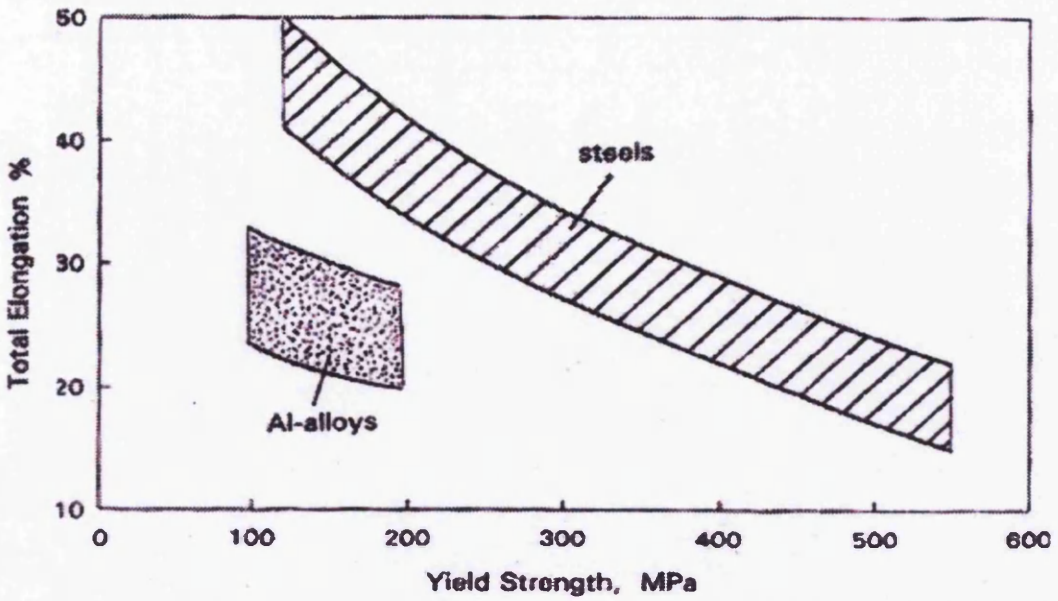


Figure 1.1- Yield strength vs total elongation of aluminum alloys and automotive steels [6]

Ultra low carbon (ULC) steels which are highly formable, non-ageing and suitable for hot dip galvanizing are firmly established to satisfy the demanding requirements of the automotive industry [7]. Traffic accidents are one of the severest social problems around the world. Thus, vehicles must not only be lightweight, but also must have improved safety performance. A high tensile strength, high r-value (Lankford value), good ductility and anti-aging property are the essential properties for a steel to be used in applications of deep-drawing parts of automobiles and appliances. To meet these requirements, High strength (HS) interstitial-free (IF) steels have been developed.

Low carbon and nitrogen contents are the main reason that interstitial free steels are highly formable. It is well known, that carbon can strengthen the steel but also decrease its ductility and formability. IF steels normally contain no more then 0.005 wt% carbon, 0.004 wt% nitrogen and 0.5 wt% of other intentional and microalloying elements, i.e. titanium, niobium, vanadium, sulphur and manganese. The high strength IF steel grades

contain higher amounts of manganese and/or phosphorus, boron and silicon [8]. The additional amount of microalloying elements is forming fine precipitated particles, in order to increase the formability and/or strength of the IF steel. High strength interstitial free steels are characterised with slightly lower elongation values and r-value, but have higher strength than conventional interstitial free grades.

The processing route and chemical composition are two major issues determining the properties of HS-IF steels. Precipitation of microalloying elements can affect the properties of HS-IF steels, such as the development of a strong {111} recrystallisation texture during annealing which is important in order to achieve high drawablility [9]. The process of removing interstitial elements with microalloying elements can promote the favorable {111} texture and produce highly drawable steels [9]. However, decreasing the interstitial atoms could cause Secondary Work Embrittlement (SWE) or Cold Work Embrittlement, since precipitates forming in the matrix from scavenging of the carbon and nitrogen atoms, control the hot band grain size which is important to the improvement of deep drawability [10]. The chemical composition of HS-IF steels can also be adjusted to meet and satisfy the different customer requirements.

Thermomechanical processing is the preferred process route in developing high quality steel products for automotive applications. In recent years, physical simulation is used to perform many thermomechanical tests. The Gleeble system is one of the most important tools in simulating thermomechanical processes. The Gleeble system is able to simulate most thermomechanical conditions, which are similar to those prevailing in the hotmill, including slab reheating temperature, heating and cooling rates, amount of deformation, strain rates, coiling temperatures, finishing temperatures and roughing temperatures. The Gleeble system could follow preset parameters to run a complete hot rolling simulation.

In this study, two experimental grades of HS-IF steels are studied, including a titanium stabilised and a titanium-vanadium stabilised grades. These have been studied using the Gleeble 3500 thermomechanical testing system. Both steel grades have been studied using carefully selected thermomechanical heat treatment cycles. Different heating

parameters are likely to have different effects on the obtained microstructures and mechanical properties. The parameters that could affect the properties include, the selected soaking temperature, finishing temperature and coiling temperature [11]. The Gleeble unit allows the designing of a suitable hot rolling processing route, in order to find the optimum processing route for HS-IF steel products.

# Chapter 2

## Aims

1. Optimise the thermomechanical processing route for both a Ti only and a Ti-V HS-IF steels to take full benefit of microalloying additions.
2. Assess the potential and effect of vanadium additions on strengthening and formability characteristics in HS-IF steels.
3. Evaluate the effect of varying the various processing parameters during the thermomechanical processing of HS-IF strip steels.

# Chapter 3

# 3. LITERATURE REVIEW

## 3.1 AUTOMOTIVE STEELS

The excellent properties of steel have maintained its position as the predominant material for the automotive industry. This is due to strip steel's characteristics of good formability, excellent elongation, high ductility, ease of welding and relatively low cost of production. Steels are also easier to recycle compared to plastics and other competitor materials, which makes its recycling environmentally friendly [6]. One of the main challenges of the automotive industry is facing in recent years is to increase fuel efficiency and reduce vehicle emissions by reducing the weight of vehicles. Car body is the main focus in this effort of reducing weight [12]. A very cost-effective method to accomplish weight savings is to decrease the thickness of automotive components and substitute mild steel by high strength steel grades.

Automotive steels can be classified into three main categories, which are conventional low-strength steels, conventional high strength steels (HSS) and advanced high strength steels (AHSS). Where interstitial free and mild steels are classified as conventional low-strength steels, carbon-manganese, bake hardening, high-strength interstitial free and HSLA steel are classified as conventional high strength steels and dual-phase, complex phase, transformation induced plasticity and martensitic steels are characterised as

advanced high strength steels (AHSS) [13]. Figure 3.1 shows this classification in relation to elongation and tensile strength [13].

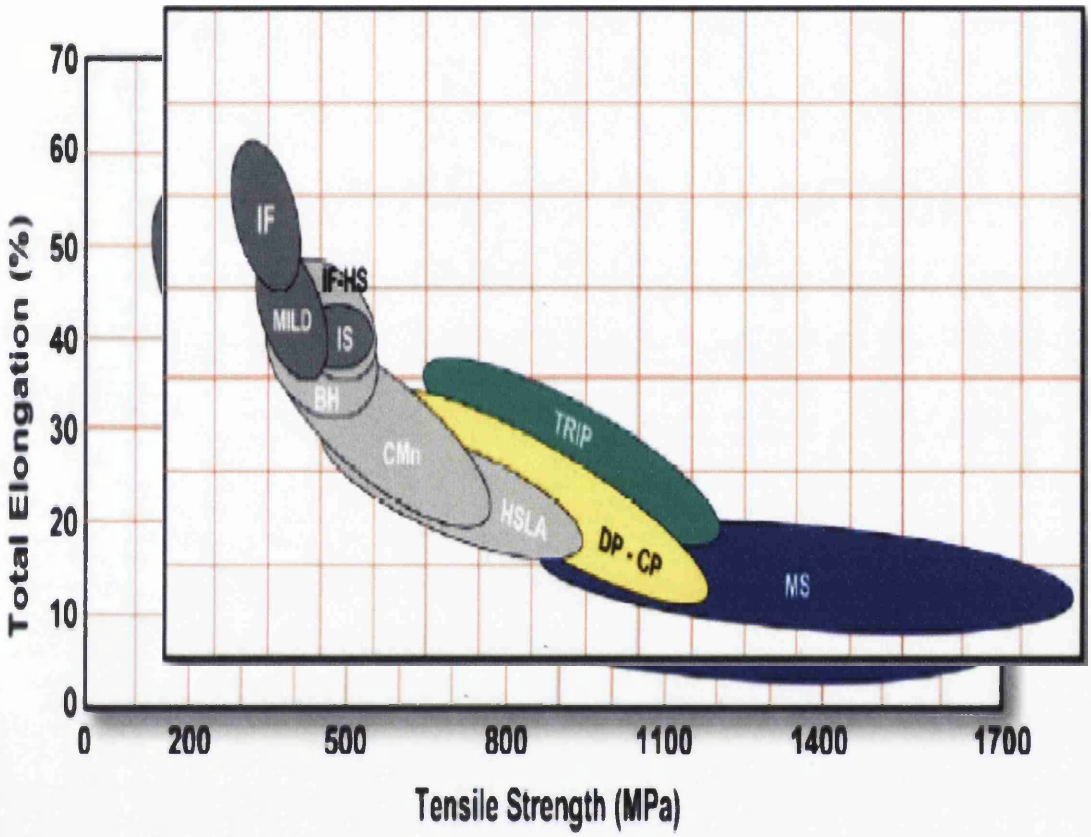


Figure 3.1: Classification of automotive steels [13].

Conventional low strength steels have yield strengths from 150-210 MPa and ultimate tensile strength less than 270 MPa, while conventional HSSs have yield strength from 210-550MPa and ultimate tensile strength from 270-700 MPa; AHSSs have yield strength greater than 550 MPa and ultimate tensile strength greater than 700 MPa. Through their microstructures, HSS and AHSS can also easily be distinguished and classified. Conventional HSS are normally single ferritic phase steels, while AHSS are

principally multi-phase steels, which may contain the combination of ferrite, martensite, bainite and/or retained austenite in critical quantities in order to produce unique mechanical properties [14].

### 3.1.1 Mild Steels

Mild steels are typically ferritic in microstructure. Drawing Quality (DQ) and Aluminium Killed (AKDQ) steels which have widespread application and high production volume are two common reference grades [13].

### 3.1.2 Interstitial Free Steels

Interstitial free steels have the best formability characteristics in comparison to all other automotive steel grades. As shown in figure 3.1 IF steels exhibit the highest elongation values. IF steels contain very low carbon and nitrogen levels, while microalloying elements such as Mn, S, Ti and Nb are normally added to remove the carbon and nitrogen from the solution. These microalloying additions are responsible for the production of extra deep drawing quality IF strip steels [8]. IF steels have low yield strength, while the dent resistance of IF steels is quite low compared to other automotive grades.

### 3.1.3 Bake Hardening Steels

Bake hardening (BH) steels have an essentially ferritic microstructure, and primarily are strengthened by solid solution strengthening. During processing of BH steels, carbon in

composition is kept in solution, and subsequently precipitates out during the paint baking state [13]. This offers steel products with combination of high formability and high strength [15]. However, High-strength IF perform better in this aspect.

### 3.1.4 Carbon-Manganese Steels

Carbon-manganese strip steels were the first steel grade manufactured for the automotive car body, carbon-manganese steel attributes are its versatility, good formability and low cost [16]. These grades are primarily strengthened by solid solution strengthening.

### 3.1.5 High-Strength Low-Alloy (HSLA) Steels

High-strength low-alloy (HSLA) steels are principally strengthened by microalloying elements. Nb, V and Ti are added to form fine carbides when combined with carbon and fine nitrides when combined with nitrogen. This results in steels with fine-precipitates fine-grain size and good combination of strength and formability [17].

### 3.1.6 Dual-Phase (DP) Steels

Dual-phase (DP) steels have both ferrite and martensite in their microstructures. DP steels are produced by controlled cooling for the austenite plus ferrite ($\alpha + \gamma$) stability field. By rapid cooling, austenite transforms to martensite. The presence of martensite increases hardenability of the steels. As shown in figure 3.2, the soft phase (ferrite) is surrounding the islands of martensite.

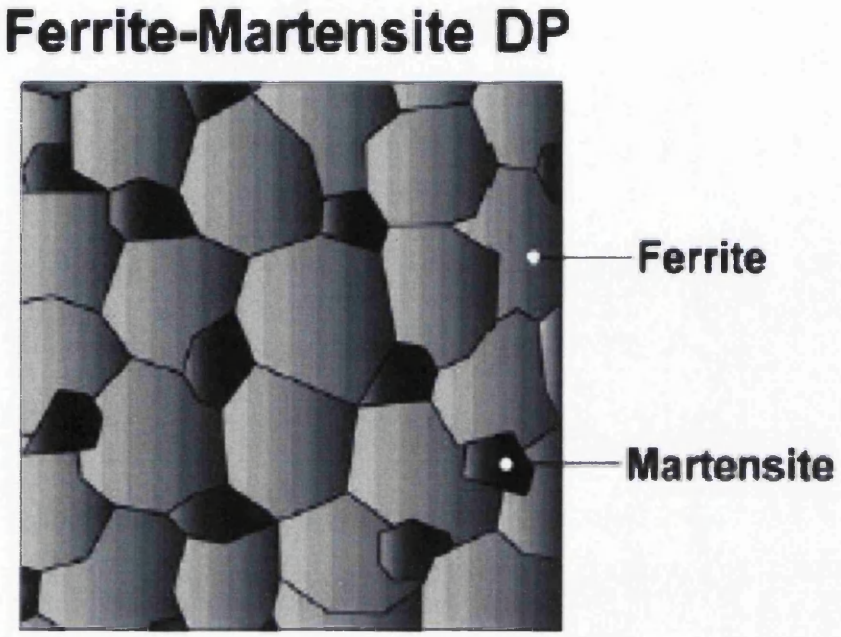


Figure 3.2: Microstructure of DP steel [13].

This combination of microstructures the steel gives good ductility, and exhibits low yield strength but high work hardening rate (n value) [13].

### 3.1.7 Transformation-Induced Plasticity (TRIP) Steels

Transformation-induced plasticity (TRIP) steels have a primary ferrite matrix with a minimum of 5% volume fraction of retained austenite embedded in the matrix. The production of TRIP steels requires the use of isothermal hold at an intermediate temperature in order to produce some bainite [13]. To increase the strength of the strip steel product, the retained austenite is progressively transformed to martensite. Thus,

TRIP steels exhibit mixed microstructure of ferrite, retained austenite, bainite and martensite, as shown in figure 3.3.

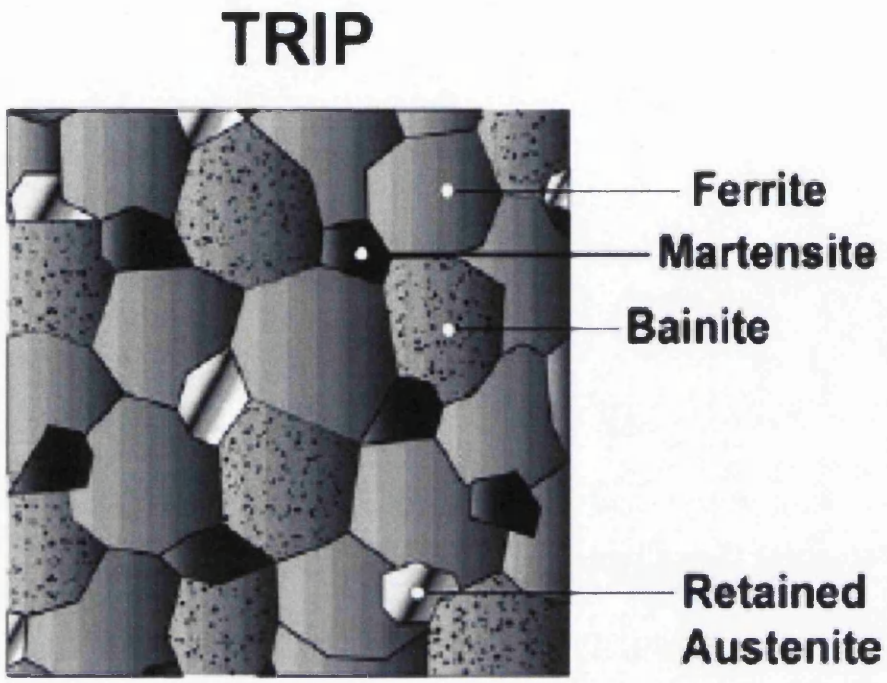


Figure 3.3: Microstructure of TRIP steel [13].

It has been reported that [13], the TRIP steels have also good work hardening rate but lower than a similar strength grade of DP steel at initial stages of deformation. However, work hardening persists at higher strains, while work hardening of an equal strength DP grade begins to diminish.

### 3.1.8 Martensitic (MS) Steel

Martensitic steels (MS) consist of a martensitic matrix with small amounts of ferrite and bainite. MS Steels are produced by rapid cooling from the austenite phase to transform almost completely austenite to martensite during hot-rolling or annealing [18]. MS steels

have the highest ultimate tensile strength levels within the family of automotive steels. Due to limitations on formability, MS steels are often subjected to further treatments to improve this property [18].

### 3.1.9 High Strength Interstitial Free (HS-IF) Steels

High strength interstitial free steels have an alloy content more variable in terms of microalloying elements than low strength IF steels do. In addition to Mn, Ti, Nb and V, they also consist P, B, Si. These elements may be used individually or in combination, in order to further strengthen and produce a range of high strength grades IF steels. Low strength IF steels have yield strength from 150-200MPa, while high strength IF grades have strength values that range from 250-300MPa [7]. High strength interstitial free steels are characterised with higher strength but slightly lower formability in order to meet the different market demands.

### 3.1.10 The Structure of Car Body

Figure 3.4 shows the exposed view of the ULSAB-AVC C-Class car body structure components and Figure 3.5 shows a pie chart of the percentage of each steel grades used in the ULSAB-AVC C-Class car body structure [19]. A car body structure is made by many different strip steel grades, each steel grade is designed to suit the specific part of the autobody, such as IF and HS-IF steels are designed for the complex and deep drawing parts and the MS grades are designed for the parts which need extra strengthening. Much effort has been paid recently to improve the performance of strip steels in order to meet the high demands of the market and the challenges from the competing materials, such as Al-alloys, plastic materials or even ceramic materials.

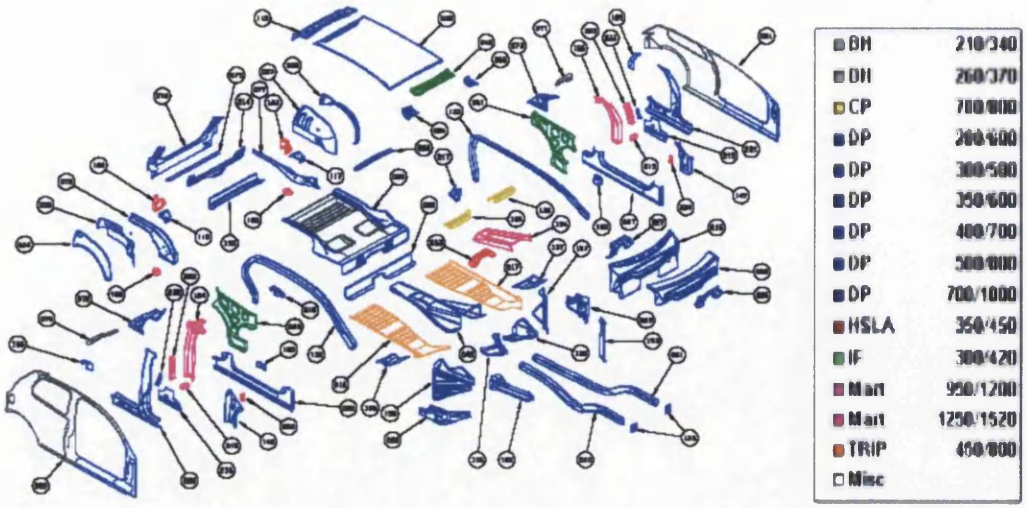


Figure 3.4: C-Class Body Structure [19].

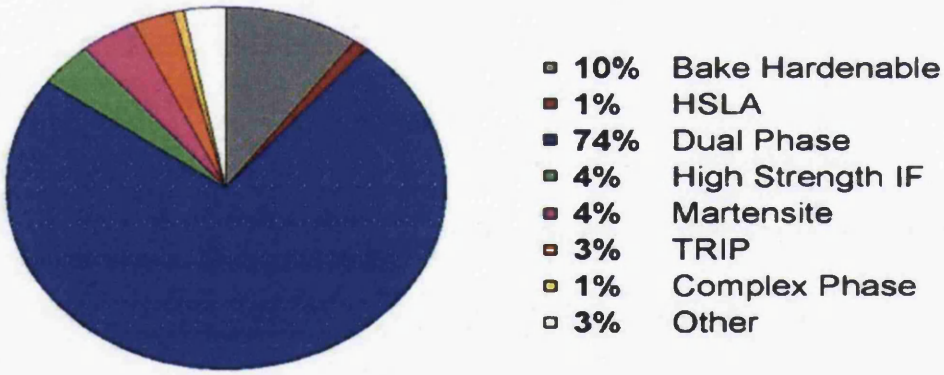


Figure 3.5: The Percentage of Each Steel Grades Used In the ULSAB-AVC C-Class Car Body [19].

## 3.2 Historical Development of HS-IF Steels.

Before the development of IF steels, Comstock [20] has observed that additions of titanium to a normal low carbon steel can promote the formation of TiC and TiN precipitates, when titanium has combined with carbon and nitrogen. He also noticed that this has made the low carbon steel become highly drawable. Due to the high price of titanium at that time when he made these characteristics, his observation could not be put into commercial practice [20].

It was in late 1960's that Ti was first used to precipitate solute carbon and nitrogen. IF steels have appeared as the first commercial products [20]. Sufficient amounts of Ti have been added to low carbon steel and precipitate the solute elements (C, N and S) at grain boundary in order to achieve the term of "interstitial-free', IF steels have then become one of the common steel grades in industry. In 1990's, IF steels have widely developed for the automotive industry, since they exhibit the excellent press-formability i.e. stretch-formability, deep-drawability and uniform appearance after press-forming required for the auto exposure panels such as side-panel and fender [21].

Many types of high-strength steels were developed in recent years. In order to meet the market demands, high-strength IF steels (HS-IF) were subsequently developed and fill the deficiency of low strength IF steels. The production of HS-IF steel is much similar to the IF steels as the HS-IF steel is IF steel strengthened by adding P, Si and Mn in order to increase the strength of IF steel and achieve the HS-IF grades [22]. HS-IF steels are also located at a superb position in the yield strength-strain hardening exponent diagrams, as shows in figure 3.6, which means HS-IF also has excellent formability.

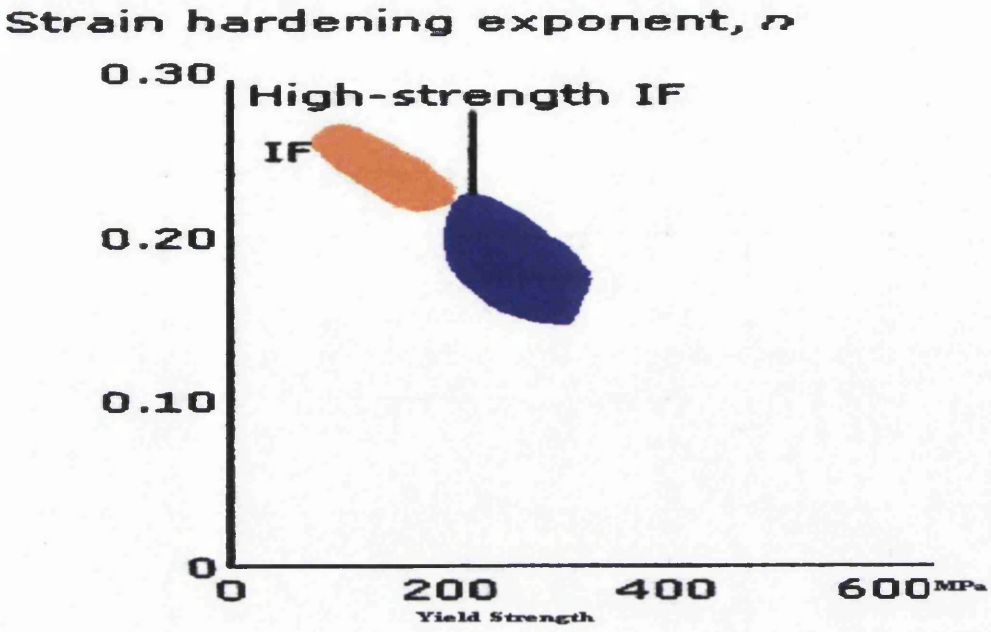


Figure 3.6: Comparison of IF and HS-IF steel in Yield Strength vs. Strain Hardening Exponent, n.

In the late of 1980's, HS-IF steels based on the IF steels and alloying with the solid solution strengthening elements have been developed, and commercialised achieving an increase in tensile strength from 230MPa and up to 440MPa grade in tensile strength.

## 3.3 High Strength Interstitial Free Steels.

High Strength Interstitial Free Steels are basically low carbon and nitrogen steels with the yield strength between 250 to 300 MPa. HS-IF steels are conventionally hot rolled at the austenite state, followed by cold rolling and annealing at the ferrite phase [23]. Every processing stage strongly influences the properties of HS-IF steels, i.e. strength, ductility, formability and etc. HS-IF steel grades are developed based on the basic compositions of the IF grades. HS-IF steels are used in the automotive industry for producing the complicated components, which need a higher strength and good deep drawing, n-value and r-value.

HS-IF steels are designed to improve the safety, fuel economy and dent resistance of the conventional low strength IF steels without loss of formability. Mn, Si and P acted as solid solution hardening elements in order to achieve high strength grades. Ti and/or Nb are added to precipitate C, S and N and reach high deep drawability values. The precipitates that could form in HS-IF steel includ TiN, TiS, MnS, $Ti_4C_2S_2$, TiC, NbC and FeTiP [24]. Previous studies [25] have indicated that, when two 60 x 60 mm square sections (Mild steel and HS-IF steel) were quasi-statically crushed using a servo-hydraulic compression machine, HS-IF was able to maintain the compact collapse modes at larger cross-sections, compared to the mild steel, as shown in figure 3.7. This demonstrates the excellent formability of HS-IF steel compared to a similar strength steel grade.

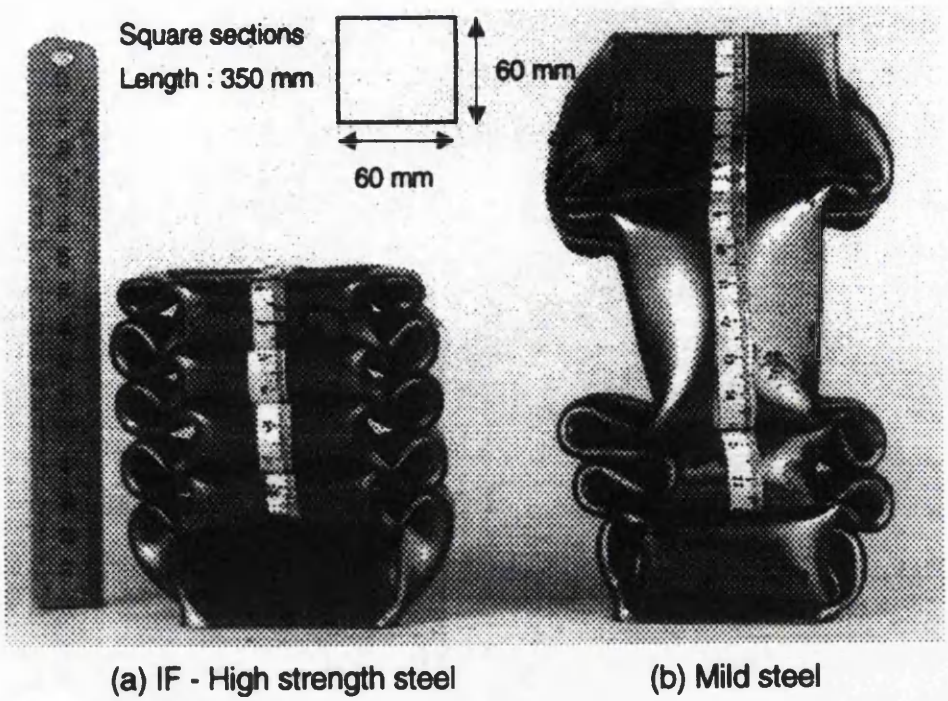


Figure 3.7: Quasi-Statically Crushed (a) HS-IF Steel (280 MPa Yield strength, 420 MPa Tensile Strength) and (b) Mild Steel (150 MPa yield strength, 300 MPa Tensile Strength) [24]

It has been reported [26] that, Phosphorus (P) is the most effective and economical solid solution strengthener to increase the strength of HS-IF steel without decreasing ductility and formability. Even though this look likes an easy and cost efficiency way to get outstanding properties, however, P segregates to grain boundaries could cause embrittlement to the steel. This could results in a catastrophic failure following forming. This phenomenon is called Secondary Work Embrittlement (SWE) or Cold Work Embrittlement [26].

To prevent this phenomenon, there are two basic methods. First, preventing or reducing the tendency of P to segregate to grain boundaries by keeping the free carbon atoms in

solution, as the solute carbon could segregate to the grain boundaries and therefore increase the resistance to SWE. However, the solute carbon is present before recrystallisation occurs and thus, the major drawback of this method is that it results in significant lowering of the r-value. When annealing is performed at high temperatures, the liberated carbon might again segregate to grain boundaries and strengthen them via the dissolution of Nb or Ti carbides [26] [27].

The second method is to add a small quantity of boron and causes significant improvement in SWE resistance. Where boron is added, it can prevent phosphorus segregation to grain boundaries. Therefore, boron addition has become a standard practice for IF steels. Boron is also one of the most effective elements to improve the hardenability and delay the recrystallisation of austenite. However, boron additions in IF steels could raise the recrystallisation temperature and decrease the r-value of steel. This are however secondary effects of boron additions in IF steels. The production of a B-added IF steels sheets with a high r-value is quite difficult [28]. Thus, increasing the strength, formability and resistance to SWE have been the matters of primary concern in IF and HS-IF steels grades.

## 3.4 Microalloying Elements, Solid-Solution Hardening and precipitation hardening.

It is well known that, chemical composition and processing route are the main parameters to determine the mechanical properties and microstructure of steels, including HS-IF steels. Microalloying elements are either individually or combined additions into the HS-IF steels as the compositions of HS-IF steels. The elements that are normally added include Ti, Si, Mn, S, P, Nb, B and V. Precipitation of these microalloying elements with carbon and/or nitrogen to form carbides, nitrides or carbonitride can determine the microstructure and mechanical properties of steels.

The deep drawing property and high r-value of HS-IF steels are normally ascribed the existence of {111} recrystallisation texture during annealing. The process of scavenging interstitial elements (carbon and nitrogen) with microalloying elements are reported [29] to promote the development of {111} texture in order to increase the formability of HS-IF steels. In order to optimise the chemical composition and processing route, the removed of solute elements via formation of precipitates is required, during the production of IF steels. Thus, microalloying elements are playing a very important role to increase the drawability of steels.

Especially in the cold rolling process, during the processing of a cold rolled produce on any carbon content steel, dynamic strain ageing will result and this could lead to the formation of shear bands in microstructure. The formation of shear bands in {111} <$\bar{1}$1$\bar{2}$> orientation grains can cause the easy nucleation of unfavorable {110} orientation [30]. Elimination of all carbon and nitrogen from the matrix before the cold rolling process takes place, is important and an efficient way of improving the formability of steels.

### 3.4.1 Carbon and Nitrogen

It is well known that the addition of carbon could increase the hardness and strength of the steel, but high carbon contents cause the steel to become brittle. HS-IF steels have normally very low carbon and nitrogen contents which are typically less than 0.005wt% carbon and 0.004wt% nitrogen. Most of the carbon and nitrogen in HS-IF steels is combined with the microalloying elements to form precipitates. These combinations have a major influence on the microstructure.

Carbide formers i.e. Ti, Nb and V would combine with carbon to form precipitates during hot rolling and coiling, this process promotes almost complete precipitation of carbon and makes all carbon to be present as precipitates in the ferrite matrix of IF steels [31]. A previous study has indicated that, if TiC does not form during this processing, the metastable compound $\epsilon$-carbide would form, in order to complete the precipitation of carbon [32]. Nitrogen most probably forms TiN or AlN in HS-IF steels.

The formation of $Ti_4C_2S_2$ may stabilize IF steel in the austenitic range, when the temperatures are greater than 950°C. Normally, the presence of a minimum amount of S is requuired. The effective C stabilization is very much influenced by the processing of HS-IF steels. The effect of the Slab Reheating temperature (SRT) and the hot rolled strip Coiling Temperature (CT) on the r-value can be easily verified. Figure 3.8 shows the specific relation between thermomechanical processing parameters, composition and the formability, measured by $r_{mean}$-value in Ti stabilized IF steels [33]. This confirms that solute carbon has a strong influence on the development of crystallographic texture and hence, influences the deep drawing property of IF steels.

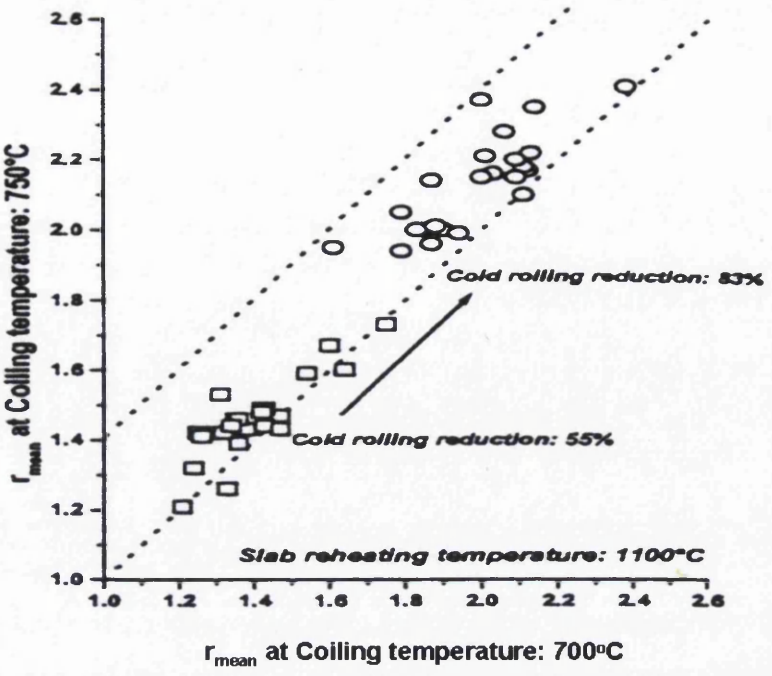


Figure 3.8: Improvement of the $r_{mean}$ -value by combination of a low SRT and a high CT for larger cold rolling reductions of Ti stabilized IF steel [33].

Removal of carbon from the grain boundaries of HS-IF could achieve an improvement in deep formability. However, lack of interstitial carbon atoms at grain boundaries could promote the Secondary Work Embrittlement (SWE) or Cold Work Embrittlement [28]. However, keeping some free carbon atoms in solution and/or an addition of small amounts of B, are two of the most efficient ways in preventing the formation of secondary work embrittlement [26].

### 3.4.2 Titanium

Titanium additions in HS-IF steels are made to lower the interstitial element contents during steelmaking, in order to produce strip products with good deep drawability.

Previous studies have indicated that the higher the Ti or Nb content the lower the yield strength (YS) / ultimate tensile strength (UTS) ratio, which means an improved in terms of formability strip steel product [33]. The influence of Ti and Nb on YS/UTS ratio is clearly reported in figure 3.9. It can be seen that TiC and TiN are very effective in delaying the recrystallisation of austenite after hot rolling and pinning the growth of recrystallised austenite grains [34]. This refinement leads to a finer ferrite microstructure and improvement of steels' properties.

Takechi [22] has reported that the improvement of mechanical properties of steel sheets in terms of the r-value can be achieved by reduction of C contents and additions of Ti. For instance, the critical amount of Ti, effective Ti% (Ti* %) necessary for obtaining an excellent r-value can be expressed by:

$$Ti^* = Ti\,(\%) - [4C\,(\%) + 3.43N\,(\%)]\ (\text{in wt. }\%) \qquad \text{equation 2.1 [22]}$$

Where the %C is carbon content and the %N is the nitrogen content.

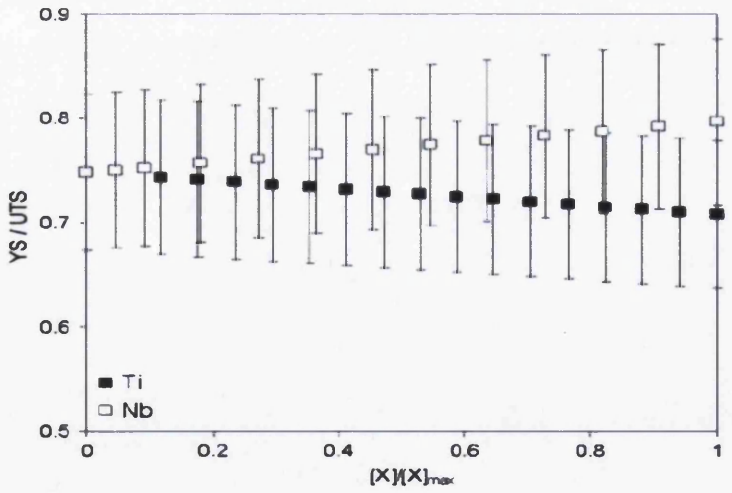


Figure 3.9: The effect of Ti and Nb on YS/UTS ratio [33].

Precipitates of TiN, TiS, $Ti_4C_2S_2$ and TiC have been detected in previous studies [9] [31] [33] in Ti-stabilised IF steels, TiN particles are detected in the ferrite matrix and at grain boundaries. They form during solidification and during the addition of the FeTi alloy to the steel bath, which means that TiN is formed in both liquid and solid phases. TiS and $Ti_4C_2S_2$ are identified in the austenite region, following reheating at approximately 1250°C and hot rolling from 1250°C – 950°C of slabs. The presence of TiC precipitates is indicated following coiling at temperatures of approximately 700°C.

TiN precipitates could promote the growth of recrystallised ferrite grains with favourable {111} texture. In order to coarsen the ultrafine TiC precipitates that form in ferrite; it is advised to set a higher coiling temperature. Precipitation of TiS can be found in the higher austenite region, while $Ti_4C_2S_2$ is present in the lower austenite region [9]. It has been reported that [35], $Ti_4C_2S_2$ possibly removes carbon from the matrix at high temperature (austenite phase), and makes the IF steel to perform as a carbon-free matrix following finishing hot rolling. This in turn results in a very favourable texture for deep drawing applications.

However, $Ti_4C_2S_2$ is not easy to form as this compound is less stable than the TiS in the austenite phase, which means that TiS is more likely to form than $Ti_4C_2S_2$. It has also been reported that, almost no $Ti_4C_2S_2$ is found above 1200°C. The results are shown in figure 3.10. It has been proven that formation of $Ti_4C_2S_2$ can be promoted through heat treatment [35].

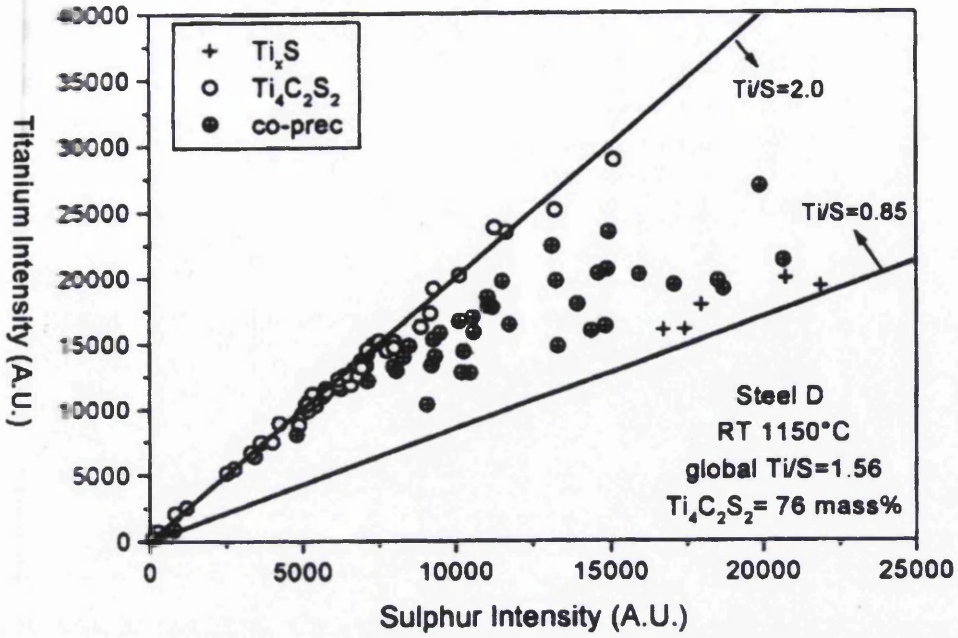


(a)

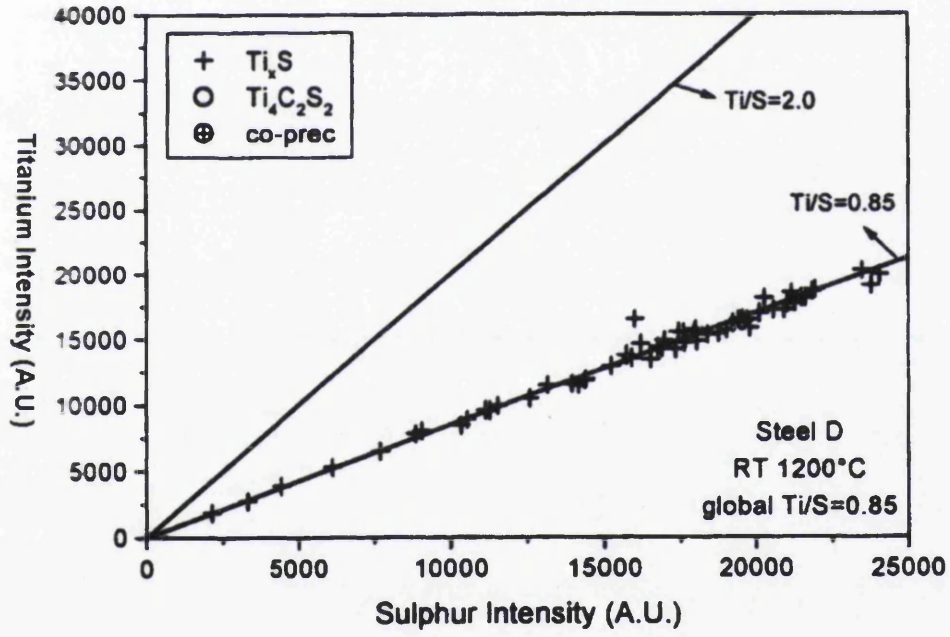


(b)

Figure 3.10: EDX results of individual particles in an IF steel, (a) reheated at 1150°C (b) reheated at 1200°C [35].

During the removal of interstitial elements by microalloying elements, precipitates that are left in the matrix may adversely affect the recrystallisation process, Ti left is excess in the matrix is far less effective than Nb in retarding the recrystallisation process. However, this is considered as a distinct advantage [9].

### 3.4.3 Sulphur

Sulphur acts as an interstitial element that is always present in IF and HS-IF steels grades. Previous studies, have detected TiS, $Ti_4C_2S_2$ and MnS in IF and HS-IF steels, and much research carried out on the behavior of these precipitates of S in IF steels, have found the ability of these particles to influence the properties of IF grades steels [32][35][36]. With the precipitation of carbosulphides ($Ti_4C_2S_2$), carbon in IF steels may be stabilised in the austenitic range. Promoting the formation of carbosulphide in the austenitic range, could reduce the formation of TiC during the annealing process, since large amounts of TiC formation could have a negative effect on the formation of favourable {111} texture [35] [36].

In other words, the promotion of the $Ti_4C_2S_2$ formation would promote the {111} texture development and this could increase the formability of the IF steels. The nucleation of $Ti_4C_2S_2$ is difficult because of the absence of sulfur supersaturation, and because the nucleation of $Ti_4C_2S_2$ requires the simultaneous presence of three different elements which are titanium, sulphur and carbon [36]. The formation of $Ti_4C_2S_2$ is strongly dependant on the process. Recently, many studies [35-39] have been carried out on the TiS- $Ti_4C_2S_2$ transformation. However, the formation of $Ti_4C_2S_2$ needs further particular analysis.

### 3.4.5 Niobium

Niobium is one of the carbide forming elements that are normally present in IF steels grades. It can form NbC when combined with carbon. It is widely accepted that, solute Nb could segregate to austenite and ferrite grain boundaries, and increase the strength of the austenite [40]. It is also reported [41] that, additions of high amounts of Nb could result in lowering of the r-value and ductility. Therefore, the Nb content should be kept to a minimum. The strength of austenite in IF steels can be enhanced by solute Nb, but this effect is reported to be relatively small, compared to Boron. Figure 3.11 has listed the overall behavior of austenite in terms of the effect of B, Mo, Nb and C solutes [42]. As shown in figure 3.11, the effect of 160 ppm of Nb addition is equal to 2000 ppm of Mo and 26 ppm C, but it is much less than the effect of B in an IF steel.

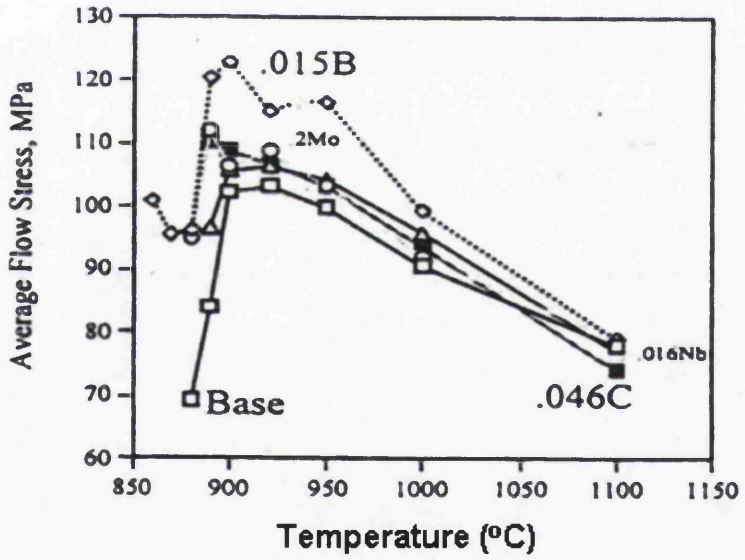


Figure 3.11: Average Flow Stress (MPa) vs. Temperature (°C) for B, Mo, and Nb and C solutes in an IF steel [42].

According to DeArdo [42], the most beneficial use of solute Nb is present in galvannealed IF steels. It is well known that Ti + Nb stabilized IF steels show much higher resistance to powdering than Ti stabilized IF steels as shows in Figure 3.12.

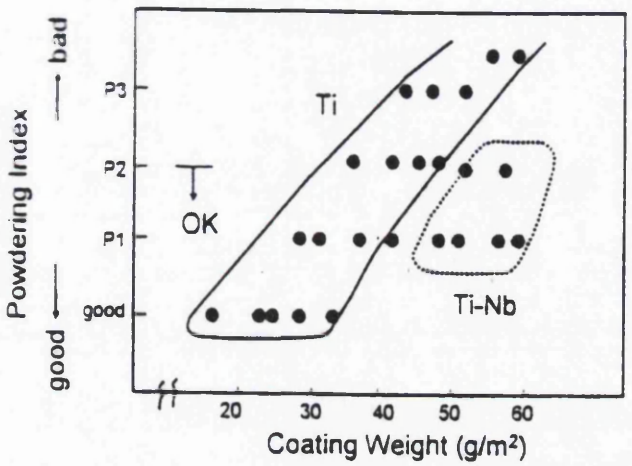


Figure 3.12: Powdering tendency for Ti and Ti + Nb galvannealed IF steels [42]

### 3.4.6 Vanadium

Ti and Nb are often added to the IF and HS-IF steels in order to increase their formability by formation of precipitates. The addition of Nb in IF and HS-IF steels grades results in severe retardation of recrystallisation during the annealing process. This kind of retardation causes much extended annealing times and/or needs higher annealing temperatures and such problem often leads to alteration of the strip during the continuous annealing cycle. Titanium additions are sufficient to stabilise the interstitial elements, but can cause problems during galvanizing. It has been advised that vanadium treated steels

could exhibit the interstitial free characteristics without such a drastic retardation of recrystallisation [43].

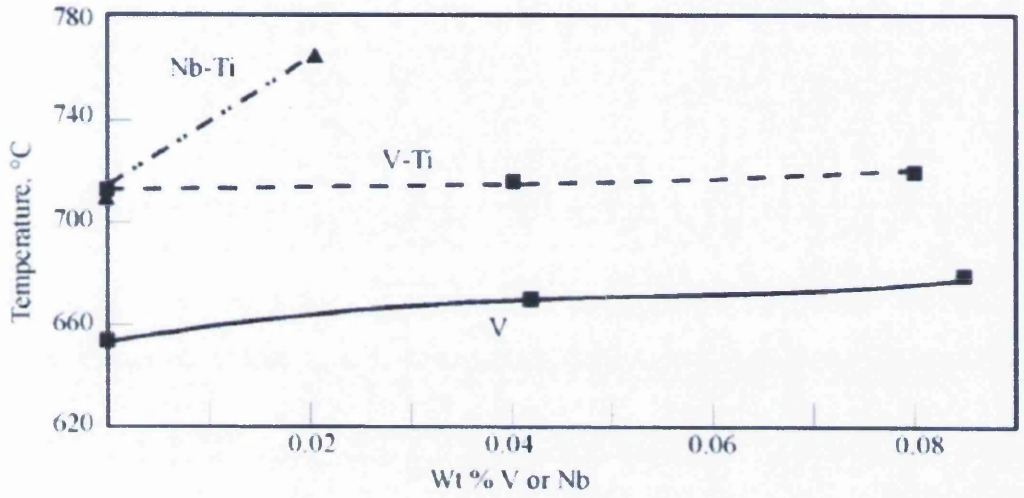


Figure 3.13: The effect of Ti + Nb, Ti + V and V stabilised IF steels on the Temperature for Complete Recrystallisation in 30 Seconds [44].

Figure 3.13 shows the temperature needed to obtain complete recrystallisation in 30 seconds, the vanadium only stabilised IF steel can recrystallise at lower temperatures than the Ti + Nb and Ti + V stabilised steel. The addition of vanadium could be made in steels containing sub-stoichiometric titanium and niobium levels as carbide and nitride stabilisers (VC and VN) [44], thus maintaining titanium content to lower levels, in order to avoiding the white powder defects seen in galvannealed steels.

For any microalloying element addition to exert its effect most efficiently it has to be dissolved into solution during processing, therefore solubility plays a key role for microalloying elements to be used most effectively. In hot rolled products, vanadium has been used with the combination of other microalloying additions for many years in high

strength products, but yet is not commonly used in high strength Interstitial Free steels. Due to the great solubility of V in austenite, it can provide efficient contributions either via ferrite grain refinement and/or precipitation strengthening [45]. During the thermomechanical processing of the steel while heating to the austenitic rolling temperature, VC solubility is much higher than TiC and NbC. Even if VN is less soluble than VC, it is more soluble than AlN and TiN. The results are shown in figure 3.14. On the other hand, the strengthening effect of V in austenite is also much higher than Ti and Nb.

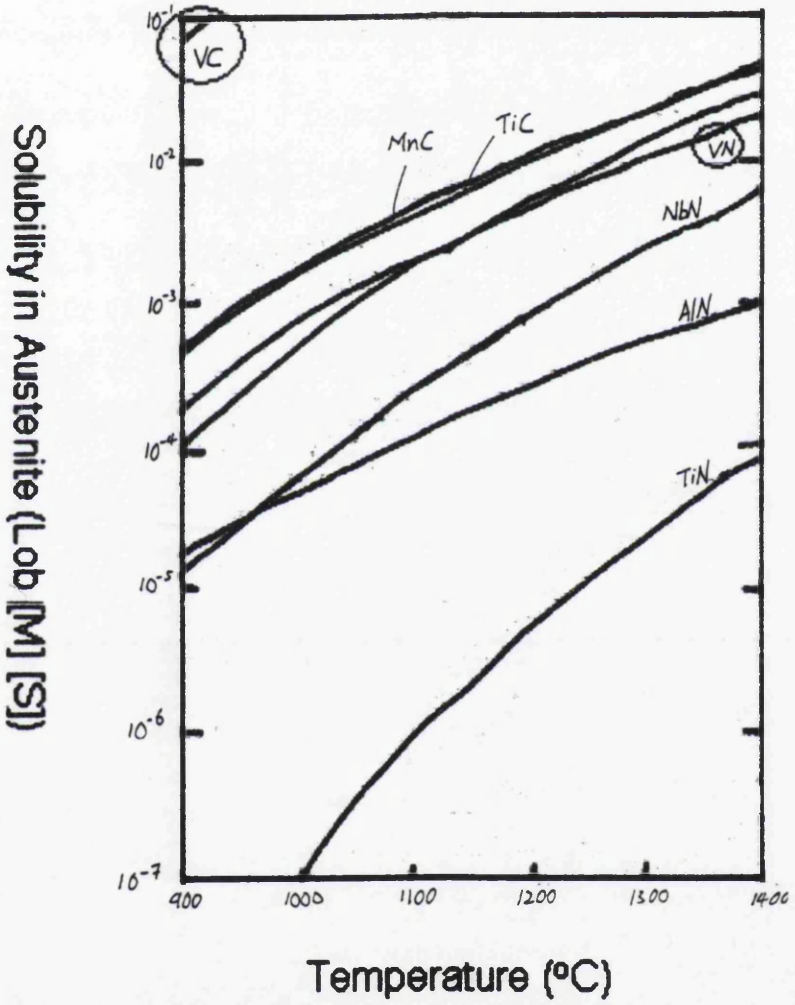


Figure 3.14: Solubility products in austenite vs. temperature [45].

In cold rolled products, vanadium provides only limited support to the steel compared to hot rolled products. This is due to the vanadium carbide coarsening rates reported to be greater than NbC or TiC.

### 3.4.7 Phosphorus

In order to achieve the weight reduction of the autobody, Manganese, Silicon and Phosphorus which act as solid solution strengthening elements are added to the IF steels and develop novel HS-IF grades steels. It is widely accepted that Phosphorus is the most effective strengthening microalloying element for use in HS-IF steels [46] [47]. It is also most cost efficient compared to Mn and Si. The effect of additions P and S on a Base steel is shown in figure 3.15. Increasing the amount of P from 20ppm to 600ppm results in a rise of the flow stress by about 8 MPa which is about 10% higher at 920°C than a S steel [42].

According to J. Rege [47], with additions of P, the yield strength and the ultimate tensile strength increase but the n-value and total elongation decrease. These are due to the segregation of P to the ferrite grain boundaries and the associated embrittlement caused. The failure of IF steel following cold forming is called cold working embrittlement (CWE) or Secondary Work Embrittlement (SWE). CWE or SWE is a critical problem in P alloyed IF steels [26].

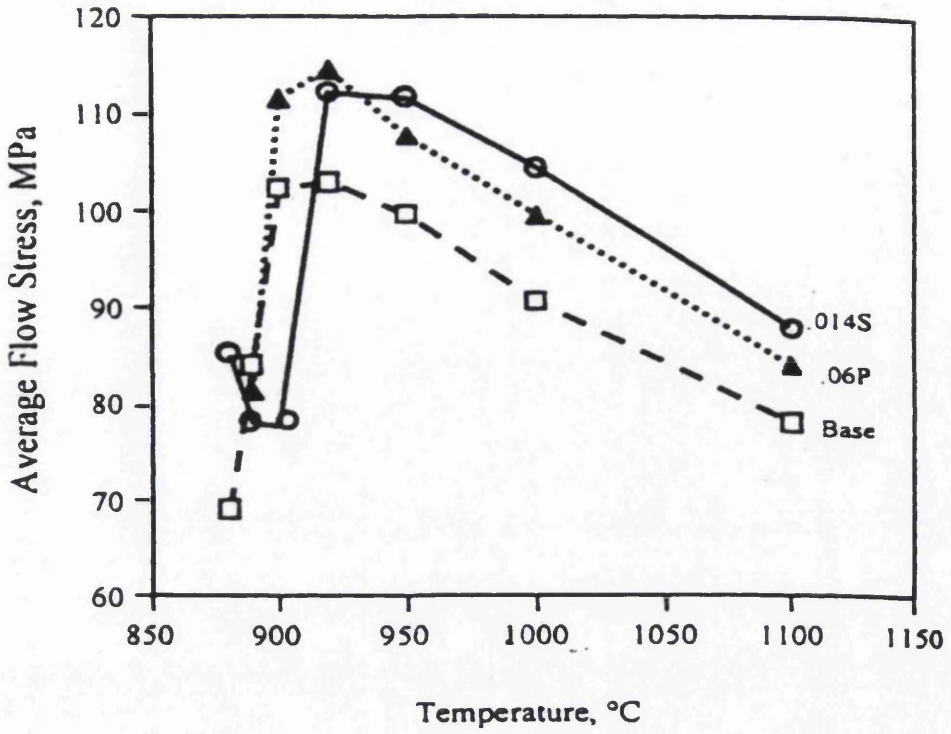


Figure 3.15: Comparison of Flow Stress vs. Temperature for Base IF grade, P and S alloyed IF Steels [26].

According to recent studies [26] [47] [48], P not only is found at grain boundaries and in the matrix but also exist as FeTiP precipitates. It is acknowledged that [48 - 51], that the presence of FeTiP leads to weakening of drawability and loss of strength. This effect is more marked in the case of batch-annealed rather than continuous-annealed HS-IF steels, due to the long soaking times allowing sufficient time for this unwanted precipitation [50]. Figure 3.16 shows the presence of FeTiP precipitates in a Ti stabilised HS-IF steel [51]. FeTiP has been reported to have better stability than TiC at the batch annealing temperature [52]. The consumption of Ti, results in the reduction of stabilizing elements in HS-IF steel to precipitate with C and N. The remaining C and N in the matrix have a direct effect on the development of the {111} recrystallisation texture [51].

FeTiP precipitates may obstruct the growth of {111} favourable recrystallisation texture, and adversely influence the r-value of the HS-IF steels, thus lowering the drawability of the steel. Although P is an efficient strengthening and inexpensive element, when added in an excess amount could cause large volume fractions of FeTiP precipitates to form which are harmful to the drawability and result in loss of strength.

P is an inexpensive element for solid solution hardening and hence it a useful element to increase steel strength. It should be added in an amount more than 0.03wt% for strengthening. Therefore, according to a recent study, the upper limit of the amount of P should be 0.20wt%, preferably between 0.10 -0.15wt% [52].

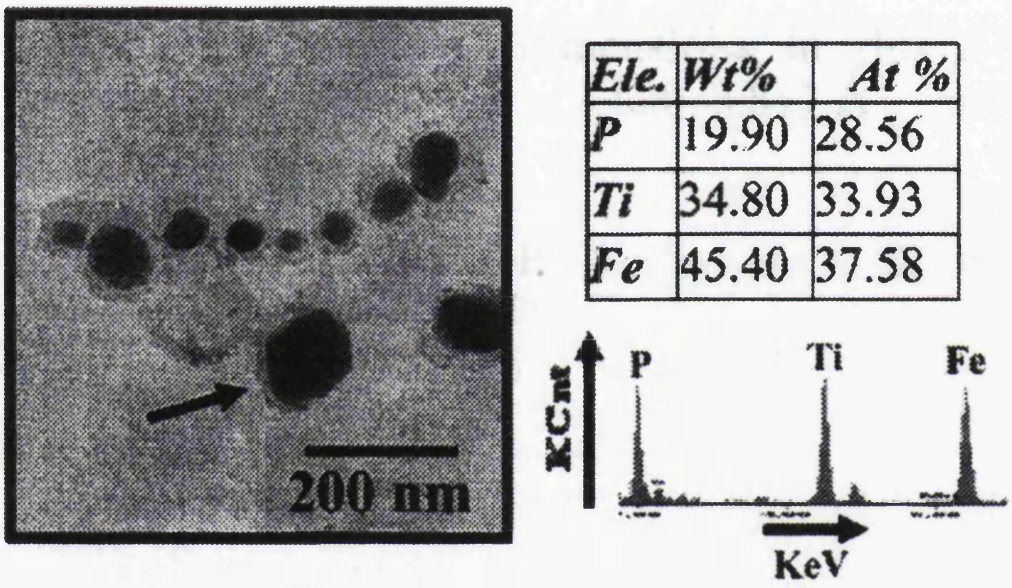


Figure 3.16: TEM micrograph of FeTiP precipitate found in Ti-IFHS steel annealed at 700°C for 60min with EDS analysis [51].

### 3.4.8 Manganese

Solid solution hardening is a widely used strengthening mechanism for high strength steels. Numerous studies have indicated that [53-55], Mn is an important microalloying element to provide sufficient level of solid solution strengthening. It is one of the hardening element which is normally added in the levels higher than 0.60wt% to HS-IF steel grades in order to achieve strengthening. Mn has a moderate solid solution strengthening effect in austenite and marked hardening effect in ferrite, as the solubility of Mn in ferrite is 10wt% higher than in austenite [12]. The amount of Mn addition in HS-IF steel is typically limited to 2wt% to prevent segregation problem [54].

Mn is an austenite stabilizing element, which implies that Mn additions could retard and lower the temperature of austenite transformation, and this retardation promotes the hardening effect in steels. By lowering the austenite heat treatment temperature during transformation to ferrite, Mn can help to promote the ferritic grain refinement in order to get finer grain size. Steels with Mn additions will be stiffer during rolling and forging, since Mn increases the strength of steels [56].

In HS-IF steels, Mn may be present as oxides (MnO), sulfides (MnS) and oxysulfides ($2MnO.SiO_2$) [56]. Mn has a high affinity to oxygen and sulphur, and this characteristic could be used for deoxidisation and desulphurisation in steels. The affinity of Mn for sulphur to form MnS, implies that the presence of MnS in steel could counteract the embrittlement in HS-IF steels. Moreover, it has been reported [57] that, steel samples containing MnS exhibit no much significant change in hardness. With the introduction of some impurities i.e. $Al_2O_3$, $SiO_2$, MnO, CaO, CaS and FeS into steel samples containing MnS, it have been reported [55] an increase in both hardness and nominal yield strength. The affinity of Mn for oxygen could give rise to a favorable diffusion of Mn to precipitates and the formation of MnO towards the outer surface in order to reduce the thin layer of iron oxides, which means increased ability of steel to prevent corrosion [55].

### 3.4.9 Silicon

The purpose of silicon additions in HS-IF steels is similar to that of manganese additions, i.e. used as a strengthening element through solid solution strengthening, Si is also used as a deoxidizer. The precipitates of $SiO_2$ can also strengthen IF steels, however, strengthening with silicon has been found to be responsible for a reduction in formability. High silicon contents result in lowering of the ductility and could cause steels to becoming brittle [12].

Additions of Si could also improve the oxidation resistance with the formation of silicon dioxides ($SiO_2$). Even if Si is a stronger in oxygen stabilization than Mn, when Si and Mn are used together singly or in combination (silicomanganese) the effect would be much higher. The reason is that the joint deoxidation product of Si and Mn would be a manganese silicate that has a lower activity in silicon less than silica were to be the only product forming [58].

### 3.4.10 Aluminum

Aluminum is normally added to HS-IF steel for deoxidization and grain refinement purposes. Al is a very strong deoxidizer, and it is added to the steel during steelmaking. The formation of skeletal like alumina crystals ($Al_2O_3$), which are removed from steel by flotation or by reaction with slag could create an oxygen free clean steel [59]. The main problem during steelmaking is that the density of Al is very low, which could cause oxidisation at the steel interface when added in large amounts to the steel bath, resulting in quick oxidisation at the steel interface.

It has been reported that, precipitation of AlN which typically could take place during recrystallisation could obstruct the selective nucleation of preferred orientations i.e. {111} and finer grain growth, leading to an unfavourable texture [60]. In order to obtain good formability, it is necessary to reduce the concentration of AlN in the solid solution. Promoting formation of TiN which is more stable than AlN is one of the best way to do. However, addition of Al should be kept to a minimum.

## 3.5 Grain Refinement

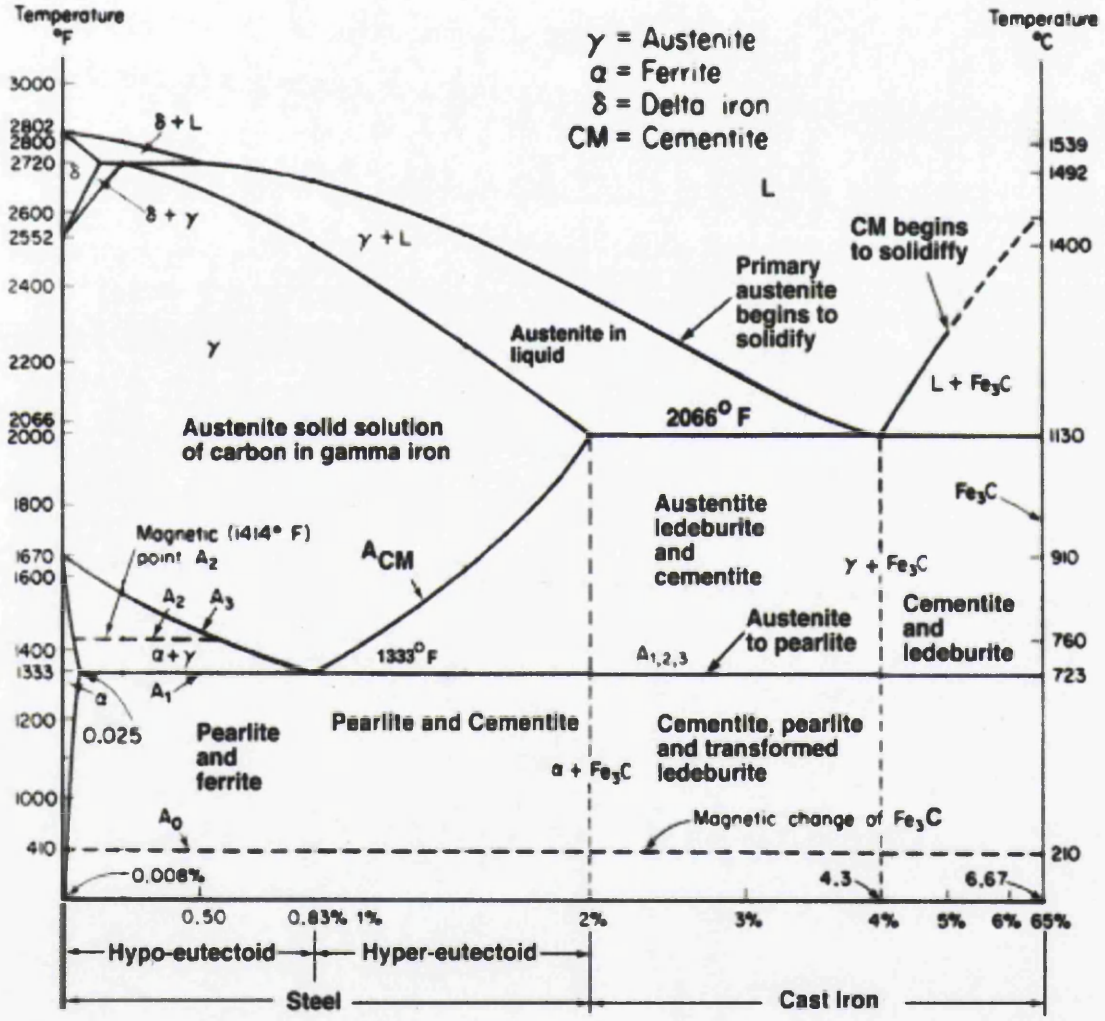


Figure 3.17: Metastable Fe-$Fe_3C$ Phase Diagram. [74]

The microstructure of HS-IF steels is typically ferritic. This can be seen in figure 3.17 where the Fe-$Fe_3C$ phase diagram is provided. In the early 1950s, Hall [61] and Petch [62] have set the groundwork for modern steel metallurgy. The creation of the Hall-Petch equation is perhaps the most important development in ferrous metallurgy, this relationship is given as:

$$\sigma_y = \sigma_i + k_y d^{-1/2} \qquad \text{Equation 2.2 [61-62]}$$

Where $\sigma_y$ is the yield strength, $\sigma_i$ is the frictional stress which opposes dislocation movement, $k_y$ is a constant which is normally called the dislocation locking term and d is the ferrite grain size. According to the equation, the outcome of the refinement of the ferrite grain size is an increase in yield strength. The relationship between ferrite grain size and yield strength is shown in figure 3.18 [63].

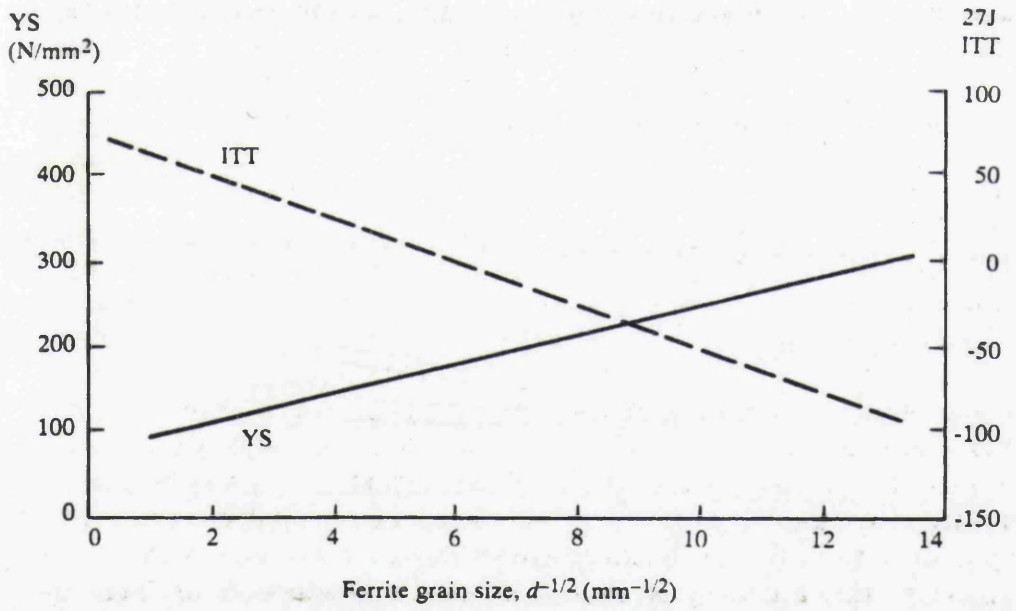


Figure 3.18: Influence of ferrite grain size on yield strength and impact properties [63].

Typically, the strengthening effect in steels is proportional to the decrease in toughness, but the refinement of ferrite grain size also produces a concurrent enhancement in toughness [63]. The Petch equation links the grain size with toughness, the equation is as follows:

$$\beta T = In\beta - In\mathrm{C} - In\, d^{1/2} \qquad \text{Equation 2.3 [63]}$$

Where $\beta$ = constant

C = constant

$T$ = ductile-brittle transition temperate (°C)

$d$ = ferrite grain size ($\mu m^2$)

As shown from the Petch equation, the reduction of ferrite grain size produces a decrease in the impact transition temperature [63]. Therefore, grain size refinement is one of the best options to increasing the toughness of a steel. Due to grain refinement increases in yield strength are noted, and these lead to lower n-value and r-value. The lowering of n-values and r-values result in a decrease of formability, which is an intrinsic drawback in IF steels.

### 3.5.1 Grain-Refined HS-IF Steels

HS-IF steels are developed as the basis of interstitial free steel and strengthened by microalloying elements like silicon, manganese and phosphorus. Strengthening by microalloying elements is subject to secondary work embrittlement, due to lack of grain boundary strength [64]. Grain refinement is an effective method to improve the resistant of secondary work embrittlement, as the finer grain can increases the strength of grain

boundaries. As mentioned previously, the decrease in formability by grain refinement is an unfortunate drawback of HS-IF steels. The balancing and combination of grain refinement, precipitation hardening and microalloying hardening is a methodology reported in recent studies to locate the optimum solution for HS-IF steels.

In HS-IF grades steels, solid-solution hardening, grain-refinement and precipitation hardening are three main strengthening method. In conventional IF steel, a larger grain size is favorable for the mean r-value which was proven by the Petch equation and this could lead to a preferable growth of the <111> texture in order to achieve excellent formability. However, in the case of HS-IF steels, coarse grains are not suitable for the surface quality of exposure panel in car-body and grain refinement is a good method to improving the surface quality [22].

On the other hand, the carbon content in HS-IF is much higher than that of the conventional IF steels. As a result, larger amounts of solid-solution hardening elements are needed to precipitate carbon in HS-IF steels. By promoting the fine precipitates and increasing tensile strength through both grain refinement and precipitation hardening, a reduction of the amounts of solid solution hardening elements is expected to take place. For example, in figure 3.19, the grain refined HS-IF steel (b) with fine precipitates of carbo-nitrides has replaced and reduced the total amount of solid-solution hardening elements (i.e. Si, Mn and P) compared to the coarse-grain HS-IF steel, even if the grain-refined IF HS steel and coarse-grain HS-IF steel have similar tensile strengths [22].

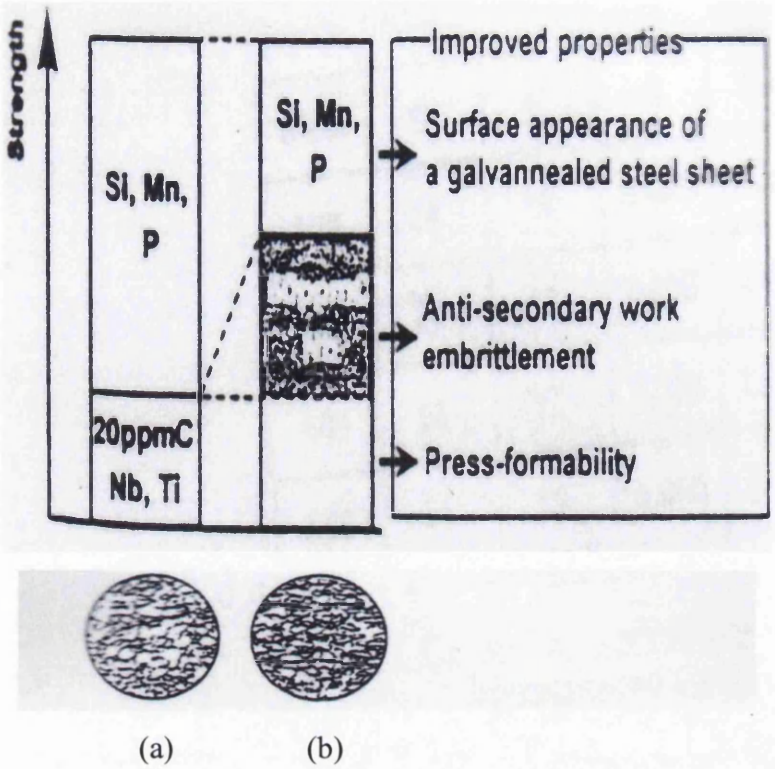


(a) (b)

Figure 3.19: Comparison of Grain-Refined HS-IF steel and Coarse-Grain HS-IF Steel in Strength, (a) Coarse Grain HS-IF Steel, (b) Grain-Refined IF_HS Steel [22].

Even though, it has been reported by Hall and Petch that the outcome of grain refinement is an increase in yield strength which could lower the formability, it is has also been reported [22] that in the case of grain-refined HS-IF steels, the grain-refined HS-IF steels exhibit lower yield strengths than the solid-solution hardened HS-IF steel which have coarser grains. The result is shows in figure 3.20

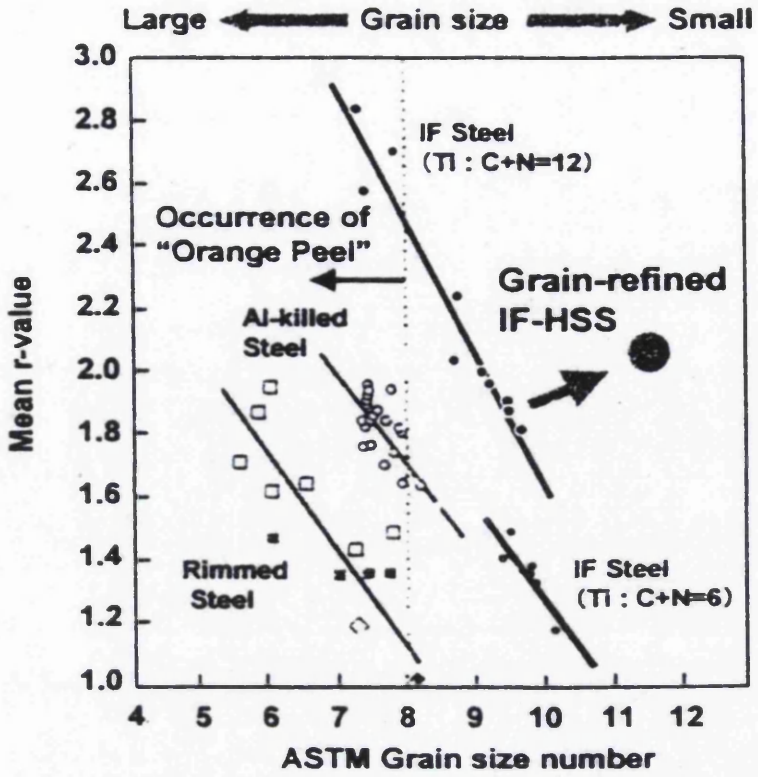


Figure 3.20: Grain Size vs. Mean r-value for Several Grades of Steels

## 3.6 Formability

Formability is defined as the ability of metal to maintain its structural integrity while being plastically deformed into various shapes [65]. The performance of a metal in a formability test is normally measured by two concepts, which are stretchability and drawability. Stretchability and drawability are measurements of the ability of metal to be stretched and drawn to form shapes without any splitting or local necking. When a sheet steel is stationary clamped around its edges and stretched over a die or a formed block, this defines the stretching process. Drawing is a process where a blank sheet steel is pressed into a die cavity by using a punch while deep drawing is a drawing process which the depth of the part is greater than its diameter [66].

The parameter that normally measures the stretchability is called the work hardening coefficient (n value). High n value steels are characterised by low yield strength and high work hardening rate, and these represent properties good stretch forming characteristics. In steels, stretch forming grades are mainly those of the advanced high strength steel family (example: DP and TRIP steels) what are used to manufacture parts that high strength and reasonably formability are required, like aircraft wings, automotive door and window panels.

The parameter which is widely accepted as an indictor of the drawability is the plastic strain ratio or normally called as r-value. High r-value materials have the ability to form into complicated shapes. The r value is defined as the ratio of the true strain in the width direction to the true thickness strain which is usually 15 or 20% in the uniform elongation region of a tensile test; this can be written as a function [67]:

$r = \epsilon_w / \epsilon_t$ [68] Equation 2.4 [68]

Where $r$ = r value

$\epsilon_w$ = True width strain

$\epsilon_t$ = True thickness strain as measured in a tensile specimen

As shown in figure 3.21, IF and HS-IF steels have excellent r values, which means they are suitable for deep drawing applications.

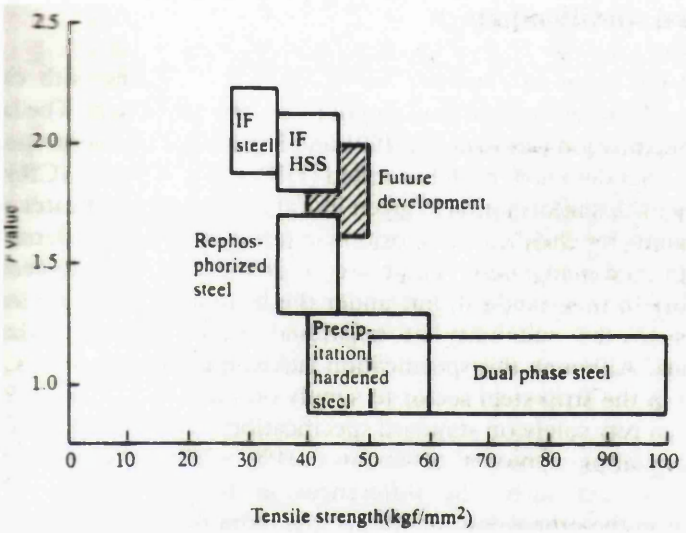


Figure 3.21: Comparison of r value for several grades for steels [68].

# Chapter 4

## EXPERIMENTAL PROCEDURES

Two experimental HS-IF steels grades were designed and used for the present study, which were a titanium only stabilised HS-IF grades and titanium-vanadium stabilised HS-IF grades. These steels were prepared using pure raw materials to control the level of unwanted alloying additions to a minimum. The composition of the experimental HS-IF steels is presented in table 4.1. Both HS-IF steels are based on controlled additions of carbon (42 – 43ppm), sulphur (50ppm), titanium (190 – 220ppm), silicon (50 – 160ppm), vanadium (up to 1000ppm) and trace amounts of niobium (10ppm). Sample designated for the experiments were provided as 35mm thick hot rolled blocks.

Table 4.1: Chemical Composition of Experimental HS-IF steels (wt%)

| Element / Steel code | 1348 (Ti) | 1349 (Ti-V) |
|---|---|---|
| C | 0.0043 | 0.0042 |
| Si | <0.005 | 0.016 |
| Mn | 0.63 | 0.60 |
| S | 0.005 | 0.005 |
| P | 0.007 | 0.011 |
| Ti | 0.022 | 0.019 |
| Nb | <0.001 | <0.001 |
| V | <0.001 | 0.10 |
| $Al_{met}$ | 0.003 | 0.010 |
| $Al_{tot}$ | 0.004 | 0.007 |
| N | 0.0035 | 0.0032 |

## 4.1 Thermomechanical Processing

For the present study, the Gleeble unit was used to simulate (physically) the thermomechanical processing of experimental HS-IF steels. The Gleeble machine is a state of the art unit for physical simulation as it is able to simultaneously simulate the thermal and mechanical processes [73]. Some of the processes that can be simulated using the Gleeble system include [72]:

1. Heat treatment
2. Hot rolling
3. Sintering
4. Continuous casting

5. Powder metallurgy
6. Upset butt welding
7. Diffusion bonding
8. Strip annealing
9. Continuous strip
10. Extrusion
11. Forging

The simulation process that is done by Gleeble systems is the reproduction of the thermal and mechanical condition of the process in the same time frames which exists under actual mill condition [72].

### 4.1.1 Grain Growth


Figure 4.1: Gleeble 3500 System located in the Materials Research Centre, Swansea University.

The Gleeble 3500 thermo-mechanical unit which is located in the Materials Research Centre, Swansea University (shown in figure 4.1) was used to study the thermo-mechanical testing of the two experimental steels. The soaking temperatures were chosen at 1200°C which is firmly in the austenite region. The heating rate is 5°C/s from room temperature to the soaking temperature. The holding time for each process is 300s at the soaking temperature. These processes were run under a partial vacuum atmosphere to avoid any significant decarburisation caused to the experimental low carbon steels. Each

heat treatment is concluded with quenching via a water spray. The complete set of reheating experiments was designed to dissolve the majority of the precipitates present in the experimental steels upon soaking and determine the size of precipitates, controlling austenite grain growth and distribution of precipitates, upon the deformation temperature applied and cooling rates chosen.

### 4.1.2 Hot Rolling Studies

The experimental hot rolled steels which were a Ti stabilised HS-IF and a Ti-V stabilised HS-IF steels (as received condition) were machined into a number of suitable cylindrical samples and prepared for experiments. Each cylindrical sample is 10mm in diameter, and 15mm in height as shown in figure 4.2. The thermocouples were then spot welded in to the mid section of the samples. The thermocouples are used to detect the temperature of the sample and send a signal to the computer in order to control the heating and cooling rate of the samples.

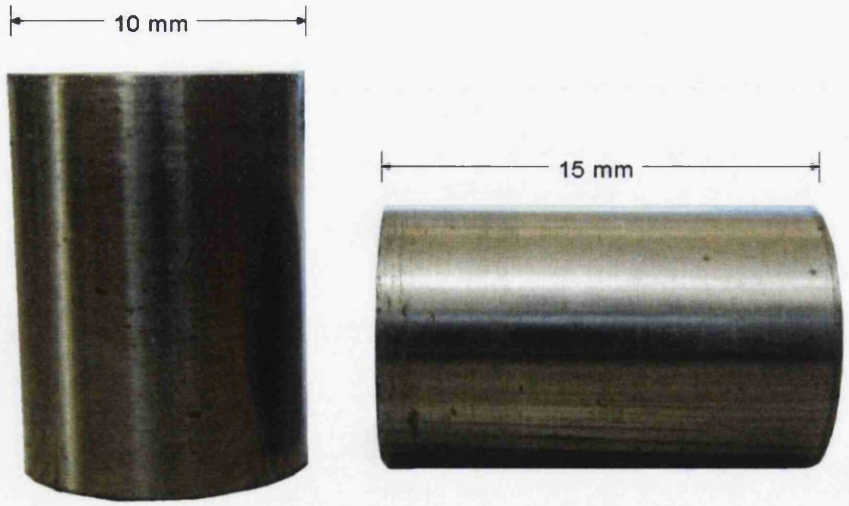


Figure 4.2: Samples in as received condition.

The prepared samples were located between two ISO-T anvils while some compression was applied; the assembled sample is shown in figure 4.3. The thermomechanical (hot rolling process) test parameters such as cooling rates, heating rates and varying finishing and coiling temperature were designed according to the metastable Fe-$Fe_3C$ phase diagram as shown in figure 3.17. The variation of thermomechanical cycles was input preset in the QuikSim Software and saved in the computer before each process started to run. The two experimental steels experienced the same conditions of thermo-mechanical processing which included soaking, controlled multi-pass deformation, controlled cooling to a variety of coiling temperatures and water quenching (water spraying) to room temperature.

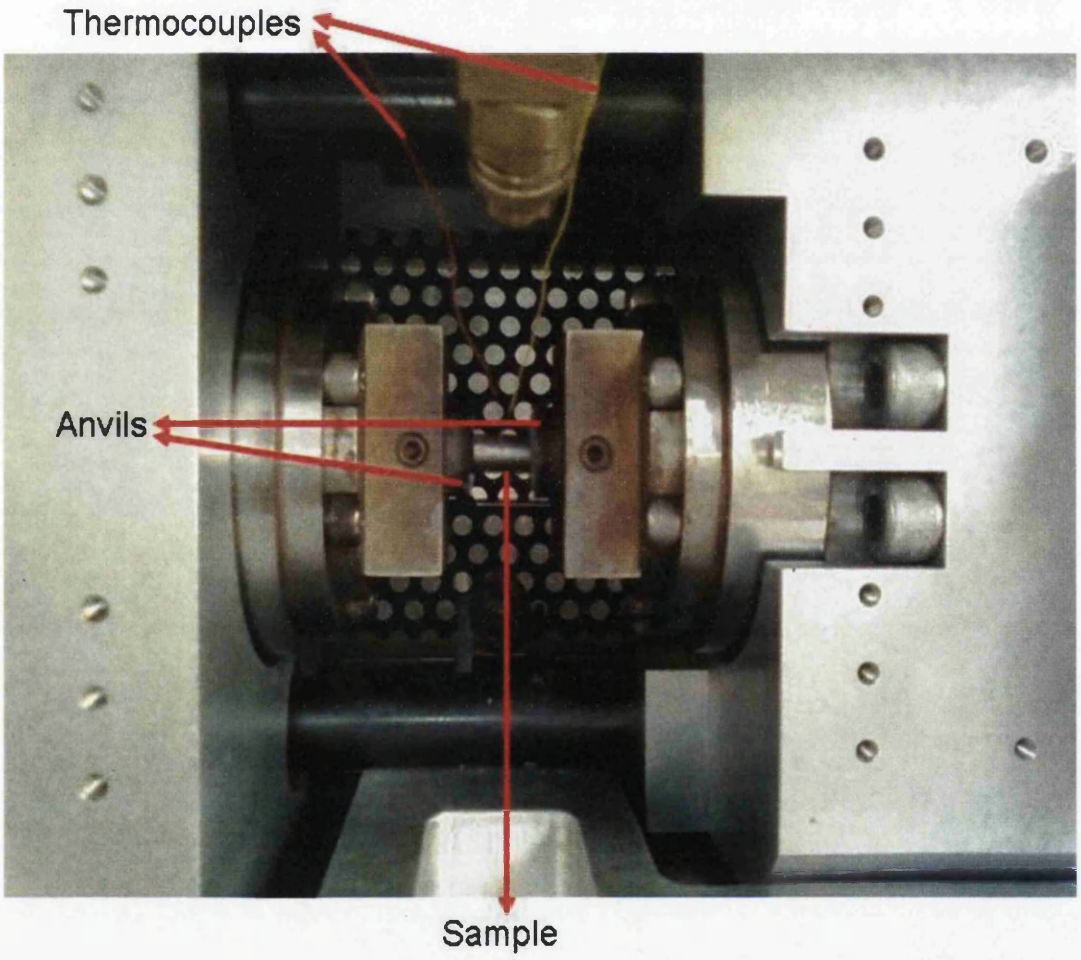


Figure 4.3: Assembled samples in the Gleeble 3500 system.

The samples were heated to the peak soaking temperature which was set at 1200°C with a heating rate of 5°C/s, in order to dissolve most precipitates that are present in the steel microstructure; the samples were kept at the peak soaking temperature for 300s. After the holding time was completed, the samples were cooled to a roughing temperature (1100°C) with a controlled cooling rate of 10°C/s. Once the temperature has reached 1100°C, samples were compressed at 0.3 true strain using a strain rate of 1/s.

After the compression, the samples were controlled cooled at 10°C/s again to a finishing temperature, the finishing temperatures studied were 950, 850 or 800°C. The samples were subjected to further deformation at a 2 x 0.2 true strains via is a double hit compression experiment, employing a strain rate of 1/s and an inter-pass time of 1s between hits.

Coiling temperature is the temperature that the sheet steel coiled and stored which ready to supply to the demanders. The samples were coiled in a variety of temperatures of 750, 650, 550 or 450°C at a cooling rate of 10°C/s from the finishing temperature. Once the samples reached the coiling temperature, the samples were directly quenched via a water spray to room temperature. The full thermomechanical cycles of these experiments is clearly shown in figure 4.4.

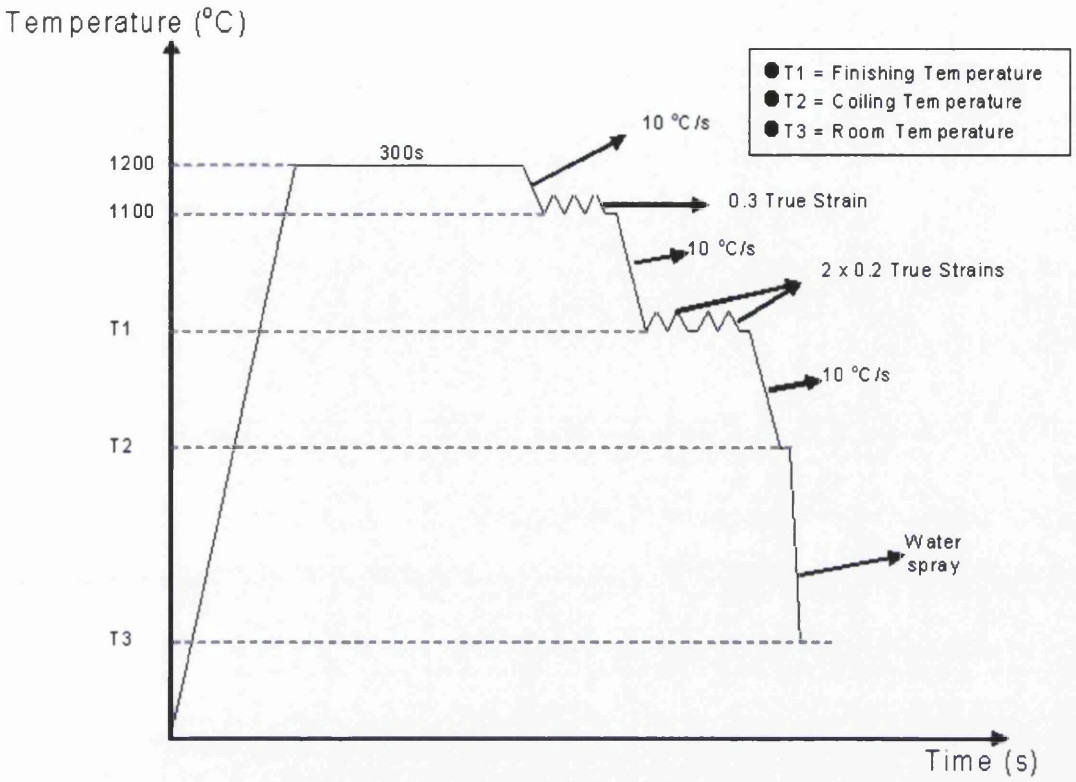


Figure 4.4: Thermomechanical Cycles employed in the Present Study.

## 4.2 Microstructural Examination

The heat treated samples were collected and cut into two sections using the Struers Accutom 50 cutting machine. The finished samples produced with Struers Accutom 50 provide a smooth cut without deformation applied to the cut surface in order to retain unaffected the actual microstructures. Heat treated sample following Gleeble testing are shown in figure 4.5 and a sectioned sample is show in figure 4.6.

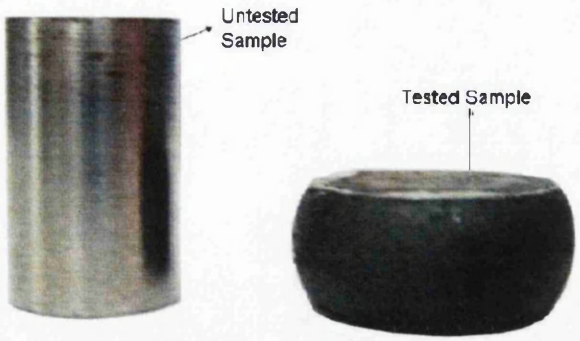


Figure 4.5: Comparison of untested sample and Gleeble tested sample.

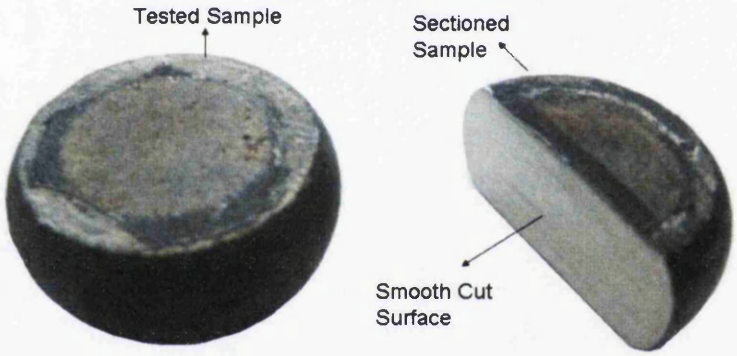


Figure 4.6: Comparison of tested sample and sectioned sample.

Sectioned samples (including the samples in the as received condition) are mounted into castable resins which consist of MetPrep Kleer-Set Type FF resin and MetPrep Kleer-Set Hardener as shown in figure 4.7. Mounted samples were subjected to grinding, starting with 240-, 320-, 600-, and finished with 1200 grit silicon carbide paper and followed by polishing using 6$\mu$m and 1$\mu$m diamond paste impregnated cloths, using paraffin as lubricant during polishing to produce a flat and scratch free surface.

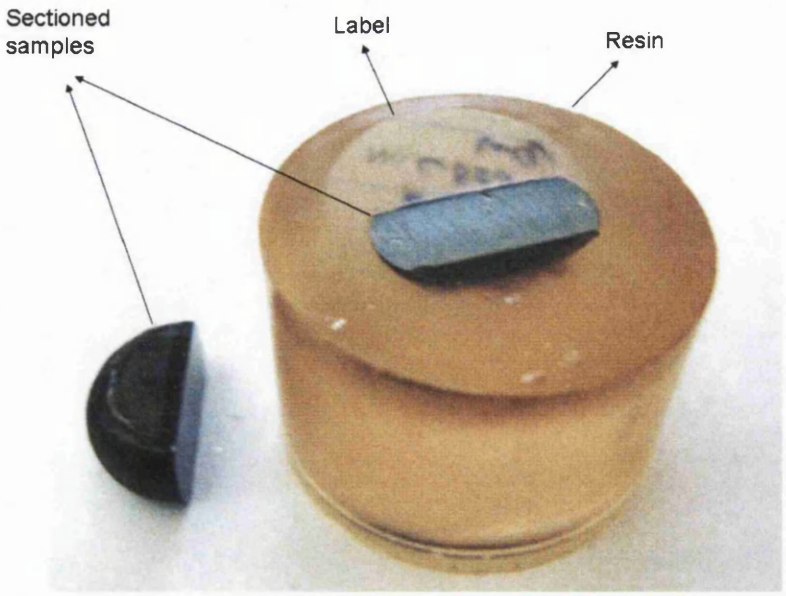


Figure 4.7: Sectioned sample mounted with resin.

Polished samples were etched using Nital solution, by immersing the sample into the solution of 2% nital for around 10s until the surface of samples became slightly cloudy. After etching was completed and dried with the dryer, the samples were studied in terms of microstructures obtained.

### 4.2.1 Scanning Electron Microscopy

Philips XL 30 Scanning electron microscopy (SEM) was used in the present study to observe and classify the obtained microstructures. SEM microscopy was employed, using an accelerating voltage of 20kV with the working distance of 10mm to obtain secondary electron images on all tested samples.

## 4.3 Hardness Test

Following scanning electron microscopy (SEM) examination, samples were subjected to a hardness testing using a Vickers pyramid diamond indenter. A load of 10 kg was used with the impression time of 10 seconds on the surface of steel samples. 18 reading were been taken for each of steel sample tested.

## 4.4 Thermodynamic Calculations

MT-Data was used in present study to predict the dissolution and formation of precipitates particles in Ti only and Ti-V HS-IF steels grades during the hot rolling simulation applied.

MT-Data thermodynamic modeling can be performed via specific software with a range for thermodynamic databases of fundamental thermochemical calculations, for the prediction of phases forming at equilibrium in systems containing a number of components and phases [69]. MTDATA permits calculations of the amount of different phases that are possible to be present under equilibrium conditions and their composition. The equation is defined as the one to minimise the free energy and is given as [70]:

$$Gs = Na\,Ga + Nb\,Gb \ldots \qquad \text{Equation 2.5 [70]}$$

Where Gs = Molar free energy of the system
Ga = Molar free energy of phase a
Gb = Molar free energy of phase b
N = Constant

The free energy of each phase can be written in as a function of its composition and of T and P:

$$Ga = Ga(T, P, xa_1, xa_2 \ldots xa_n) \qquad \text{Equation 2.6 [70]}$$

Where $xa_1, xa_2 \ldots xa_n$ are the weight or mole fraction of each component in phase and T is the temperature and P is phase. in a system with a number of phases and a number of components all phases are consider will dissolve all the components, then the equation of free energy can be written as a function:

$$m*n+2 \text{ variables [70]} \qquad \text{Equation 2.7 [70]}$$

Where m = number of phases
n = number of components

With abovementioned basics, MTDATA is able to calculate and work with many different elements and several phases together, in order to produce predictions and describe the fundamental properties of tested materials in phase diagram [71].

## 4.3 Grain Size Measurement

Grain size measurements have been carried out on the Ti only and Ti-V HS-IF steels for all samples at a finishing temperature of 850°C, using a variety of coiling temperature.

Grain size measurements permit quantification of the effect of coiling temperature on grain the evolution.

# Chapter 5

# Experimental Results

## 5.1 Microstructural Examination

### 5.1.1 As received condition

The effect on microstructure and hardness evolution of two experimental Ti only and Ti-V steels was assessed via the Gleeble 3500 themomechanical simulation unit. Due to the limited size of the samples tensile testing could not be carried out. The parameters that were studied were the choice of the finishing temperature and the choice of the coiling temperature on two experimental HS-IF grades. Figure 5.1 presents the as received microstructure of the Ti only and Ti-V steels. Both micrographs consist purely of coarse ferrite.

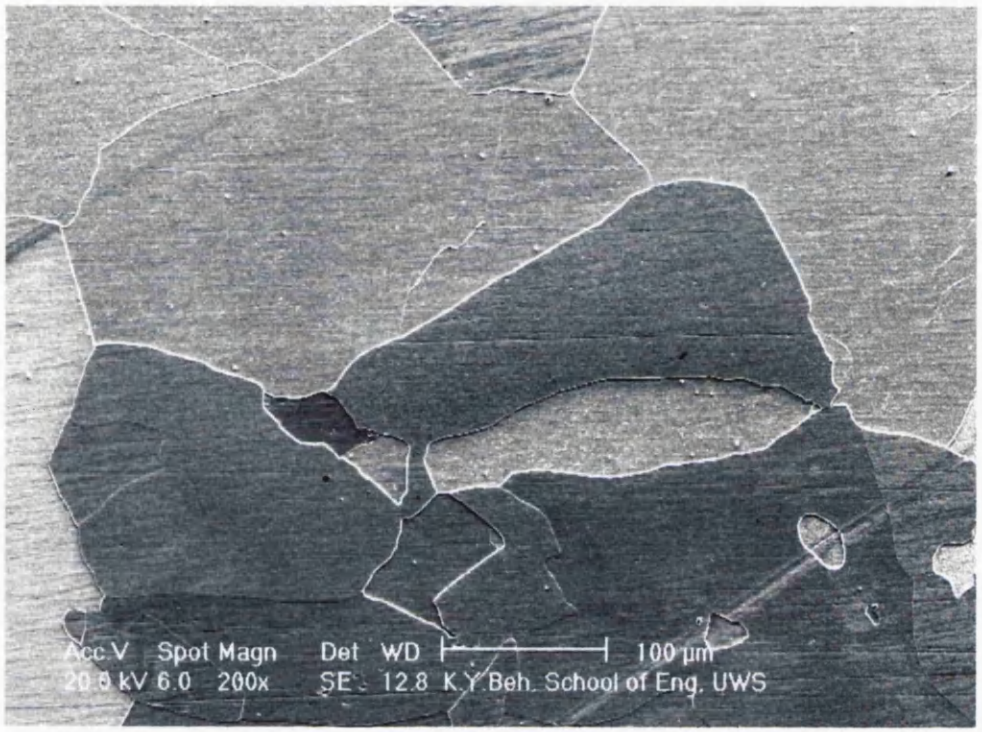


(a)

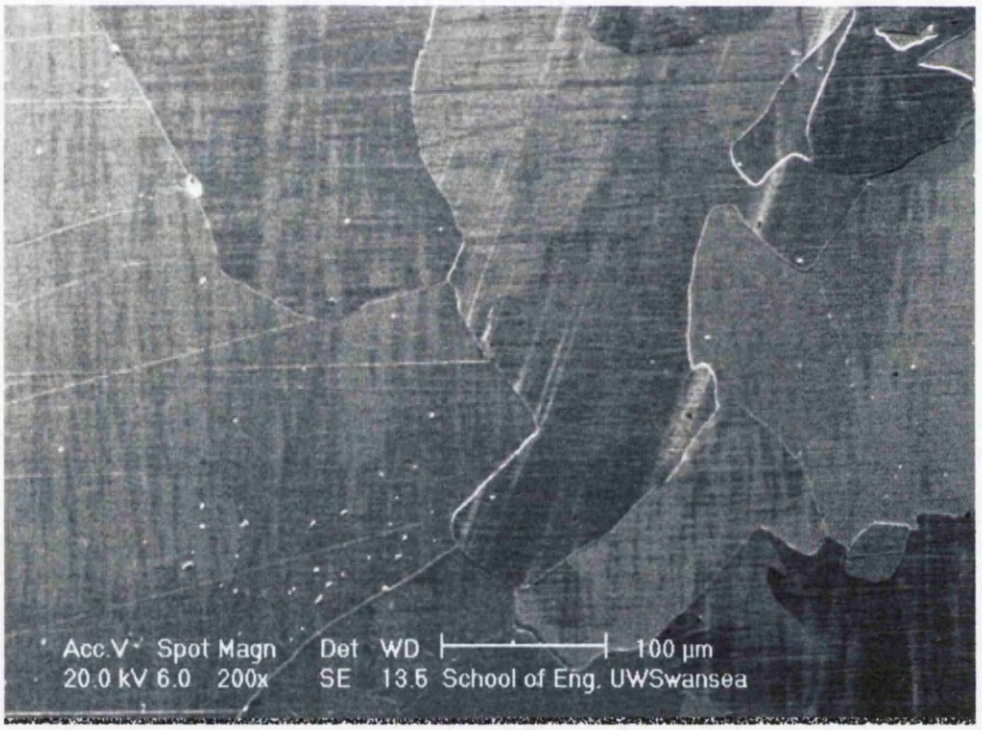


(b)

Figure 5.1: Scanning electron Micrograph of (a) Ti only Steel in the as received condition (b) Ti-V steel in the as received condition.

### 5.1.2 Tested condition

Figure 5.2 shows the scanning electron micrographs representing the evolution of microstructures in relation to varying finishing temperature i.e. 950°C, 850°C or 800°C, followed by cooling at a rate of 10°C/s to a coiling temperature of 750°C in the Ti only HS-IF steel.

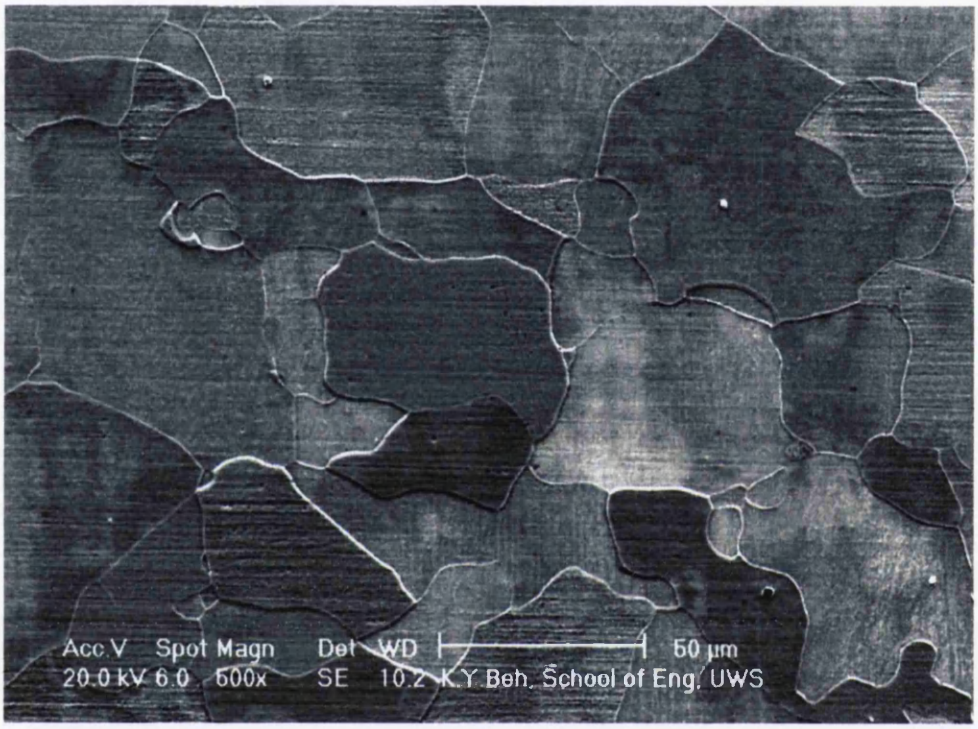


(a)

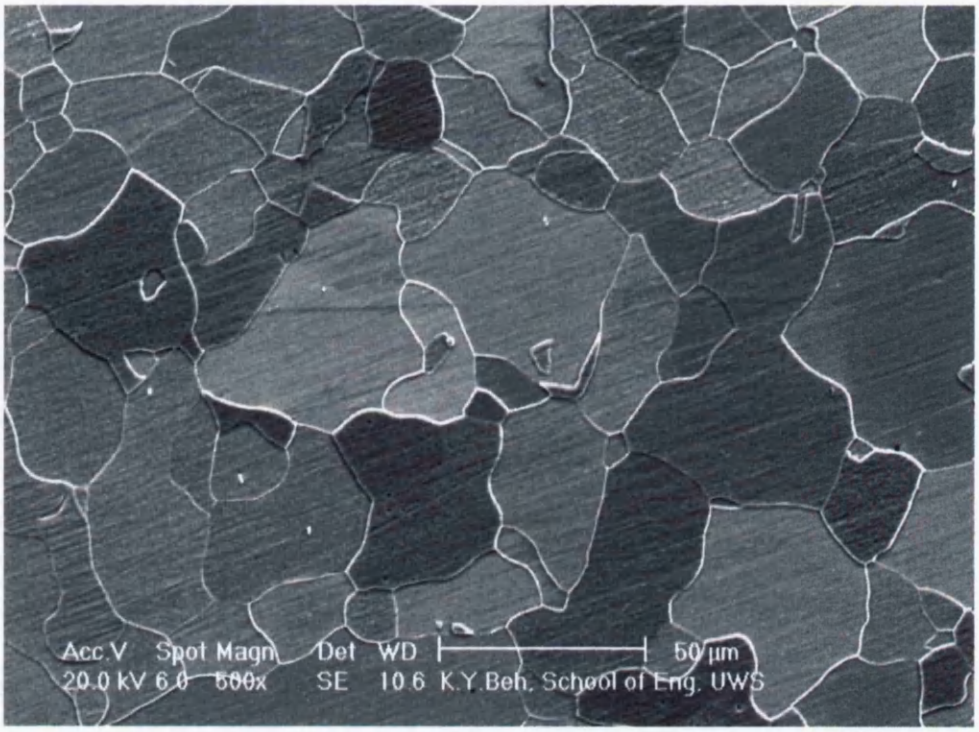


(b)

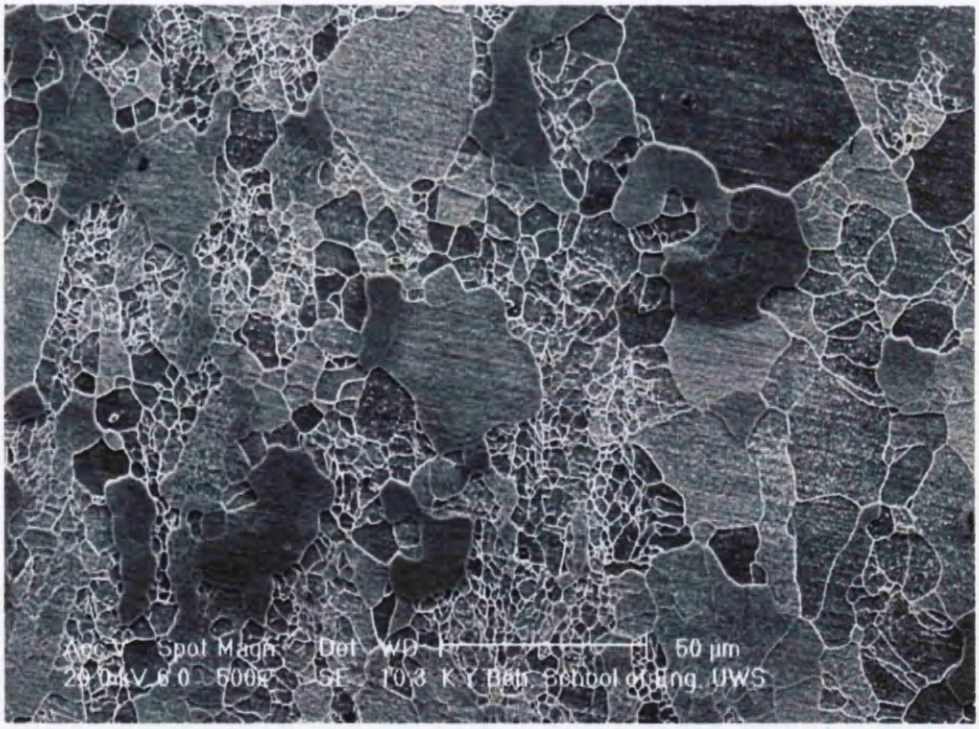


(c)

Figure 5.2: Scanning electron micrographs recorded in the Ti only HS-IF steel employing variable finishing temperatures (a) 950°C, (b) 850°C and (c) 800°C, followed by coiling

at a coiling temperature of 750°C employing a cooling rate of 10°C/s and water quenched from the coiling temperature to room temperature. The arrow indicates the direction of deformation on all three samples.

In figure 5.3a set of micrographs for the Ti-V HS-IF steels are presented, employing variable finishing temperatures of 950°C, 850°C or 800°C, and coiling at temperature of 750°C followed by water quenching to room temperature.

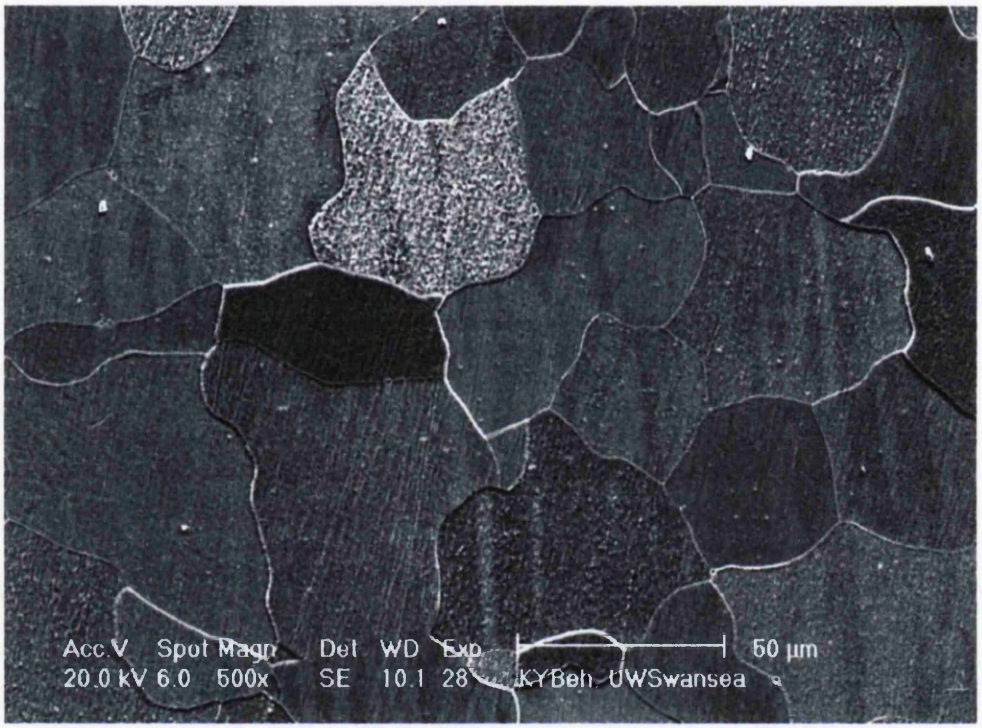


(a)

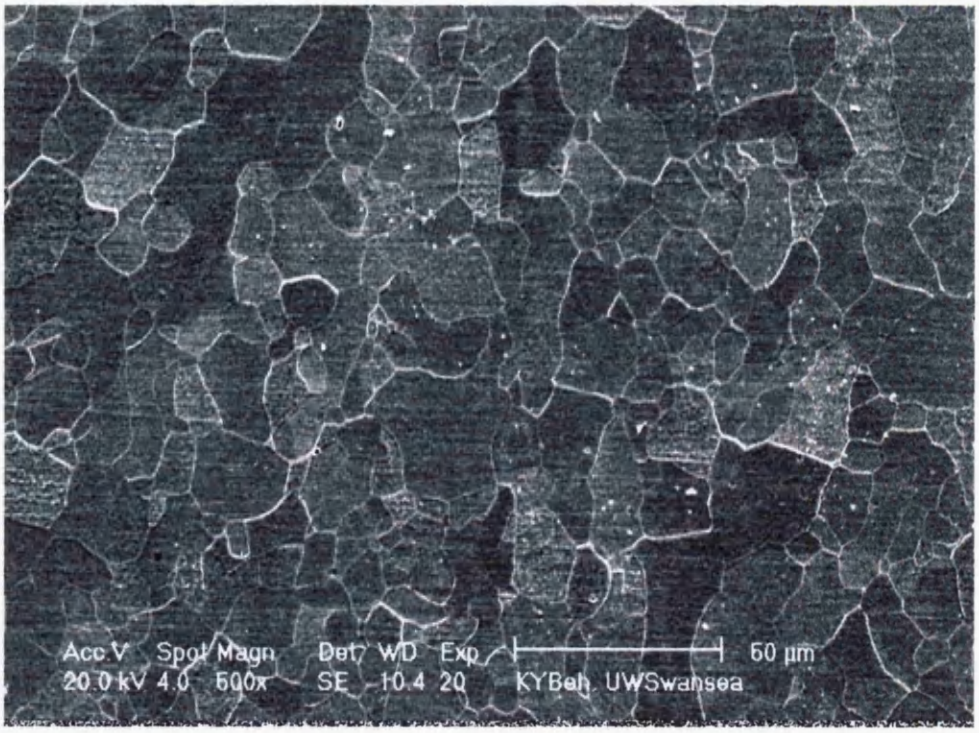


(b)

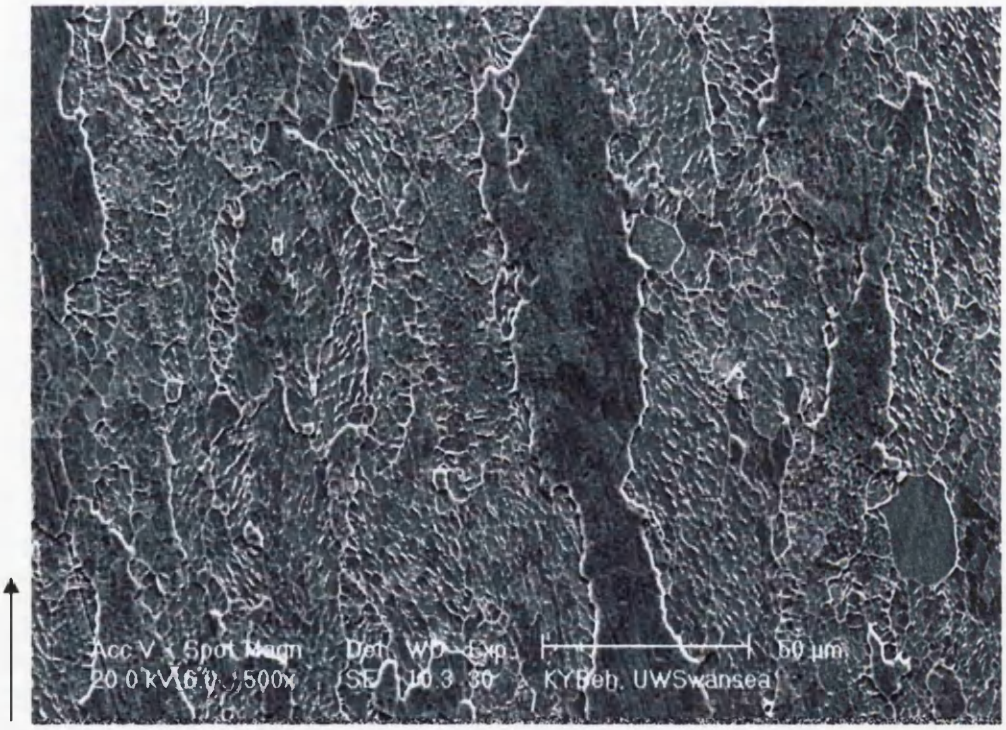


(c)

Figure 5.3: Scanning electron micrographs recorded in the Ti-V HS-IF steel employing variable finishing temperatures (a) 950°C, (b) 850°C and (c) 800°C, followed by coiling

at a coiling temperature of 750°C employing a cooling rate of 10°C/s and water quenched from the coiling temperature to room temperature. The arrow indicates the direction of deformation on all three samples.

With regards to establishing the effect of coiling temperature on the microstructure, several sets of micrographs were obtained on both the Ti only and the Ti-V HS-IF steels. Figure 5.4 presents a set of micrographs on the Ti only steel employing variable finishing temperatures (a) 950°C, (b) 850°C and (c) 800°C, followed by coiling at a temperature of 650°C with the cooling rate of 10°C/s and water quenching to the room temperature. Figure 5.6 and figure 5.8 are the micrographs for the Ti only steel employing the same testing parameters as those in figure 5.12, however, the samples were coiled at 550°C or 450°C. Figure 5.4 present the micrographs for the Ti-V steel employing variable finishing temperatures (a) 950°C, (b) 850°C and (c) 800°C followed by a cooling rate of 10°C/s to a coiling temperature of 650°C and water quenching to room temperature. Figure 5.7 and figure 5.9 employed the same testing parameters as those on the Ti-V steels but involved coiling temperatures of either 550°C or 450°C.

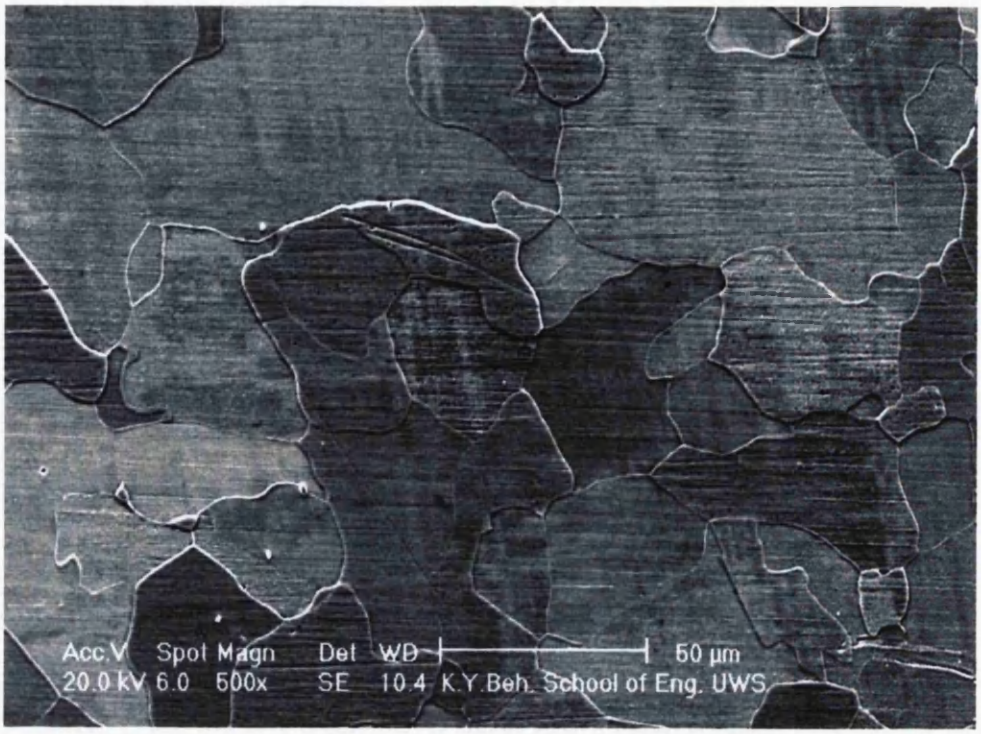
Acc.V Spot Magn Det WD 50 µm
20.0 kV 6.0 500x SE 10.4 K.Y.Beh, School of Eng, UWS

(a)

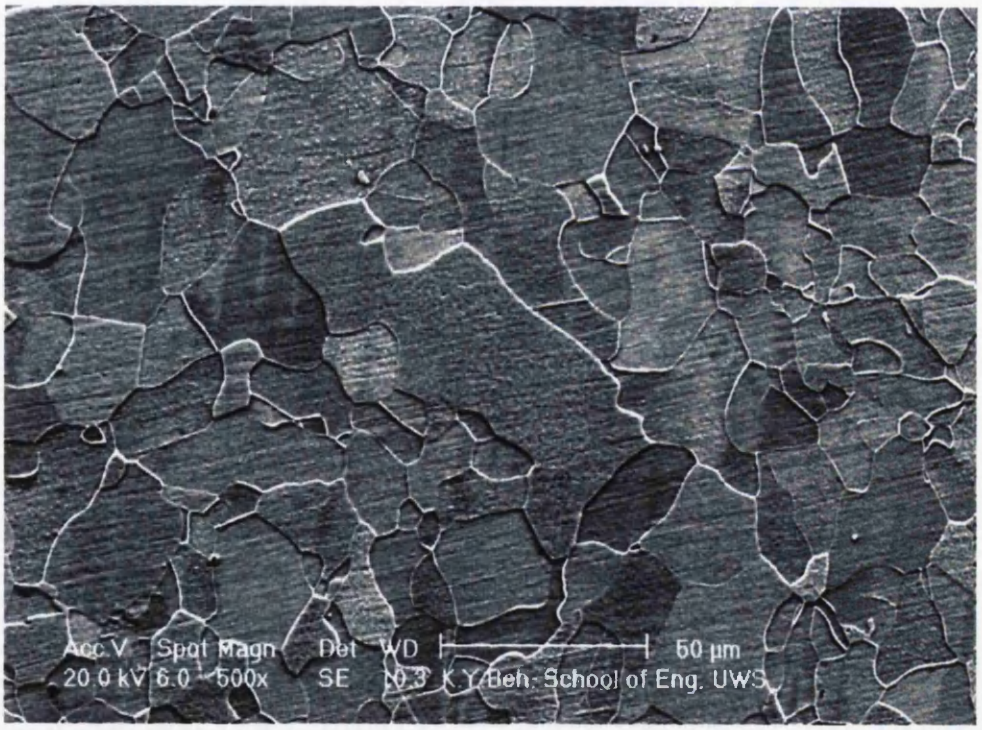
Acc.V Spot Magn Det WD 50 µm
20.0 kV 6.0 500x SE 10.3 K.Y.Beh, School of Eng, UWS

(b)

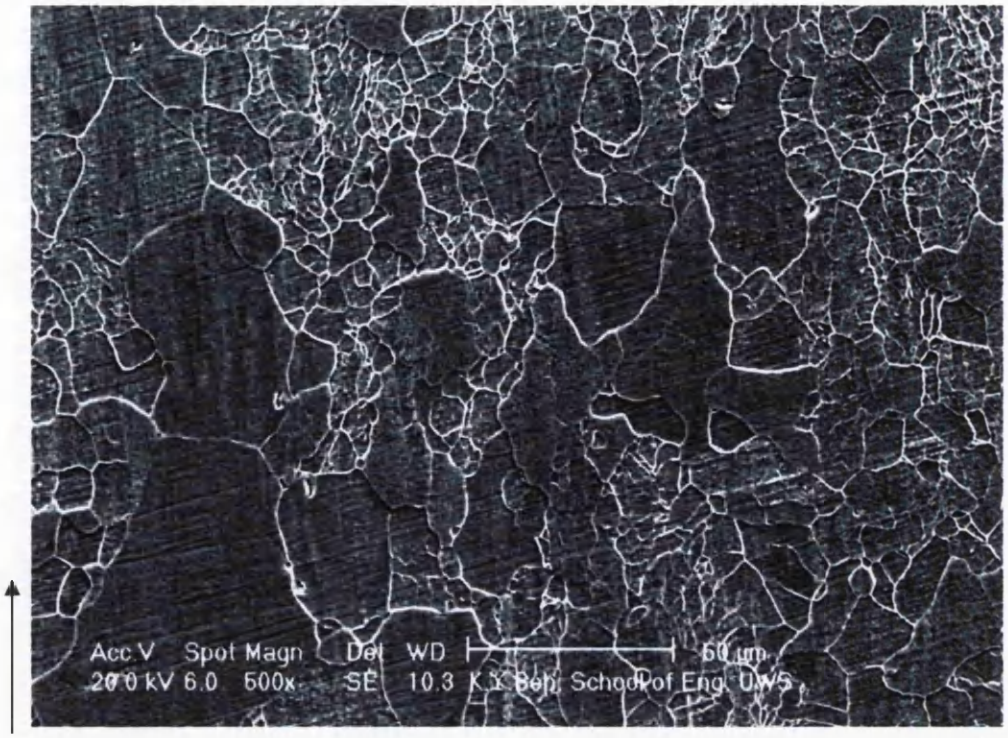


(c)

Figure 5.4: : Scanning electron micrographs recorded in the Ti only HS-IF steel employing variable finishing temperatures (a) 950°C, (b) 850°C and (c) 800°C, followed by coiling at a coiling temperature of 650°C employing a cooling rate of 10°C/s and water quenched from the coiling temperature to room temperature. The arrow indicates the direction of deformation on all three samples.

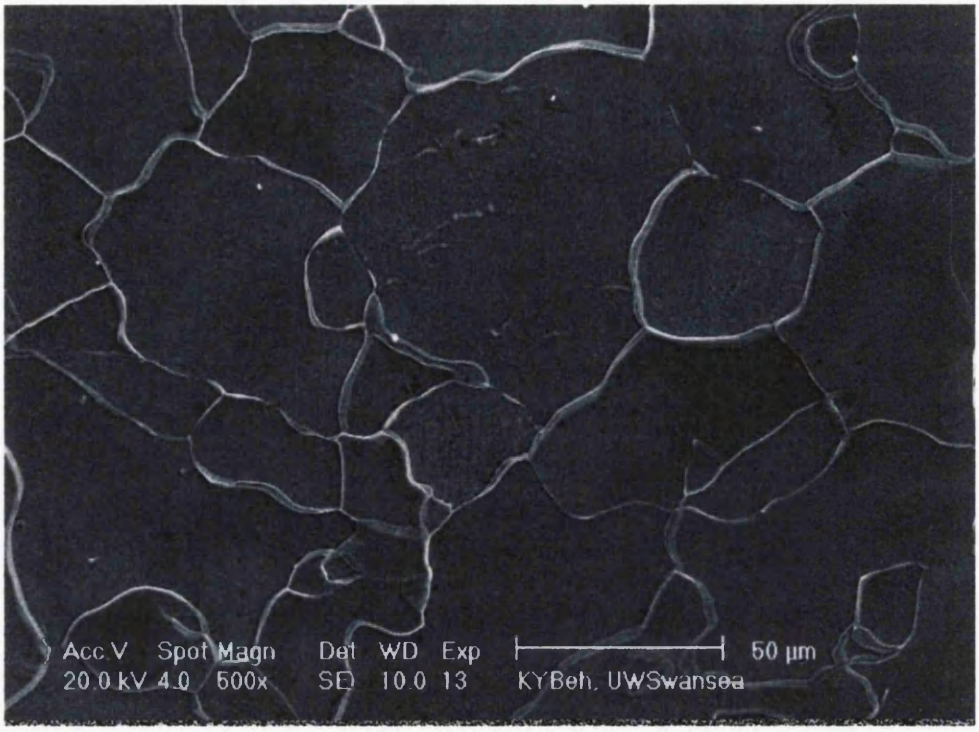
Acc.V Spot Magn Det WD Exp 50 µm
20.0 kV 4.0 500x SE 10.0 13 KYBeh, UWSwansea

(a)

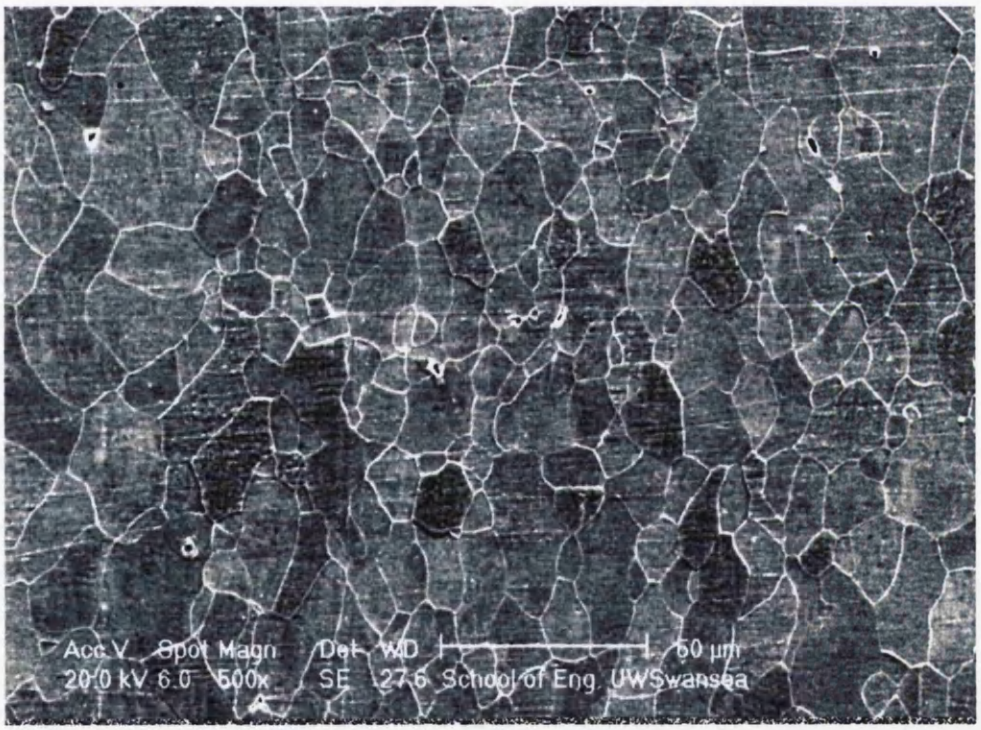
Acc.V Spot Magn Det WD 50 µm
20.0 kV 6.0 500x SE 27.6 School of Eng, UWSwansea

(b)

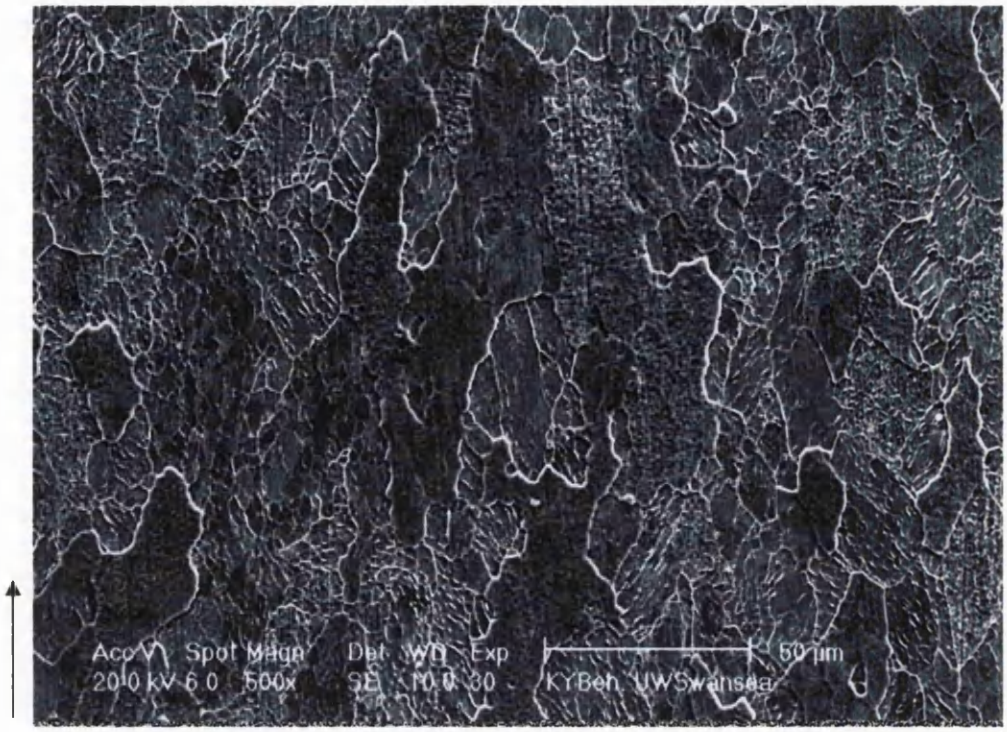


(c)

Figure 5.5: Scanning electron micrographs recorded in the Ti-V HS-IF steel employing variable finishing temperatures (a) 950°C, (b) 850°C and (c) 800°C, followed by coiling at a coiling temperature of 650°C employing a cooling rate of 10°C/s and water quenched from the coiling temperature to room temperature. The arrow indicates the direction of deformation on all three samples.

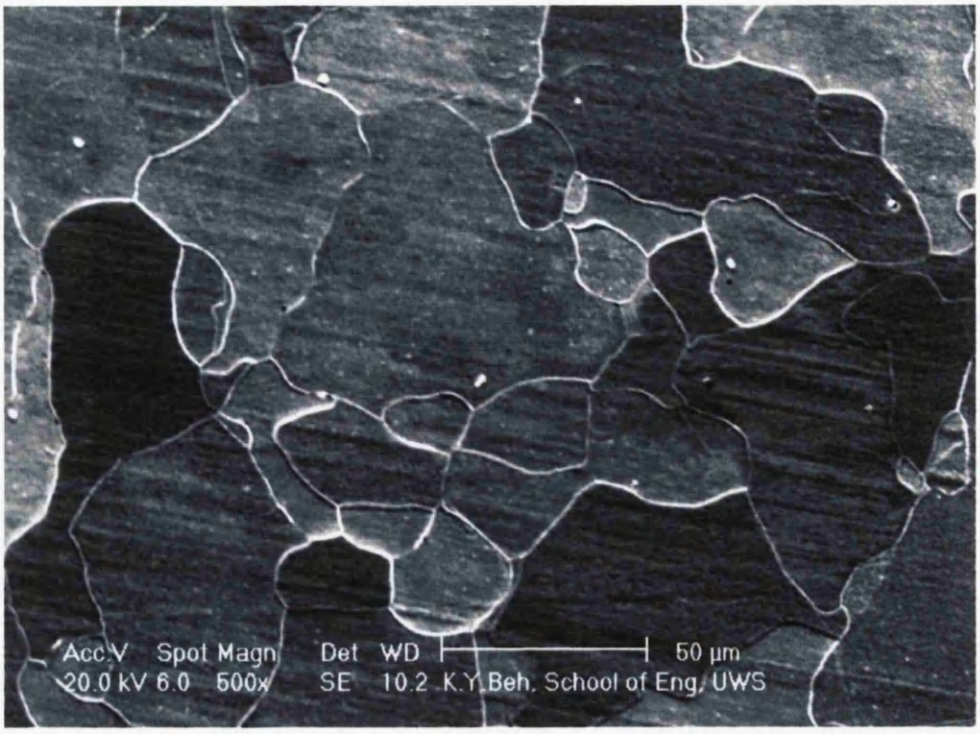
Acc.V Spot Magn Det WD 50 µm
20.0 kV 6.0 500x SE 10.2 K.Y.Beh, School of Eng, UWS

(a)

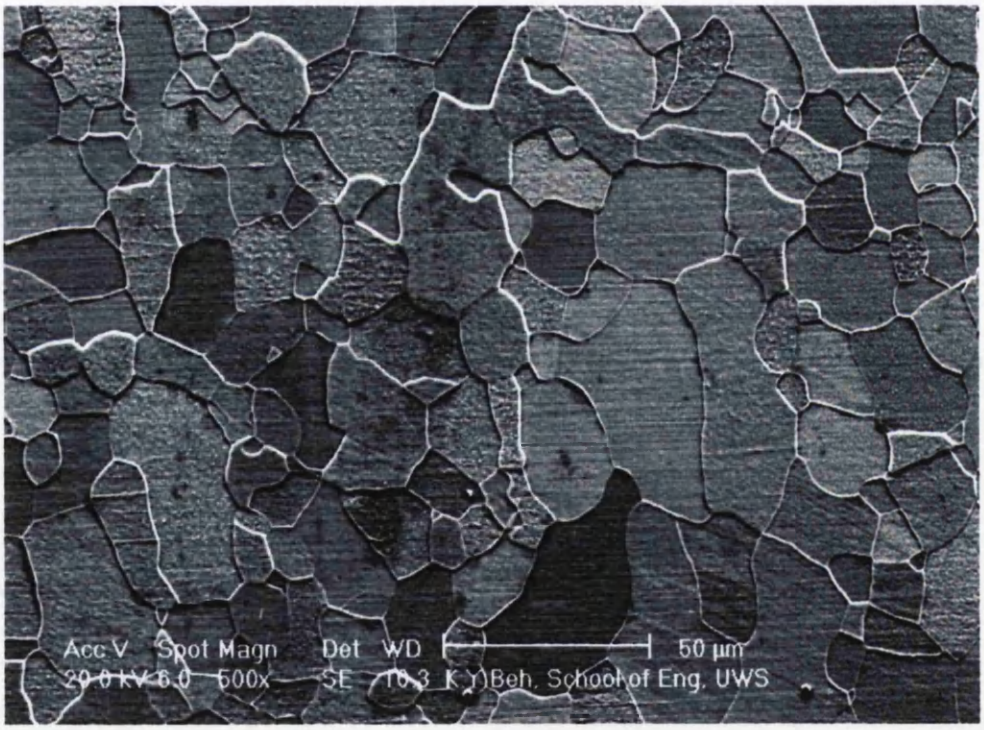
Acc.V Spot Magn Det WD 50 µm
20.0 kV 6.0 500x SE 10.3 K.Y.Beh, School of Eng, UWS

(b)

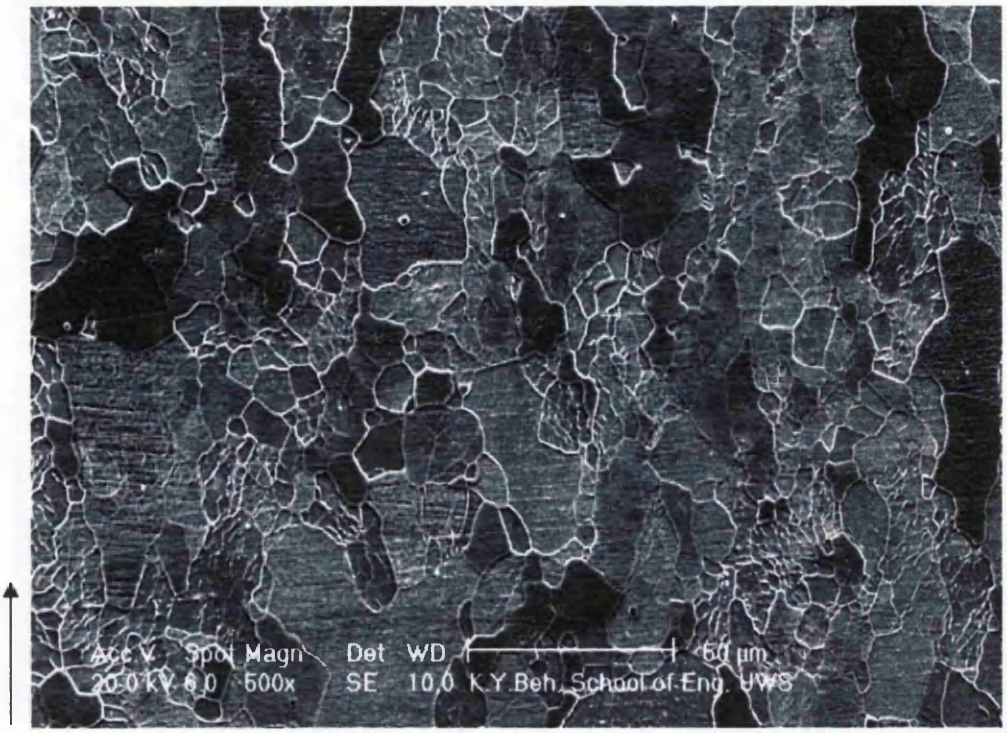


(c)

Figure 5.6: Scanning electron micrographs recorded in the Ti only HS-IF steel employing variable finishing temperatures (a) 950°C, (b) 850°C and (c) 800°C, followed by coiling at a coiling temperature of 550°C employing a cooling rate of 10°C/s and water quenched from the coiling temperature to room temperature. The arrow indicates the direction of deformation on all three samples.

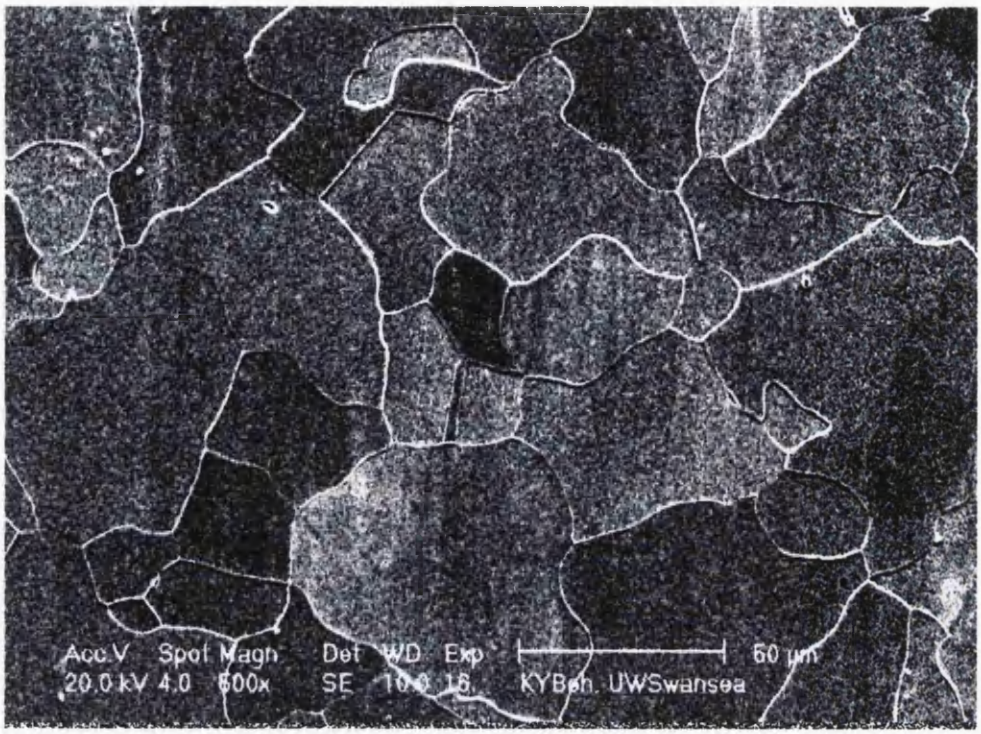
Acc.V Spot Magn Det WD Exp 50 µm
20.0 kV 4.0 500x SE 10.0 16. KYBph. UWSwansea

(a)

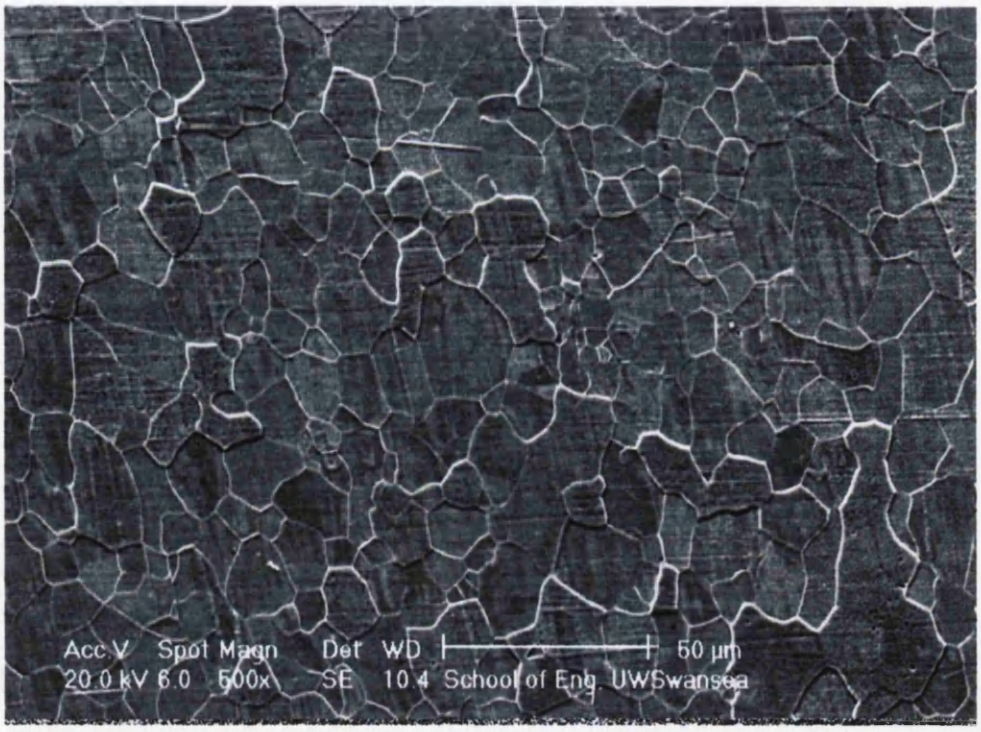
Acc.V Spot Magn Det WD 50 µm
20.0 kV 6.0 500x SE 10.4 School of Eng. UWSwansea

(b)

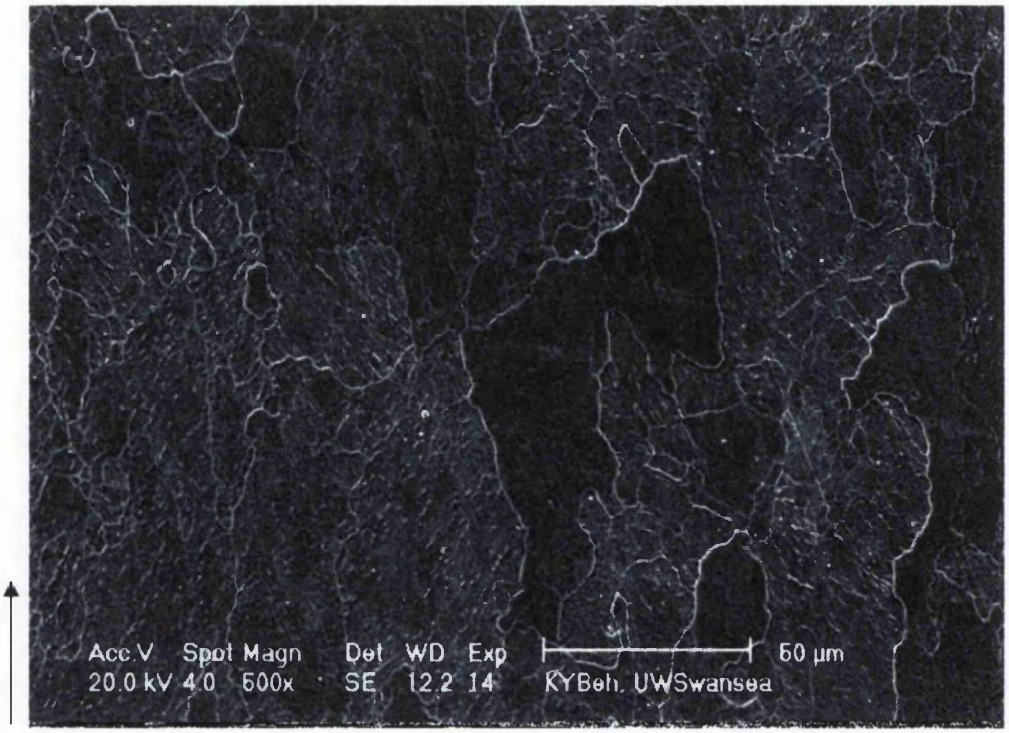


(c)

Figure 5.7: Scanning electron micrographs recorded in the Ti-V HS-IF steel employing variable finishing temperatures (a) 950°C, (b) 850°C and (c) 800°C, followed by coiling at a coiling temperature of 550°C employing a cooling rate of 10°C/s and water quenched from the coiling temperature to room temperature. The arrow indicates the direction of deformation on all three samples.

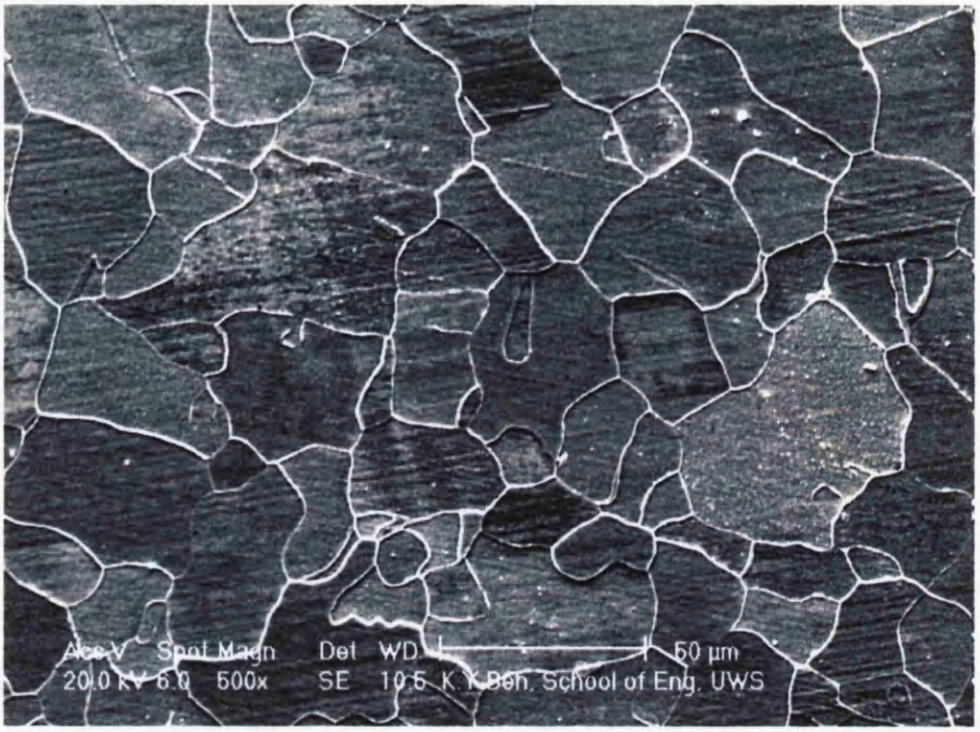
Acc.V Spot Magn Det WD 50 µm
20.0 kV 6.0 500x SE 10.5 K.Y.Beh, School of Eng, UWS

(a)

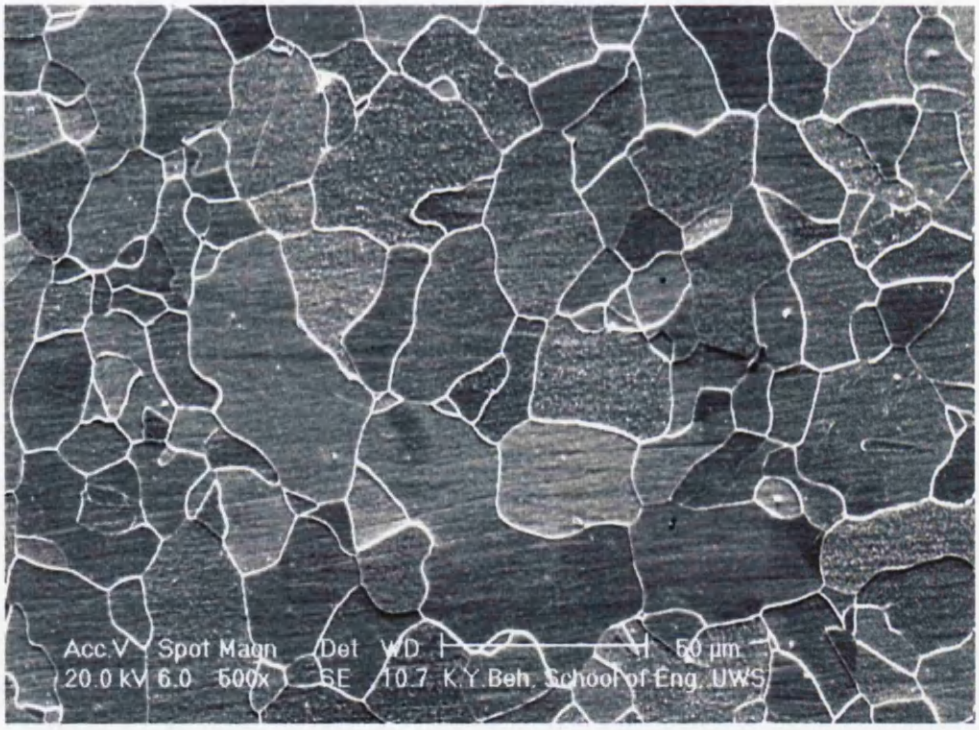
Acc.V Spot Magn Det WD 50 µm
20.0 kV 6.0 500x SE 10.7 K.Y.Beh, School of Eng, UWS

(b)

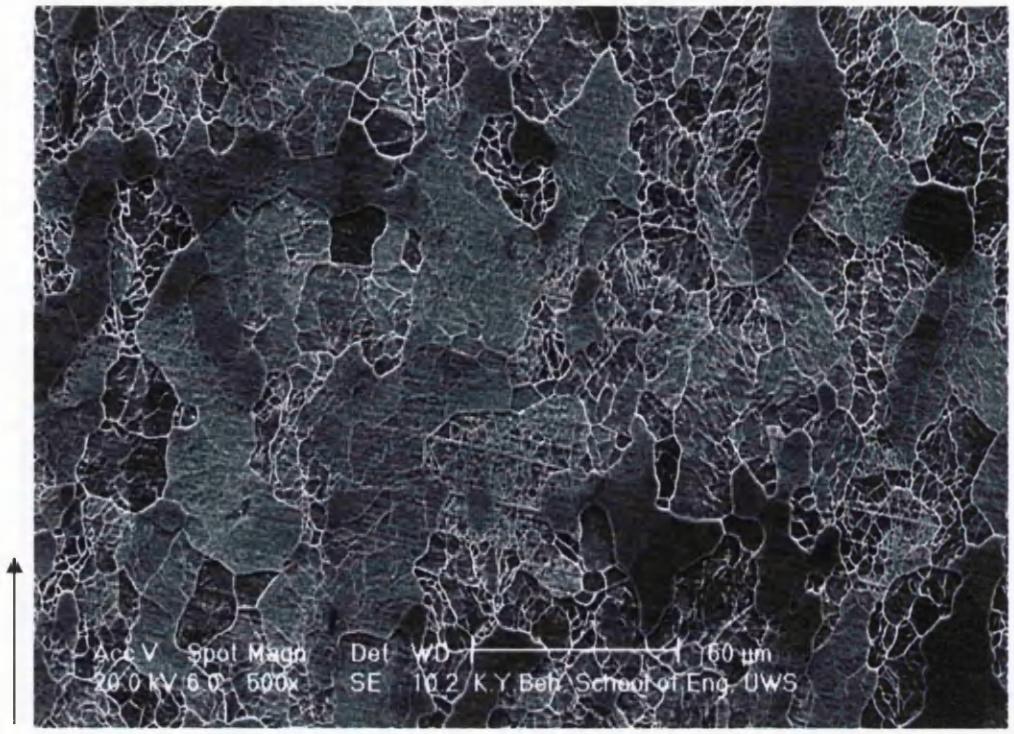


(c)

Figure 5.8: Scanning electron micrographs recorded in the Ti only HS-IF steel employing variable finishing temperatures (a) 950°C, (b) 850°C and (c) 800°C, followed by coiling at a coiling temperature of 450°C employing a cooling rate of 10°C/s and water quenched from the coiling temperature to room temperature. The arrow indicates the direction of deformation on all three samples.

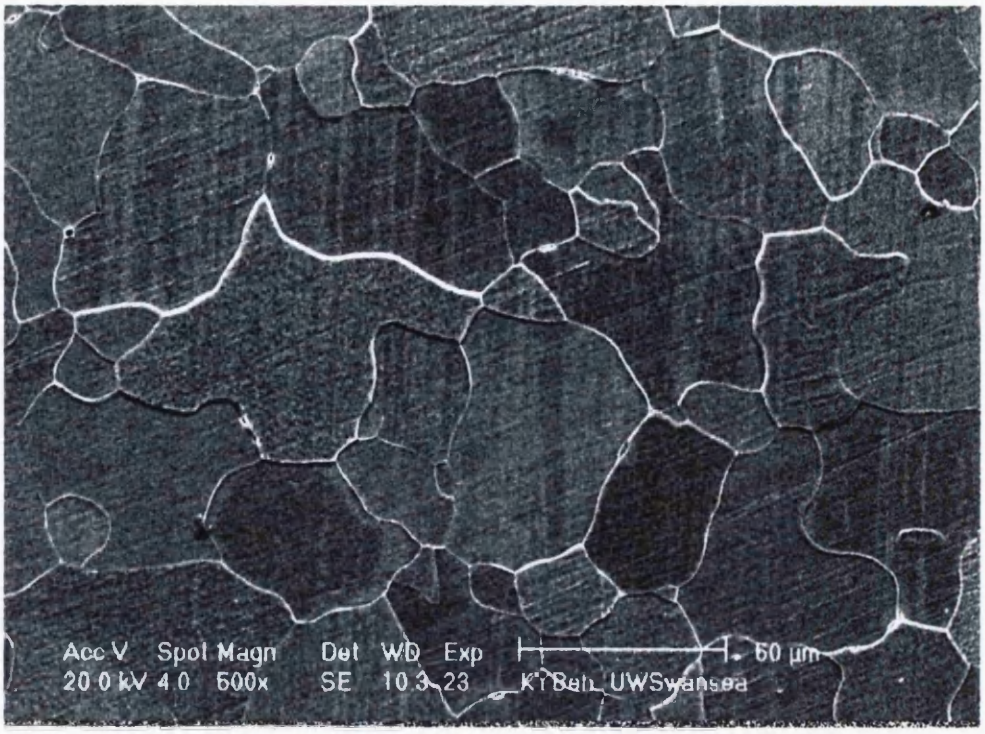
Acc.V Spot Magn Det WD Exp
20.0 kV 4.0 500x SE 10.3 23 KYBeh UWSwansea
50 µm

(a)

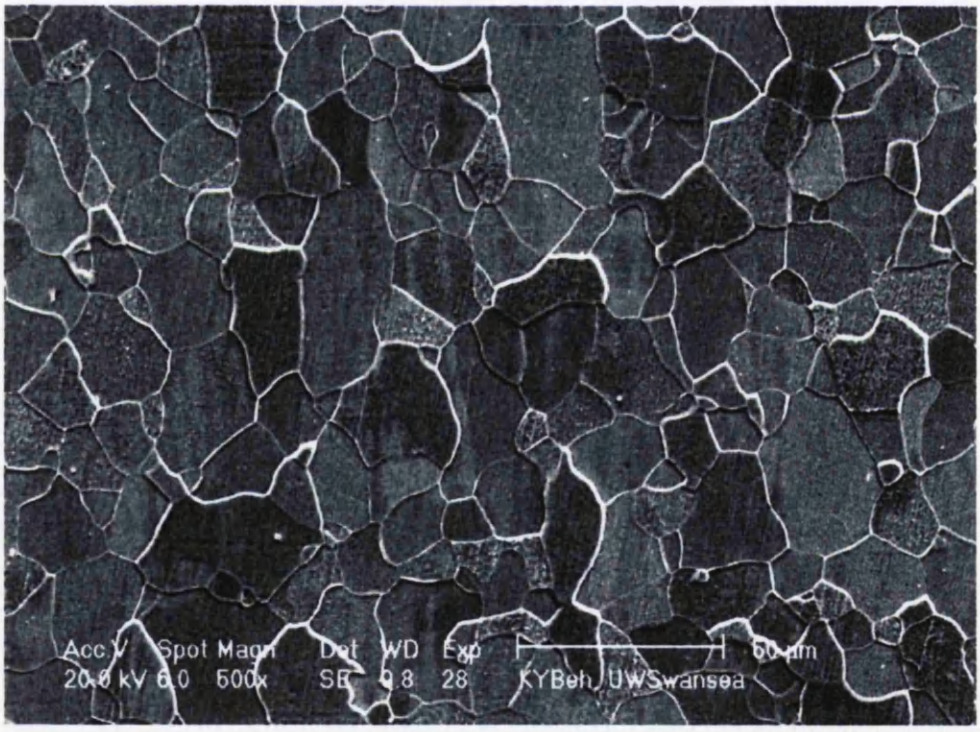
Acc.V Spot Magn Det WD Exp
20.0 kV 6.0 500x SE 9.8 28 KYBeh UWSwansea
50 µm

(b)

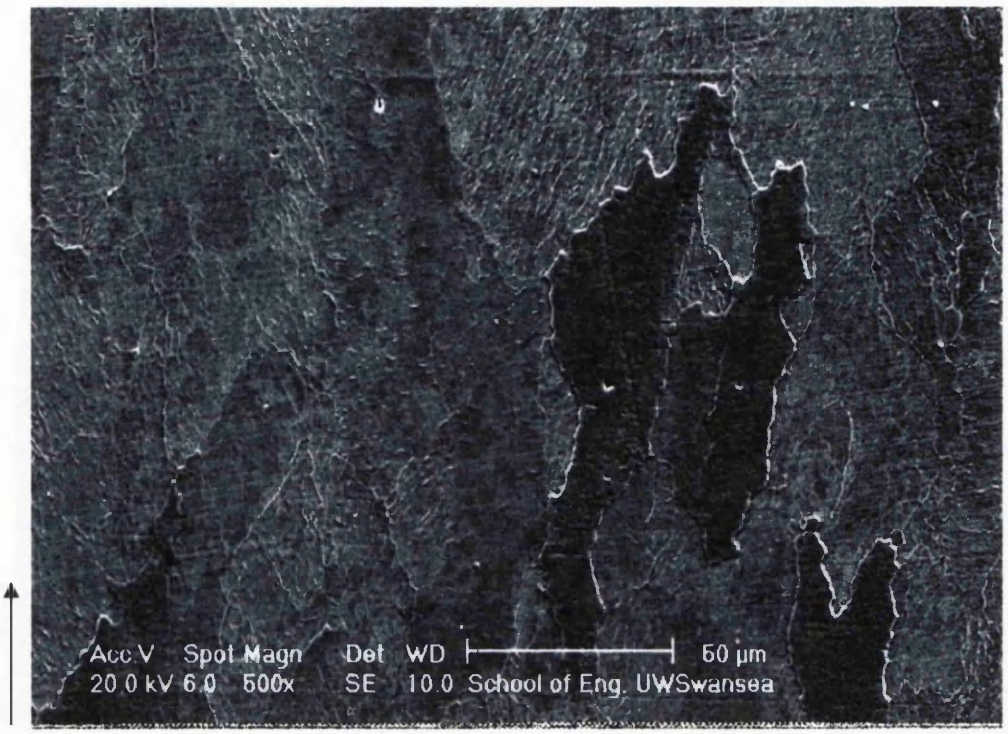


(c)

Figure 5.9: Scanning electron micrographs recorded in the Ti-V HS-IF steel employing variable finishing temperatures (a) 950°C, (b) 850°C and (c) 800°C, followed by coiling at a coiling temperature of 450°C employing a cooling rate of 10°C/s and water quenched from the coiling temperature to room temperature. The arrow indicates the direction of deformation on all three samples.

## 5.2 Hardness

### 5.2.1 Effect of Finishing Temperature

Table 5.1: Hardness (MPa) evolution for the Ti only HS-IF steel as a function of finishing temperature when variable coiling temperatures were applied.

| Finishing Temperature (°C) | Coiling Temperature,(°C) | | | |
|---|---|---|---|---|
| | 450 | 550 | 650 | 750 |
| 800 | 981.4 +/- 41.1 | 971.8 +/- 36.1 | 989.8 +/- 34.3 | 1023.6 +/- 35.7 |
| 850 | 902.5 +/- 11.8 | 904.7 +/- 17.5 | 928.1 +/- 23.8 | 967.4 +/- 35.7 |
| 950 | 847.8 +/- 9.6 | 854.7 +/- 8.4 | 855.3 +/- 13.6 | 879.5 +/- 19.8 |

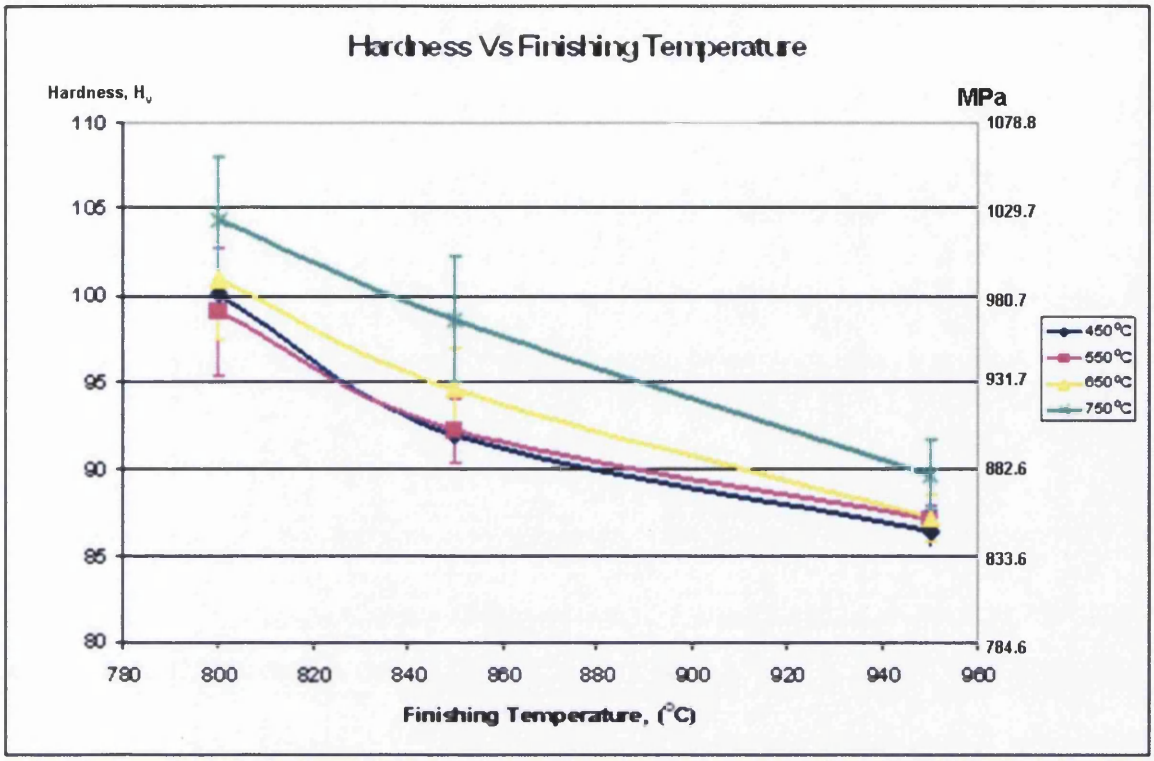


Figure 5.10: Hardness evolution for the Ti only HS-IF steel as a function of finishing temperature following coiling at 750°C, 650°C, 550°C, and 450°C.

Table 5.2: Hardness (MPa) evolution for the Ti-V HS-IF steel as a function of finishing temperature when variable coiling temperatures were applied.

| Finishing Temperature (°C) | Coiling Temperature,(°C) | | | |
|---|---|---|---|---|
| | 450°C | 550°C | 650°C | 750°C |
| 800 | 1079.5 +/- 22.6 | 1071.6 +/- 18.7 | 1089.9 +/- 28.4 | 1066.3 +/- 38.8 |
| 850 | 920.3 +/- 10.1 | 916.5 +/- 14.7 | 939.9 +/- 18.8 | 911.6 +/- 11.8 |
| 950 | 855.7 +/- 12.6 | 859.6 +/- 13.3 | 920.1 +/- 10.1 | 861.3 +/- 20.0 |

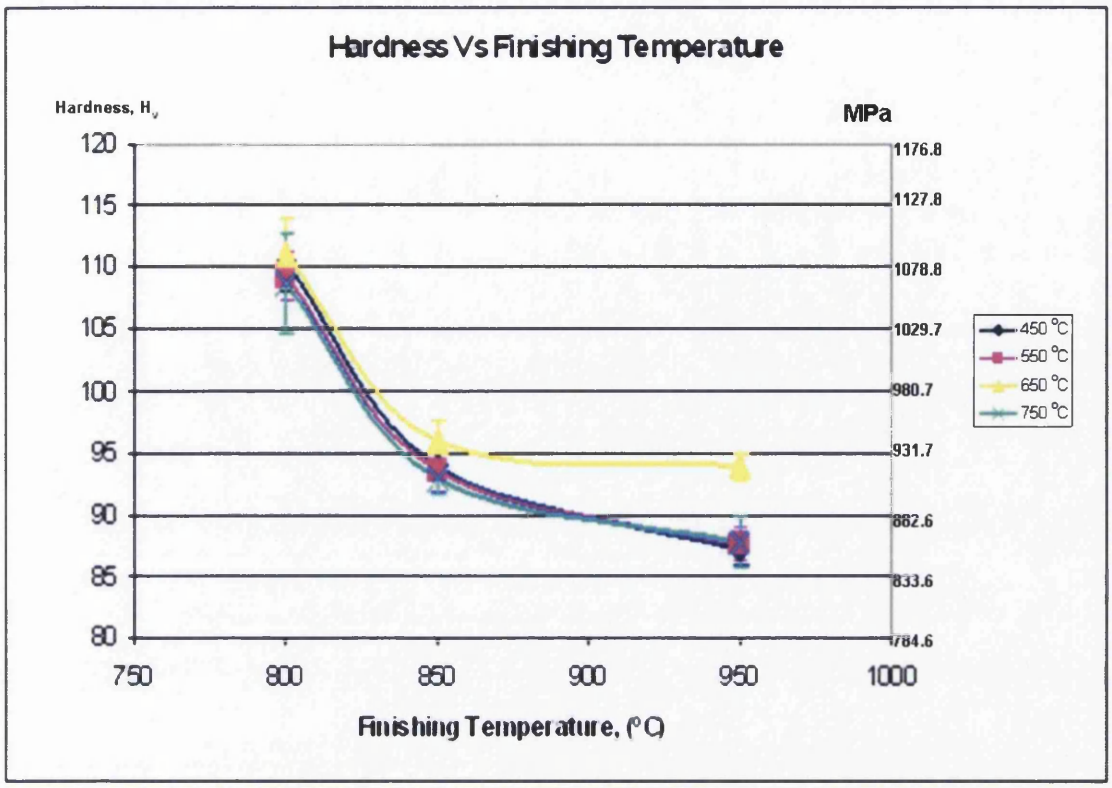


Figure 5.11: Hardness evolution for the Ti-V HS-IF steel as a function of finishing temperature following coiling at 750°C, 650°C, 550°C, and 450°C.

### 5.2.2 Effect of Coiling Temperature

Table 5.3: Hardness (MPa) evolution for the Ti only HS-IF steel as a function of coiling temperature.

| Coiling Temperature (°C) | Finishing Temperature, (°C) | | |
|---|---|---|---|
| | 800 | 850 | 950 |
| 450 | 981.4 +/- 41.1 | 902.5 +/- 11.8 | 847.8 +/- 9.6 |
| 550 | 971.8 +/- 36.1 | 904.7 +/- 17.5 | 854.7 +/- 8.4 |
| 650 | 989.8 +/- 34.3 | 928.1 +/- 23.8 | 855.3 +/- 13.6 |
| 750 | 1023.6 +/- 35.7 | 967.4 +/- 35.7 | 879.5 +/- 19.8 |

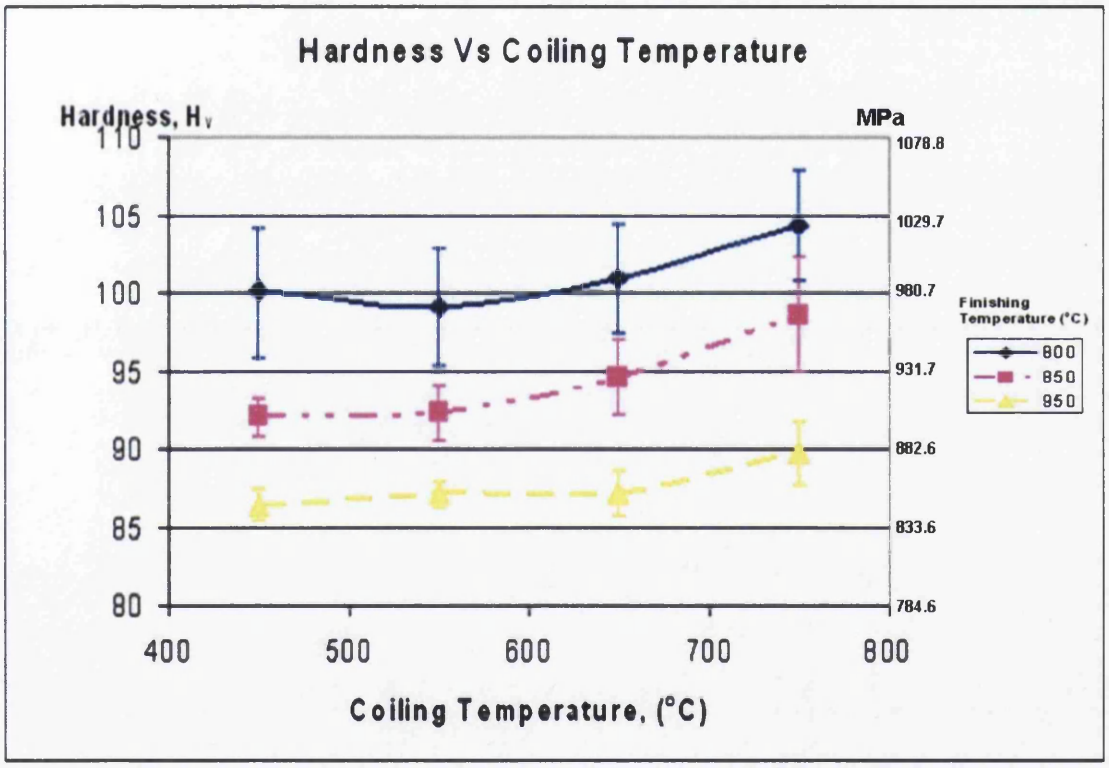


Figure 5.12: Hardness evolution of the Ti only HS-IF steel as a function of coiling temperature.

Table 5.4: Hardness (MPa) evolution for the Ti-V HS-IF steel as a function of coiling temperature.

| Coiling Temperature (°C) | Finishing Temperature, (°C) | | |
|---|---|---|---|
| | 800 | 850 | 950 |
| 450 | 1079.5 +/- 22.6 | 920.3 +/- 10.3 | 855.7 +/- 12.6 |
| 550 | 1071.6 +/- 18.7 | 916.5 +/- 14.7 | 859.6 +/- 13.3 |
| 650 | 1089.9 +/- 28.4 | 939.9 +/- 18.8 | 920.3 +/- 10.3 |
| 750 | 1066.3 +/- 38.8 | 911.6 +/- 11.6 | 861.3 +/- 20.0 |

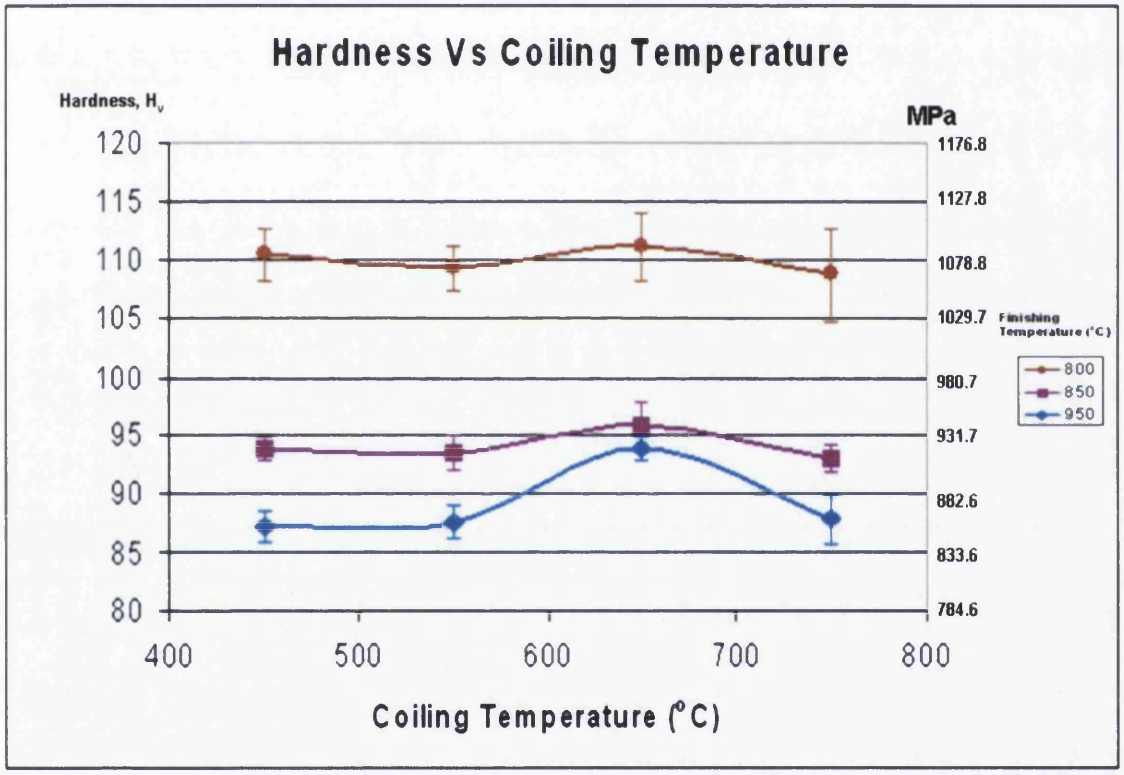


Figure 5.13: Hardness evolution for the Ti-V HS-IF steels as a function of coiling temperature.

## 5.3 MT-Data Thermodynamic Calculations.

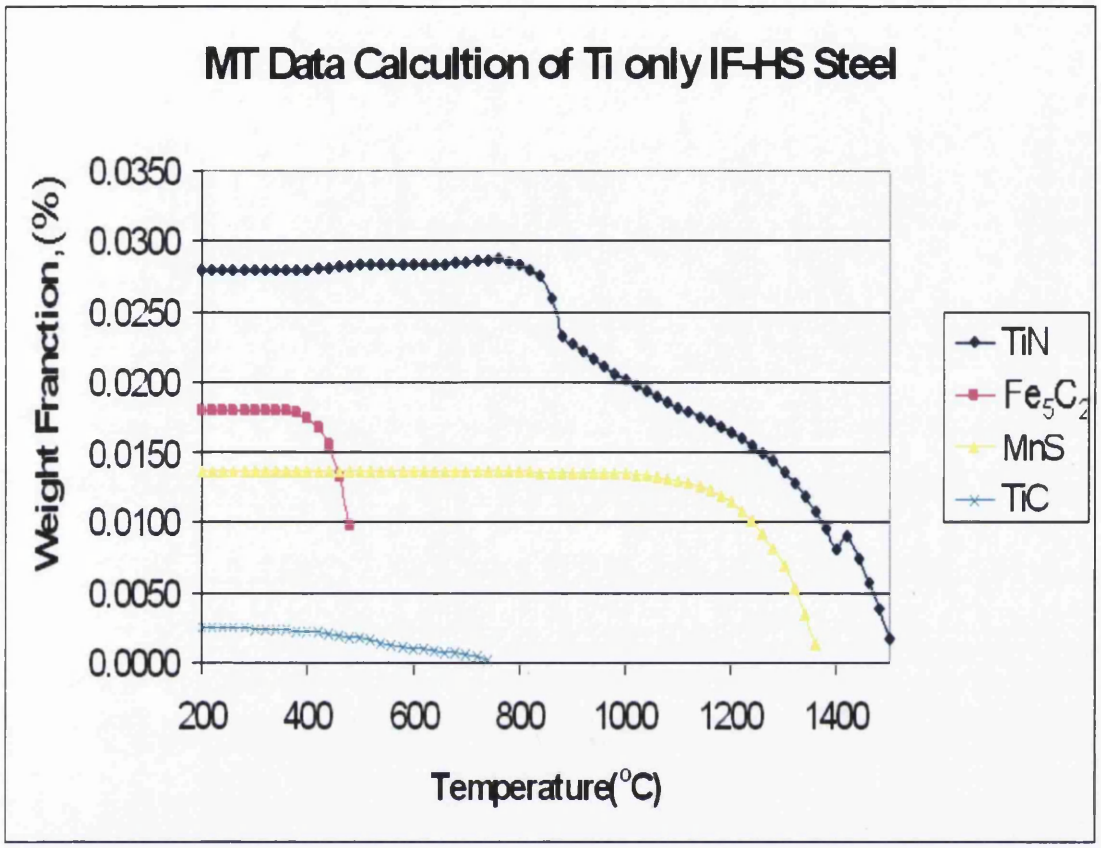


Figure 5.14: MT-Data thermodynamic calculations of equilibrium phases on the Ti only HS-IF steel as a function of weight fraction versus temperature.

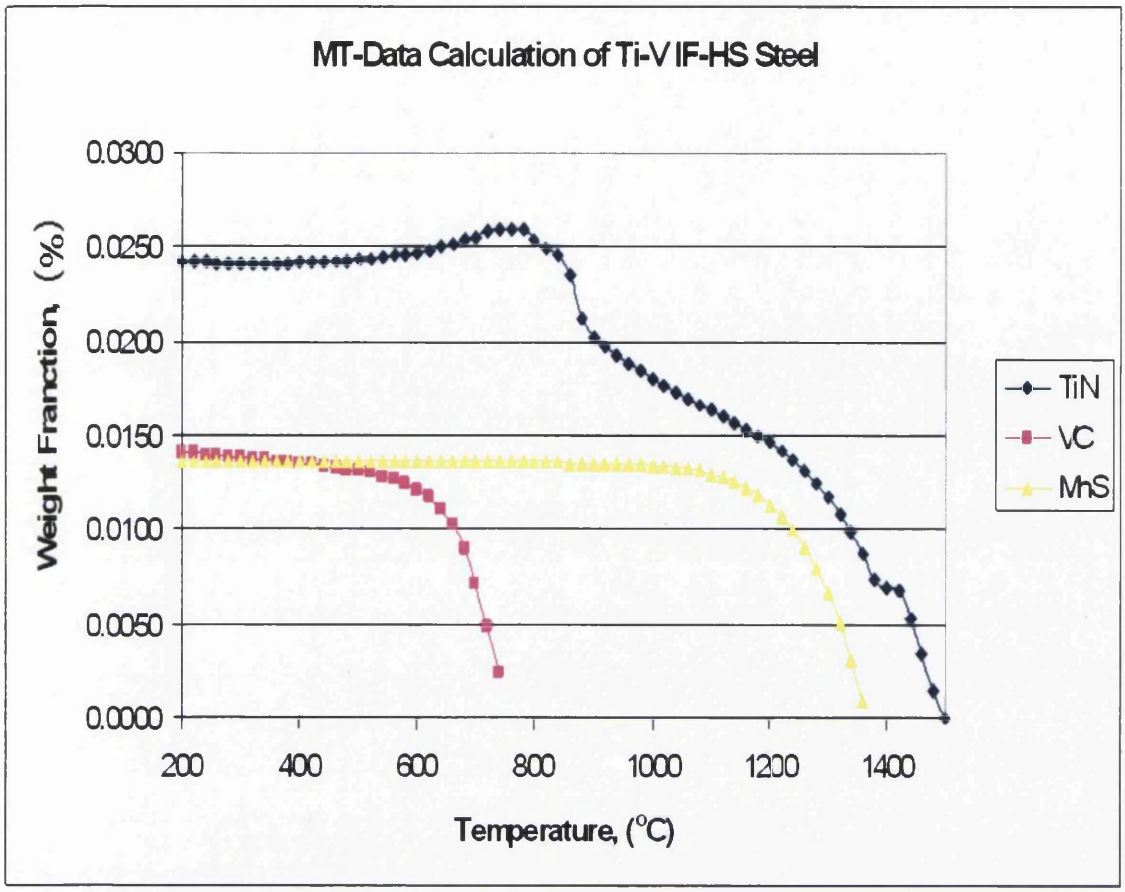


Figure 5.15: MT-Data thermodynamic calculations of equilibrium phases on the Ti-V HS-IF steel as a function of weight fraction versus temperature.

Figure 5.14 and 5.15 show the MT data calculations for Ti only HS-IF steel and Ti-V IF-HS steel. The thermodynamic calculations imply that titanium nitride (TiN), manganese sulphide (MnS), titanium carbide and $\epsilon$-carbide ($Fe_5C_2$) are predicted to be present in Ti only HS-IF steel. Since Ti-V HS-IF steel contains vanadium additions, vanadium carbide (VC) is predicted to be present as well as TiN and MnS.

## 5.4 Grain Size measurements

Due to the complicated grain morphology developed during Gleeble simulation and the difficultly on performing accurate measurements, grain size measurements were only carried out on samples that were finished rolling at 850°C. The measurement was performed using the optilab software. The results are shown in table 5.5.

Table 5.5: Grain size evolution for samples tested at a finishing temperature of 850°C for (a) Ti only HS-IF steel and (b) Ti-V HS-IF steel.

| Coiling Temperature (°C) | Mean Area ($\mu m^2$) | Standard Deviation | Minimum Area ($\mu m^2$) | Maximum Area ($\mu m^2$) |
|---|---|---|---|---|
| 750.00 | 202.98 | 159.77 | 1.46 | 1207.43 |
| 650.00 | 211.27 | 242.84 | 1.80 | 1590.92 |
| 550.00 | 216.39 | 239.53 | 1.27 | 1304.55 |
| 450.00 | 291.49 | 340.95 | 2.05 | 1595.48 |

(a)

| Coiling Temperature (°C) | Mean Area ($\mu m^2$) | Standard Deviation | Minimum Area ($\mu m^2$) | Maximum Area ($\mu m^2$) |
|---|---|---|---|---|
| 750.00 | 216.79 | 224.39 | 1.71 | 1163.37 |
| 650.00 | 149.95 | 152.02 | 2.56 | 970.56 |
| 550.00 | 231.95 | 194.36 | 5.41 | 898.50 |
| 450.00 | 211.93 | 216.86 | 1.60 | 1157.09 |

(b)

# Chapter 6

# Discussion

## 6.1 Hot Rolling Simulation.

The Gleeble 3500 thermomechanical simulation unit was used to perform the hot rolling simulation experiments on the Ti only and the Ti-V HS-IF steels during the present study. The scanning electron micrographs of the as received condition were presented in figure 5.1, where figure 5.1a represents the Ti only steel and figure 5.1(b) the Ti-V steel. The presented micrographs reveal the presence of equiaxed ferritic only microstructures for both steel grades.

The hot rolling deformation during the present study took place at temperatures, within the austenite and/or austenite + ferrite stability field. Both the Ti only and the Ti-V HS-IF steel samples have undergone transformation from austenite to ferrite during the reheating and cooling sequences applied. The purpose of this exercise was to induce this transformation, so as to simulate conditions applicable in the hot mill. Essentially, this approach would lead to the production of refined ferrite for both steels grades. In addition, such a refined microstructure could lead to optimised mechanical properties i.e. strength, drawability and toughness for both steel grades.

At the beginning of the hot rooling sequences, specimens were heated up to the soaking temperature, which was set at 1200°C. In this condition, both the Ti only and the Ti-V

HS-IF steel specimens have experienced the transformation from ferrite to austenite. When held at the soaking temperature, austenite grain growth and coarsening could take place. The dissolution of precipitate particles is time and temperature dependent, certain types of chosen precipitates (present in the steel microstructure) could totally dissolve at the soaking temperature chosen. Especially, TiC and VC which have been reported to dissolve at lower austentisation temperatures [74], and predicted to be present in the experimental Ti only or Ti-V steels studied by MT-Data thermodynamic equilibrium calculations as these were presented in figures 4.30 and 4.31. TiN is also predicted to be present in both the Ti only and the Ti-V steel and it is expected to partially dissolve at the soaking temperature chosen.

The first uniaxial compression took place, once the samples were cooling down to the roughing temperature of 1100°C, which is still within the austenite region. The equiaxed coarse austenite grains (formed and grown at the soaking temperature) of the Ti only and the Ti-V HS-IF steel specimens are deformed at this stage, the austenite grains are elongated and further defined.

## 6.2 Effect of finishing temperature

The steel samples have undergone controlled cooling to the finishing temperature following the first deformation at the roughing temperature. The finishing temperature is the temperature at which the deformation of the samples is completed. Mechanical properties of the steels are strongly affected by the finishing temperature, which consists of the final deformation (compression) during the hot rolling sequences. The samples have been subjected to further compression via a two stage (2 x 0.2 true uniaxial strain compressions) at the finishing temperatures.

The finishing temperatures were set at 950°C, 850°C, or 800°C. The micrographs presented in figure 5.2 have shown that in the Ti only steel, different microstructures

have developed at the variable finishing temperatures employed such as (a) 950°C, (b) 850°C, and (c) 800°C, followed by coiling at 750°C with the cooling rate of 10°C/s and water quenched to the room temperature. These micrographs reveal that when the finishing temperature was set at (a) 950°C, a purely recrystallised uniform ferrite microstructure has been obtained. Due to the finishing temperature set at the recrystallised austenite region; a fully recrystallised ferrite microstructure is subsequently obtained following the transformation from the austenite microstructure. Even if TiN particles are predicted (MT-Data calculation, figure 5.14) to be present in this state, they do not appear to be sufficient enough to inhibit recrystallisation from taking place. The ferrite grain size is fairly dependent on the recrystallised austenite grain size [75]. However, the obtained grain size is refined compared to the as received condition. Hägg carbide ($\epsilon$-carbide) ($Fe_5C_2$) [76] is predicted (MT-Data calculation, figure 5.14) to be forming at around 450°C or below, however, both the Ti only and the Ti-V HS-IF steel samples are water quenched from the finishing temperature which are above/equal to 450°C, thus the Hägg carbide is predicted to play no major role in the development of the microstructures.

When the finishing temperature was further reduced to 850°C, the finishing temperature is now set below the recrystallisation start temperature for austenite. DeArdo [77] has reported that deformed austenite structure with deformation bands would be produced in microalloyed steels. Once the temperature has cooled down to the $\alpha$ region, ferrite nucleates not only on the austenite grain boundaries but also on the deformation bands as shown in figure 5.2b, The recorded micrographs have shown that mixtures of fine ferrite and elongated grains ferrite have found. In particular, the elongated grains are parallel to the rolling direction. Grain size measurements have revealed, further refinement of the microstructures compared to the finishing temperature of 950°C.

When the finishing temperature was set to 800°C, the finishing temperature is firmly within the $\alpha + \gamma$ region. Priestner [78] has reported that when deformation has occurred in the two phase region this is responsible for a hardening of austenite and newly formed ferrite grains. In such a scenario, both austenite and ferrite grain would develop sub

grains and ferrite would nucleates on the austenite grain boundaries and within austenite grains on dislocation. Panigrahi [79] has reported that the strain hardened ferrite (newly formed in $\alpha + \gamma$ region) can recrystallise to a finer ferrite, remaining in a recovered state or remaining in an unresolved state and this is depend upon the temperature, alloying elements present in steel and the amount of reduction. It is also reported that the recovered ferrite has no unfavourable toughness characteristics, the recrystallised fine ferrite could increase the toughness but the unresolved hardened ferrite would cause a negative effect on the toughness. The remaining austenite would transformed to ferrite when the temperature has drop below the $\alpha/\gamma$ transition temperature.

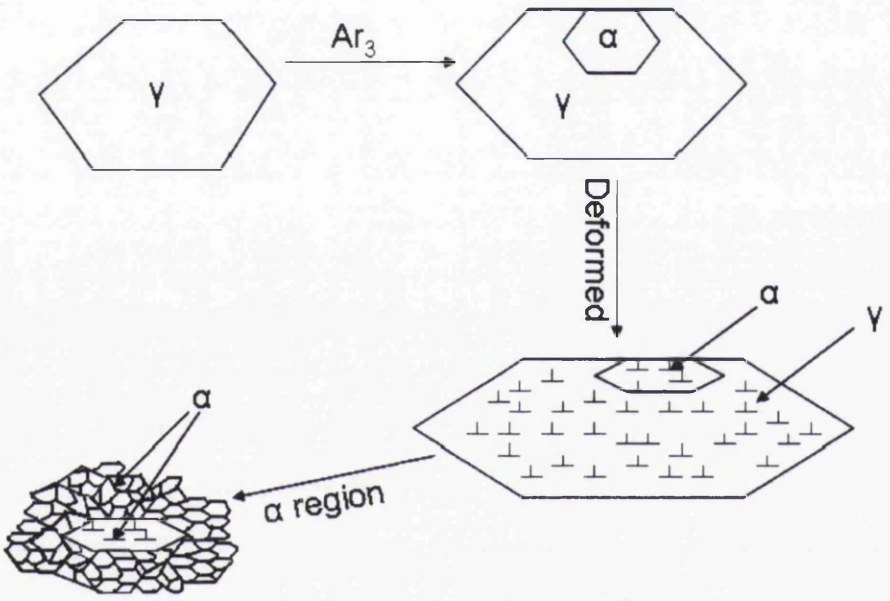


Figure 6.1: The microstructure development developing during finish rolling in the two-phase region of HS-IF steels.

According to the micrographs shown in figure 5.2b, it can be deduced that finishing rolling in the $\alpha + \gamma$ region, results into markedly different microstructure from those developing at a higher finishing temperature, which consist of a very fine transformed ferrite grain with islands of recrystallised ferrite, where recrystallised fine ferrite is shown

to develop parallel to the deformation direction. The grain sizes when measured are proven to be refined compared to these observed in figure 5.2a, which indicates micrographs developed when the finishing temperature was set at 950°C or 850°C. The full process of development of such a microstructure when deformation was performed in the $\alpha + \gamma$ stability field as shown in figure 6.1.

Similar microstructures has also been observed in the Ti-V HS-IF steel. In Figure 5.3 a set of micrographs is presented of the Ti-V HS-IF microstructures obtained when variable finishing temperatures (a) 950°C, (b) 850°C or (c) 800°C, were employed followed by controlled cooling at cooling rate of 10°C/s to the coiling temperature of 750°C, followed by water quenching to room temperature.

When samples were finished rolling at 950°C, a fully recrystallised ferrite grain is developed, as shown in figure 5.3(a), due to the finishing deformation carried out in the recrystallised austenite region.

When the finishing rolling temperature was set at 850°C, similar microstructures, as in the case of the Ti only steel were observed, i.e. a mix of ferrite and elongated ferrite grains. However, in terms of the grain size, the degree of grain refinement in the Ti-V steel is much higher than that observed in the Ti only steel. This provides direct experimental evidence that the vanadium addition in the steel is responsible for the absence of any retardation of recrystallisation. MT-data calculations presented in figure 5.15 predict the presence of VC precipitates in the Ti-V steel. Through the experimental results obtained on this study, it is hypothesized that these VC particles are responsible for the ferrite grain refinement observed.

When the finishing temperature was further reduced to 800°C, the micrographs consisted of a very fine transformed ferrite with 'islands' of recrystallised ferrite. These recrystallised ferrite regions, however, appear to be more elongated than the recrystallised ferrite areas that were observed in the Ti only steel. This is attributed to the absence of any additional retardation effect by vanadium on the recrystallisation. Ferrite

nucleates faster when vanadium additions are performed in HS-IF steels. The temperate drops below the Ar3 and large ferrite grains are produced which are elongated when the sample was deformed. This effect is demonstrated in figure 5.3(c), where large elongated ferrite grains are present parallel to the rolling direction.

One of the aims of the study is to establish the effect of finishing rolling temperature on the microstructures and grain size of the two IF studied steels. Several sets of micrographs are presented for both the Ti only and the Ti-V HS-IF steels. Figure 5.4 presents a set of micrographs of the Ti only steel employing variable finishing temperatures (a) 950°C, (b) 850°C, or (c) 800°C, followed by coiling at 650°C at a cooling rate of 10°C/s followed by water quenching to room temperature. Figure 5.6 and figure 5.8 present the micrographs for the Ti only steel, which was finished rolled under the same conditions as that of figure 5.4 but coiled at 550°C or 450°C.

Figure 5.5 presents the micrographs for the Ti-V steel employing variable finishing temperatures, ie (a) 950°C, (b) 850°C, or (c) 800°C followed by controlled cooling at the rate of 10°C/s to a coiling temperature of 650°C, followed by water quenching to room temperature. Figure 5.15 and figure 5.17 present the micrographs of the Ti-V steel finished rolled under the same conditions as those described in figure 5.5 but coiled at either at 550°C or 450°C.

From the sets of these micrographs, it is evident that when the temperature was set at 950°C, fully recrystallised ferrite grains were obtained. At 850°C, a mix of ferrite and elongated ferrite grains were obtained. Further lowering of the finishing temperature to 800°C resulted in microstructures, which were significantly different. The micrographs consisting of very fine transformed ferrite grains with 'islands' of recrystallised ferrite, which are now evident. It is also evident that vanadium additions in the HS-IF steel is efficient in producing a refined ferrite microstructure.

Table 5.1 and figure 5.10 present the hardness evolution results versus the finishing temperature when variable coiling temperatures are employed, observed on the Ti only

HS-IF steels. The curves in figure 5.10 show that higher hardness values are obtained when the finishing temperature is decreased from 950°C to 800°C, regardless of the applied coiling temperature. In the case of the Ti-V HS-IF steel, a gradual increase in hardness values is also observed, when the finishing temperature decreases form 950°C to 850°C (table 5.2 and figure 5.11), irrespective of the coiling temperature employed. The effect of the finishing temperature on the hardness evolutions is believed to be directly related to the grain size and the associated microstructural changes observed. As observed in figure 5.2 – 4.9, the grain sizes of (a)s are coarser compared to (b)s and (c)s. It is revealed that hardness increases when a finer grain size is obtained. However, the standard deviation of hardness at a finishing temperature of 800°C is much higher than that obtained at lower finishing conditions as observed on both the Ti only and the Ti-V steels (tables 4.1 and 4.2). This is due to the uneven and complex grain sizes observed in the recorded microstructures at 800°C.

## 6.3 Effect of the Coiling Temperature.

The coiling temperatures employed during the hot rolling simulations studied, could influence the grain size and precipitate morphology of the steel product. In the present study all samples were coiled in the ferrite region, therefore, only pure ferrite microstructures were observed under all coiling temperatures. Barrett and Wilshire [80] have reported that lowering the coiling temperature could result in a finer grain, but the finest grain size have been observed at the highest coiling temperature for the Ti only steel (750°C) and second highest coiling temperature for Ti-V steel (650°C) in the present study (as shown in table 5.5).

This is attributed to the fact that samples were rapidly water quenched to room temperature once samples have reached the designated coiling temperate and also due to the fact that the controlled cooling rate (10°C/s) applied from the finishing temperature to the coiling temperature is lower than water spraying. Therefore, it has been proven in the

present study that rapid cooling at a higher ferrite temperature region could produce a finer ferrite microstructure. According to the hardness results shown in table 5.3 and figure 5.12, it is evident that quenching from the higher coiling temperature increases the hardness, regardless of the applied finishing temperature. On the other hand, it is also demonstrated that the finer grains obtained, are responsible for the higher hardness values of the steels.

In the case of the Ti-V HS-IF steels samples, the finest grain sizes (table 5.5b) and highest hardness values (table 5.4 and figure 5.13) are obtained at a coiling temperature of 650°C. This result is associated with precipitation strengthening by vanadium carbide (VC) particles. As predicted by the MT-Data calculations (figure 5.15); there is lack of VC formation at 750°C, hence, rapid cooling from this coiling temperature provides insufficient time for VC to form and result in coarser grain sizes and lower hardness values which (table 5.5b and 4.4).

As predicted by MT-Data calculations, significant quantities of vanadium carbide (VC) particles are expected to have formed at 650°C. Water quenching from this coiling temperature could therefore result in an optimisation of grain refinement and precipitation strengthening. Consequently the optimum coiling temperature for the Ti-V steel has been found to be at 650°C. It is evident that the hardening mechanism and the mechanical properties of steels are not solely depend on the grain refinement but also due to the presence of alloying elements and the active precipitation strengthening mechanism.

# Chapter 7

## Conclusions

1. It has been revealed that in both the Ti only and the Ti-V HS-IF steels that when the finishing temperature was set at (a) 950°C, a purely recrystallised uniform ferrite microstructure has been observed. It is considered that transformation has taken place within the austenite recrystallisation region. When the finishing temperature was set at 850°C, ferrite nucleates on the austenite grain boundaries and any present deformation bands. Hence, a mix of fine ferrite and elongated ferrite grains are observed. It is considered that the finishing temperature was set below the austenite recrystallisation start region. While, when deformation was carried out at a finishing temperature of 800°C, markedly different micrographs consisting of very fine transformed ferrite grains with 'islands' of recrystallised ferrite were observed. It is considered that deformation has taken place within the $\alpha + \gamma$ region.
2. It has also been revealed that the presence of vanadium additions in the steel is responsible for the interstitial free characteristics without any retardation of recrystallisation. The presence of vanadium carbide (VC) particles is hypothesized to have a positive effect in controlling the ferrite grain size, since the finest ferrite grains were obtained on the Ti-V HS-IF steel grade, regardless of the finishing and coiling temperatures employed.
3. Hardness is demonstrated to be increasing with lowering of the finishing temperature in both the Ti only and the Ti-V HS-IF steels and this is reflected in the finer grain sizes obtained. Standard deviation of hardness values for

deformations carried out at a finishing temperature at 800°C are much higher, due to the uneven and complex grains observed in the microstructures.

4. Higher hardness values are obtained at higher coiling temperature due to faster cooling from the coiling temperature to room temperature for the Ti only steels. In the Ti-V HS-IF steels optimum hardness values were measured at a coiling temperature of 650°C. It is hypothesized that the presence of VC precipitates particles could efficiency contribute to a hardness increase, via a precipitation strengthening mechanism.
5. It is evident that the mechanical properties of HS-IF steels employed in the present study are dependent on the microalloying elements used, involving not only precipitation strengthening but also grain refinement.

# Chapter 8

## Suggestions for Further Work

In order to optimize further the processing route of HS-IF grades based on combined Ti-V additions, it would be advantageous to perform additional experimentation correlating the mechanical properties of cold rolled and annealed HS-IF strips, that have been subjected to the hot rolling processing route identified in the present study, and their obtained microstructures.

Thermomechanical processing can be further investigated with the effect of varying the various cooling rates. The control of cooling rates from the coiling temperature to finishing temperature and from the finishing temperature to room temperature plays an important role on the mechanical property and microstructures attained. The applied cooling rates could also determine the precipitation characteristics in the experimental steel studied.

The effect of deformation and strain rate are also important to determine the mechanical properties of steel. Applying variable amounts of deformation and strain rates could help to further refine the ferrite grain size of IF-HS steel and this in turn could lead to positive effect on the attained mechanical properties.

Additional work could focuses on above-mentioned processing parameters to enhance the quality of strip steel products and maximise the benefits of ferritic hot rolling.

# Chapter 8

# References


1. Wagner, Donald B: 'Early iron in China, Korea and Japan'. Britannica, 2/2007
2. Needham: 'Methods of forging steel', Coves Book ltd, Volume 4, Part 3, 563 g, 1986.
3. Bessemer process. Britannica 2: 168. 2005. Encyclopedia Britannica.
4. "Smelting". Britannica. Encyclopedia Britannica.2007
5. C. Newey: 'The Open University: Car Body', The Open University Press, 1973, 13.
6. P. Pichant: 'Competition between steel and Al for the passenger car', International iron and steel institute, 1994, 5.
7. K.Berchem, M.G.Hocking: 'The influence of pre-straining on the high-cycle fatigue performance of two hot-dip galvanised car body steels. Materials Charaterization 2007, 58, pp. 593-602.
8. N. Takahashi, M. Shibata, Y. Fruno, H. Hayakawa, K. Kakuta, and Y. Yamamota: 'to produce Deep Drawing and high Strength Steel Sheets'., Proc. Metallurgy of Continuous annealed sheet steel, TMS-AIME, 1982, PP. 133-153.
9. R.Mendoza, M. Alanis, O. Alvarez-Fregoso, J.A. Juarez-Islas: 'Processing Conditions of an ultra low carbon/Ti stabilized steel developed for automotive applications', Seripta mater. 2000, 43, pp. 771-775

10. E. Yasuhara, K. Sakata, T. Kato, and O.Hashimoto: 'Effect of Boron on the resistane to Secondary Working Embrittlement in extra- Low-C cold Rolled Steel Sheet, ISIJ International, 1994, 34, pp. 99-107.
11. S.L. Porter and G. Fourlaris: 'Thermo-mechanical simulation and microstructural control in IF strip steels. Proceeding of simpro'04, 2004, pp. 173-180
12. K.Berchem and M.G. Hocking: 'The influence of per-straining on the high-cycle fatigue performance of two hot-dip galvanized car body steels. Materials Characterization, 2007, 58, pp.593-602
13. International Iron & Steel Institute; Committee on Automotive Applications: 'Advanced High Strength Steel (AHSS). 2006, Version 3. www.autosteel.org
14. H. Beenken, 'Processing state-of-the-art multi-phase steel, European Automotive supplier conference', Berlin 2004
15. M. Abe: 'Formable Steels', Material Science and Technology, 1992,chapter 7, 285-333
16. D.T.Llewellyn: 'Steel: Metallurgy and Applications', Butterworth-Heinemann Ltd, Great Britain, 1992.
17. T. Gladman: 'The Physical Metallurgy of Microalloyed Steels', The institute of Materials, London, 1997.
18. J.R. Davies: 'Carbon and Alloy Steels', ASM Specialty Handbook, ASM International, USA, 1996.
19. ULSAB-Advanced Vehicle Concepts, 'Steel Materials And Processes', 2002, overview report 5.
20. R. Robinson: 'The Future of Interstitial-Free Steels, Iron and Steel International', 1982, vol 55, pp. 83-86
21. H. Takechi: 'Metallurgical Aspects on Interstitial Free Sheet Steel From Industrial Viewpoint, ISIJ International, 1994, Vol. 34, No. 1, pp. 1-8
22. T. Urabe, Y. Ono, H. Matsuda, A. Yoshitake and Y. Hosoya: 'Practical Properties of HS-IFSS for the Application to Automotive Usage', JFE Steel Corporation, International Forum For The Properties And Application Of IF Steels, 2003, pp. 170-177

23. G.Krauss, D.O.Wilshynsky, and D.K. Matlock: 'Proc. Int. Symp. On IF steel Sheet: "Processing , Fabrication and Properties", Ottawa, ON, Canada, August 1991, pp. 1-14.

24. Kyooyoung Lee, Sang-Ho Han and Young-Sool Jin: 'Effects Of Substitutional Elements On Precipitation Behavior And Mechanical Properties Of High Strength IF Steels', Technical research Laboratories, Korea, International Forum For The Properties And Application Of IF Steels, 2003, pp. 286-290

25. D.Anthony Jones, Stephen R. Daniel: 'A Review of the Development and Use of ULC Steels Manufactured by Corus Group (Wales) and Current Challenges for Further Development', International Conference On The Processing, Microstructure And Properties of IF Steel, 2000, pp.55-67.

26. O.Girina, D. Bhatacharya: 'Effect of boron on the Microstructure and mechanical properties of a high-strength, interstitial-free steel'. Ispat Inland Research Laboratories, International Conference On The Processing, Microstructure And Properties of IF Steel, 2000, pp35-44

27. S.I. Kim, S.H. Choi, Y. Leec, 'Influence of phosphorous and boron on dynamic recrystallization and microstructures of hot-rolled interstitial free steel' Materials Science and Engineering, 2005 A406, pp. 125–133

28. Huang-Chuan Chen, Liuwin Chang, Peng-Kuen Lee, Yie-Shing Hwang, 'Effect of alloying elements and processing Parameters on the properties of cold-rolled IF steel sheets', International Conference On The Processing, Microstructure And Properties of IF Steel, 2000, pp23-33

29. Y.Yasushi, U. Toshiaki and N. Yasunobu: 'A New Type of High Strength Steel for Exposed Panels- High-Strength Steel with Excellent Formability, Superior Surface Precision after Press Forming, and Uniform Surface Appearance, JFE Technical Report, 2004, No.4,pp. 15-21

30. L.J. Ruiz-Aparicio, C.I.Garcia and A.J. DeArodo: ' Deveropment of {111} Transformation Texture in Interstitial-Free Steels, Metallurgical And Materials Transaction A, 2001, Vol. 32A, 2235.

31. Y. Ishiguro, T. Murayama, A. Chino, K. Sato, Y. Shima, A.Kido, and M. Morita: 'A Precise Quantitative Analysis of Precipitates in Ti-Bearing

Interstitial-Free Steel, Proc. Conf. on 39th Mechanical Working and Steel Processing Conference Proceedings', Iron & Steel Society, Indianapolis, IN, 1998, pp. 225-264

32. S. Carabajar, J. Merlin, V. Massardier and S. Chabanet: 'Precipitation Evolution During the Annealing of an Interstitial-Free Steel, Materials Science and Engineering A-Structural Materials Properties Microstructure and Processing, 2000, vol. 281, pp132-142.
33. C.Capdevila, C. Garcia-Mateo, F.G. Caballero, C. Garcia de Andres: 'Neural Network Analysis of the Influence of Procession on Strength and Ductility of Automotive Low Carbon Sheet Steels, Computational Material Science, 2006, vol. 38, pp. 192-201.
34. David San Martin, F.G. Caballero, C. Capdevila, C. Garcia de Andres: 'Material Transformation', JIM, 2004, 45, pp.2797-2804.
35. R.A.Hubert, G. Dupuis and R. Taillard: 'Percipitation Reactions in Ti-IF Steels: A Comparision between Austenite and Ferrite., IF Steels 2000 Proceedings, ISS, 2000, pp. 45-54.
36. B.C.De Cooman and A.De V yt: 'Ti-Containing Precipitates In IF Steels', The Iron and Steel Institute of Japan, IF Steels 2003, pp. 249-258
37. G. Dupuis, R.A. Hubert and R. Tailard, Proc. 40th MWSP conference, Pittsburgh, Iss, 1998, pp117.
38. R.A. Hubert, G.Dupuis, R. Taillard, 'Solid-Solid Phase Transformation', Proceedings International Conference, Kyoto, 1999, pp. 99
39. I. Tolleneer, F. Horzenberger and B.C. De Cooman: 'Properties of IF Steel Grades for Enamelling', IF Steel 2000, Proceedings, ISS, 2000, pp. 301-311
40. M. Hua, C. I. Garcia and A. J. DeArdo, 40th Proceedings MWSP Conf., Volume XXXVI, ISS, Warrendale, PA, 1998, pp.887
41. I. Gupta, and D.Bhattacharya: 'Metallurgy of Formable Vacuum Degassed Products', Warrendale, Minerals Metals & Materials Society, 1990, pp. 43-72.
42. A.J. DeArdo: 'Role of Solutes In IF Steels', International Forum for The Properties and Application of IF Steels, IF Steels 2003, pp. 240-249.

43. V. Krupic, T. Gladman and P. Mitchell: 'Vanadium in Interstitial-Free Steels', Hamilton, Ontario, Canada, V0595, 1995, 22-25.

44. T. Gladman and P.S. Mitchell: 'Vanadium in Interstitial Free Steel', University of Leeds, 1997, Vanitec Publication V0497.

45. John Speer: 'Vanadium in Cold-Rolled Sheet Steels', Colorado School of Mines Golden, Co, USA, International Seminar on Application Technologies of Vanadium In Flat – Rolled Steels, 2005, pp.34-42.

46. I.Hertveldt, B.C. De Cooman, and S. Claessens, 'Influence of Annealing Conditions on the Glavanizability and Galvannealing Properties of TiNb Interstitial-Free Steels, Strengthened with Phosphorous and Manganese, Metallurgical and Materials Transactions A, 2000, Vol. 31A, pp.1125.

47. J. Rege, M. Hua, C.I. Garcia and Anthony J. DeArdo, 'The Role of Phosphorus in Interstitial-Free Steels, IF Steel 2000, Proceedings, ISS, 2000, pp.327-338.

48. P. Ghosh, B. Bhattacharya and R.K. Ray, 'Comparative Study of Precipitation Behavior and Texture Formation in Cold Rolled-Batch Annealed and Cold Rolled-Continuous Annealed Interstitial-Free High Strength Steels, Scripta Materialia 56, 2007, pp. 657-660

49. Z.D. Wang, Y.H.Guo, D.Q. Sun, X.H. Liu and G.D. Wang, 'Texture Comparison of an Ordinary IF steel and a High-Strength IF Steel Under Ferritic Rolling and High-Temperature Coiling, ScienceDirect, Material Characterization, 2006, Issues 4-5, Vol 57, pp. 402-407.

50. P.Ghosh, R.K.Ray, B.Bhatacharya and S. Bhargave, 'Precipitation and Texture Formation in Two Cold Rolled and Batch Annealed Interstitial-Free High Strength Steels, ScienceDirect, 2006, Vol 55, pp. 271-274

51. P.Ghosh, R.K.Ray and B.Bhatacharya, 'Determination of the Crystal Structure of FeTiP-type Precipitates in a few Interstitial-Free High-Strength Steels, ScienceDirect, Scripta Materialia, Article in Press, 2007, doi:10.1016/jascriptamat.2007.04.003

52. A.Okamoto, N.Mizui, 'Metallurgy of Vacuum Degassed Steel Products', TMS, Warendale, PA, 1990, pp. 161-180.

53. A.Uenishi, C.Teodosiu, 'Solid Solution Softening at High Strain Rates in Si- and/or Mn-added Interstitial Free Steels, ScienceDirect, Acta Materialia, 2003, vol 51, pp. 4437-4446.

54. H.A. Akbarzadeh, M. Tamizifar, Sh. Mirdamadi and A. Abdolhosseine, 'Mechanical Properties and Microstructures of Zr-Microalloyed Cast Steel', ISIJ International, 2005, Vol. 45, No. 8, pp1201-1204.

55. S. Feliu Jr., M.L. Perez-Revenga, 'Effect of Alloying Elements (Ti, Nb, Mn and P) and the Water Vapour Content in the Annealing Atmosphere on the Surface Composition of Interstitial-Free Steels at the Galvanising Temperature, ScienceDirect, Applied Surface Science, 2004, vol 229, pp 112-123.

56. Shieldalloy Metallurgical Corporation, 'Mn Manganese', 2002, http://www.shieldalloy.com/manganesepage.html.

57. F.Matsuno, Shun-ichi Nishikida and H. Ikesaki, 'Mechinical Properties of Manganese Sulphides in the Temperature Range between Room Temperature and 1000°C, Transactions ISIJ, 1985, Vol 25, pp. 989-998.

58. Shieldalloy Metallurgical Corporation, 'Si Silicon', 2002, http://www.shieldalloy.com/manganesepage.html.

59. T.Vladman: 'The Physical Metallurgy of Microalloyed Steels', The Institute of Materials, London, 1997.

60. C.Capdevila, T.De Cock, C. Garcia-Mateo, F.G. Caballero, C. Garcia de Andres, Materials Science Forum 500-501, 2005, pp. 803-810.

61. Hall, E.O. Proc. Phys. Soc. Series B. 1951, Vol 64, pp. 747

62. Petch, N.J. Proc. Swampscott Conf., MIT Press, 1955, pp. 54.

63. DT. Llewellyn: 'Steels: Metallurgy & Applications 2nd Edition', Butterworth Heinemann Ltd, 1994, pp.65-74.

64. Fusato KITANO, Toshiaki URABE, Takeshi FUJITA, Katsumi NAKAJIMA and Yoshihiro HOSOYA: 'New Type of IF-High Strength Steel with Superior Anti-secondary Work Embrittlement', ISIJ International, 2001, Vol. 41, No. 11, pp. 1402–1410.

65. J.R. Davies: 'Carbon and Alloy Steels', ASM Specialty Handbook, ASM International, United State, 1996.

66. Wikipedia: 'Sheet Metal', http://en.wikipedia.org/wiki/Sheet_metal.

67. C.A. Khoo: 'Microstructure-Mechanical Property Relationships in Vanadium Bearing High Strength Low Alloy Strip Steels', PhD Thesis, 2005.

68. DT. Llewellyn: 'Steels: Metallurgy & Applications 2nd Edition', Butterworth Heinemann Ltd, 1994, pp.12-64.

69. H. Davies and J. Robinson: 'Introduction of MTDATA', Thomas Sourmail, Cambridge, 2003, http://cml.postech.ac.kr/mtdata/introduction.html.

70. H. Davies and J. Robinson: 'General Principle of MTDATA', Thomas Sourmail, Cambridge, 2003, http://cml.postech.ac.kr/mtdata/theory_general.html.

71. Alan Dinsdale, Hugh Davies, John Gisby, Susan Martin and Jim Robinson: 'Thermodynamic Modeling: MTDATA', NPL, 2002, http://www.msm.cam.ac.uk/phase-trans/2002/MTDATA/MTDATA.PPT#256,1,Slide 1

72. Todd A. Bonesteel, David E.Ferguson, and Hugo Ferguson, 'Physical Simulation in the 21st Century. Thermo-Mechanical Simulation and Processing of Steels, Ranchi, India, Viva Book Private Limited, 2004, pp. 91-105

73. H.G. Suzuki: 'Physical Simulation of Continuous Casting to Get Crack-Free Slabs in Steels and other Metals', Thermo-Mechanical Simulation and Processing of Steels, Ranchi, India, Viva Book Private Limited, 2004, pp. 3-9.

74. Kim Ballentine: 'Iron-Iron Carbide Phase Diagram Example', Material Science and Metellurgy, 4th edition, Pollack, Prentice-Hall, 1988.

75. K Easterling: 'physical metallurgy of welding', London, butterworths, 1992, pp. 112.

76. André Schneider and Gerhard Inden, 'Carbon diffusion in cementite (Fe3C) and Hägg carbide (Fe5C2)', Computer Coupling of Phase Diagrams and Thermochemistry, vol. 31, 2007, pp. 141–147.

77. E Underwood; ' Quantitative Stereology', Wesley, 1970, New York.

78. R Priestner and E de Los Rios: 'heat treatment', London: Metal Society, 1976, p.129

79. A.J. DeArdo, Editor: D. P. Dunne and T Chandra, "High Strength Low Alloy Steels', Springer India, vol. 24, No.4, 2007, pp.361-371.

80. C.J.Barrett and B.Wilshire: 'Metallurgical aspects relating to the production of ferritically hot-rolled interstitial-free steel', Professional Engineering Publishing, vol.215, No. 8, 2001, PP. 361-371.